FOSSIL ENERGY

DOE/BC/14941-6
(DE97008428)

ADVANCED OIL RECOVERY TECHNOLOGIES FOR IMPROVED RECOVERY FROM SLOPE BASIN CLASTIC RESERVOIRS, NASH DRAW BRUSH CANYON POOL, EDDY COUNTY, NEW MEXICO

Annual Report
September 25, 1995 to September 24, 1996

RECEIVED
DEC 09 1997
OSTI

By
Mark B. Murphy

August 1997

Performed Under Contract No. DE-FC22-95BC14941

Strata Production Company
Roswell, New Mexico

National Petroleum Technology Office
U. S. DEPARTMENT OF ENERGY
Tulsa, Oklahoma

DISTRIBUTION OF THIS DOCUMENT IS UNLIMITED

DISCLAIMER

This report was prepared as an account of work sponsored by an agency of the United States Government. Neither the United States Government nor any agency thereof, nor any of their employees, makes any warranty, expressed or implied, or assumes any legal liability or responsibility for the accuracy, completeness, or usefulness of any information, apparatus, product, or process disclosed, or represents that its use would not infringe privately owned rights. Reference herein to any specific commercial product, process, or service by trade name, trademark, manufacturer, or otherwise does not necessarily constitute or imply its endorsement, recommendation, or favoring by the United States Government or any agency thereof. The views and opinions of authors expressed herein do not necessarily state or reflect those of the United States Government.

This report has been reproduced directly from the best available copy.

Available to DOE and DOE contractors from the Office of Scientific and Technical Information, P.O. Box 62, Oak Ridge, TN 37831; prices available from (615) 576-8401.

Available to the public from the National Technical Information Service, U.S. Department of Commerce, 5285 Port Royal Rd., Springfield VA 22161

DOE/BC/14941-6
Distribution Category UC-122

Advanced Oil Recovery Technologies For Improved Recovery From Slope Basin Clastic Reservoirs, Nash Draw Brushy Canyon Pool, Eddy County, New Mexico

Annual Report
September 25, 1995 to September 24, 1996

By
Mark B. Murphy

August 1997

Work Performed Under Contract No. DE-FC22-95BC14941

Prepared for
BDM-Oklahoma/
U.S. Department of Energy
Assistant Secretary for Fossil Energy

Jerry Casteel, Project Manager
National Petroleum Technology Office
P.O. Box 3628
Tulsa, OK 74101

MASTER

Prepared by:
Strata Production Company
PO Box 1030
Roswell, NM 88202

DISCLAIMER

Portions of this document may be illegible in electronic image products. Images are produced from the best available original document.

TABLE OF CONTENTS

LIST OF FIGURES

LIST OF TABLES

EXECUTIVE SUMMARY

A producing property operated by Strata Production Company in the Nash Draw Brushy Canyon Pool, Eddy County, New Mexico is a field demonstration site in the Department of Energy Class III program. The five-year project has just completed the first year of activity.

The basic problem at the Nash Draw Pool is the low recovery typically observed in similar Delaware Basin reservoirs. By comparing a control area using standard infill drilling techniques to a similar area developed using advanced reservoir characterization methods, the goal of the project is to demonstrate that a development program based on advanced methodology can significantly improve oil recovery.

The advanced characterization effort integrates geological, geophysical, petrophysical, geostatistical, production, and reservoir engineering data. During the first year of the project, four new producing wells were drilled, serving as data acquisition wells. Vertical seismic profiles and a 3-D seismic survey were acquired to assist in interwell correlations and facies prediction. The stratigraphic framework is being quantified in petrophysical terms using innovative rock-fabric/petrophysical relationships calibrated to wireline logs. Geostatistical techniques are being coupled with 3-D seismic attributes to extrapolate petrophysical properties into the interwell area.

Reservoir characterization and simulation studies are being used to predict the distribution of remaining oil saturation and to optimize development drilling programs. Limited surface access at the Nash Draw Pool, caused by the proximity of underground potash mining and surface playa lakes, limits development with conventional drilling. Various combinations of vertical and horizontal wells combined with selective completions are being considered for optimizing production performance. Based on the production constraints due to high gas-oil ratios observed in similar Delaware Basin fields, pressure maintenance is a likely requirement at the Nash Draw Pool. Using the geological model developed in the first year of the project, a detailed reservoir description of the pilot area has been made, and current efforts are concentrating on defining the reservoir volume which supports the pilot area wells. In the next quarter, a preliminary evaluation of enhanced recovery options, including waterflooding, lean gas, and carbon dioxide injection, will be made for the pilot area. By the end of 1996, the next generation geological model will include 3-D seismic input and greater use of statistical methods.

This first annual report will highlight the progress made to date.

INTRODUCTION

The basic driver for this project is the low recovery observed in Delaware reservoirs, such as the Nash Draw Pool (NDP). This low recovery is caused by low reservoir energy, less than optimum permeabilities and porosities, and inadequate reservoir characterization and reservoir management strategies which are typical of projects operated by independent producers. Rapid oil decline rates and high gas/oil ratios are typically observed in the first year of primary production. Based on the production characteristics that have been observed in similar Delaware fields, pressure maintenance is a likely requirement at the Nash Pool. Three basic constraints to producing the Nash Draw Brushy Canyon Reservoir are: (1) limited areal and interwell geologic knowledge, (2) lack of an engineering tool to evaluate the various producing strategies, and (3) limited surface access prohibiting development with conventional drilling. The limited surface access is caused by the proximity of underground potash mining and surface playa lakes.

OBJECTIVE

The objectives of this project are: (1) to demonstrate that a development drilling program and pressure maintenance program, based on advanced reservoir management methods, can significantly improve oil recovery compared with existing technology applications and (2) to transfer these advanced methodologies to oil and gas producers, especially in the Permian Basin.

PROJECT STATUS

This is a 5-year project that has just completed the first year of activity. This project has two budget periods; duration of the first budget period is two years and duration of the second budget period is three years. A milestone chart for the project is shown in **Figure 1**. The first period of the DOE cost-shared project is the "Science Phase" in which detailed reservoir characterization and project data are being analyzed to provide the basis for delineating appropriate reservoir management strategies. During the first period, the feasibility of a pilot project will be determined and the results will be extrapolated to a full field implementation, if technically and economically feasible. Phase Two, if pursued, will be the "Implementation Phase" in which results of the pilot testing will be considered for expansion to the remainder of the Unit.

PROJECT PLAN

The plan in the first year calls for developing a control area using standard reservoir management techniques and comparing the performance of the control area with an area developed using advanced reservoir management methods. During Budget Period #1, eight new wells will be drilled for data acquisition in a pilot demonstration project area. Results from reservoir characterization and simulation studies from the pilot project will be used to design an optimum field demonstration program for Budget Period #2, which is anticipated to involve the drilling of ten wells using various combinations of vertical and horizontal drilling techniques and to employ selective completions to optimize production performance. The program anticipates that the 3-D seismic data analysis, reservoir simulations, production and geostatistical studies, and additional well drilling will facilitate the unitization of the project area.

RESULTS AND DISCUSSION

Discussion of the results obtained during the first year of the Nash Draw Pool project follows the statement of work that was originally prepared for the project.

I. MANAGEMENT

Strata Production Company (Strata) is the lead organization and the operator of the Nash Draw Brushy Canyon Pool. Strata has put together a diverse team of experts to manage and analyze the Nash Draw Class III project. Strata is responsible for the management and day-to-day operations of the Unit; the Petroleum Recovery Research Center (PRRC) of the New Mexico Institute of Mining and Technology (NMIMT) provides technical support and technology transfer functions; Dave Martin and Associates, Inc., with Drs. Richard Kendall, Earl Whitney, and John Killough, provides reservoir characterization and simulation services; Dr. Bob Hardage of the Bureau of Economic Geology (BEG) provides seismic and geophysical expertise; Territorial Resources, Inc. provides geological expertise; and Pecos Petroleum Engineering, Inc. (P.P.E.) provides reservoir, production, and drilling engineering services. The organizational chart is presented in **Figure 2.**

One challenge to this type of organization is providing communication and coordination between the team members located in a diverse geographic area. Reporting and coordinating of five subcontractors uses advanced technologies to communicate and coordinate efforts. The use of E-mail, the Internet, and high capacity data transfer are used successfully to exchange data and conclusions between each group.

II. DATA COLLECTION

The Nash Draw Brushy Canyon Pool produces from Sections 12-, 13-, and 14-T23S-R29E and Section 18-T23S-R30E, in Eddy County, NM. General characteristics of the Nash Draw Pool are listed in Table 1. Production at Nash Draw Pool is from the basal Brushy Canyon zones of the Delaware Mountain Group of Permian, Guadalupian age. The Brushy Canyon intervals of interest have been subdivided into four mappable stratigraphic units, designated the "J", "K", "K-2", and "L" sands. All are productive and fall within the scope of this project; however, the three main pay zones are the "K", "K-2", and "L" sands.

The data acquisition portion of the project included compiling existing reservoir and engineering data as well as acquiring new data. As part of the project, four new wells have been drilled to date for data acquisition, and the Nash Draw Pool now consists of 15 producing wells and one salt water disposal well **(Fig. 3)**. Multiple sidewall cores were obtained for analysis when each new well was drilled, and, when Well No. 23 was drilled, 203 ft of full core was cut for laboratory analysis. Normal suites of logs were obtained in all of the wells, and a magnetic resonance tool was run in Well No. 23 for comparison to the core analysis.

Compile Core Data - Sidewall Cores - Well Data

Wireline log and core data for all wells within and adjacent to the Nash Draw Pool were compiled. These include data from offset wells provided by Texaco and Maralo, Inc., as well as logs in the E.

Loving Field analog area provided by RB Operating. Whenever possible, the logs were obtained in digital and hard copy formats. Where only hard copy logs were available, they were digitized across the "K", "K-2", and "L" sands for use with the rest of the database. Well No. 1 was hand digitized from microfiche logs. That well was originally drilled as a deeper gas well, and logs across the lower Brushy Canyon interval and the original log files were not available.

Sidewall core data from each well were compiled, and porosity/permeability (ϕ=k) relationships were determined. These relationships were compared to the whole core data and found to be in good correlation. The graphical representation of these relationships is shown in **Figure 4**. Porosity /permeability relationships were determined by performing a regression analysis of the data to determine the best straight-line fit of the data. Core data from the offset and analog wells were calibrated to characterize the uniformity of the zones over the area. As it turns out, the porosity and permeability relationships for each of the basal Brushy Canyon sands in the study area are very uniform from well to well.

Permeability (k_a)/ Porosity Relationships for Each Interval

Porosity/permeability relationships were developed from the sidewall cores and full core analyses. The flow unit variables *a* and *b* are given in Table 2 for the power function:

$$k = 10^{a\phi - b} \qquad (1)$$

A data file was prepared for each well, including digitized logs, perforations, cement programs, tracer logs, completion information, and frac treatments. These data were used to allocate production, estimate drainage areas, determine productivity, estimate saturations for each interval, and prepare data files for reservoir simulation.

Additional log and core data were obtained from wells in the E. Loving Delaware Pool and the Texaco wells southeast of the Nash Draw Pool. These data were analyzed to determine if the zone characteristics were uniform over this general area. As can be seen in **Figure 5**, the core data are in good agreement, especially in the "L" Zone.

Data Wells

Four data wells have been drilled during the first year of the project: Well Nos. 12, 23, 24, and 25. Each well was drilled in different areas of the field to determine the producing characteristics of different field positions. The locations and initial producing rates of the data from each of these wells are shown in Table 3.

Well Nos. 12 and 24 were drilled in prime locations exhibited by good log response and favorable oil saturations, especially in the "L" Zone. Well Nos. 23 and 25 were in areas where the "L" zone was less developed and the water production was higher. The data from the wells have been integrated into the geologic model and adjustments have been made to the reservoir maps. Porosity and permeability data from the sidewall cores taken in Well Nos. 12, 24, and 25, and plugs from the full core in Well No. 23 have been calibrated to the logs and entered into the database.

Whole Core I

A 203 ft whole core was cut from the "J" Zone through the "L" Zone in Well No. 23. Basic core data including porosity, permeability, oil and water saturations, grain density, show description, and lithology description were measured for each foot of core as presented in **Figure 6.**

The core data were used to prepare a transform to correct the log cross-plot porosity to yield a true porosity based on the whole core porosity. Presented in **Figure 7**, the relationship between cross-plot log porosity (logs run on a limestone matrix) and core porosity was determined to be:

$$\phi_{CORR} = (\phi_{x\text{-}plot} - 3.7685)/.848294 \qquad (2)$$

Permeability was plotted against porosity, and a regression analysis was performed to generate equations of the line through the data. These relationships were used to predict the permeability of each zone based on corrected log porosities. Permeability/porosity distributions were prepared for each zone as presented in **Figure 8.**

Generally, the rock is fine to very fine-grained, massive to very thinly laminated. There is some evidence of turbulence as exhibited by sets of low-to-medium angle cross bedding within some of the sand units. Evidence of bioturbation occurs in some of the shaley and silty zones. There is also carbonate clastic debris present in some intervals within the core. Examination of the core under ultraviolet light shows the discontinuous character of the hydrocarbon distribution throughout the reservoir. This correlates with the erratic vertical distribution of calculated oil and water saturations seen in the log analysis.

These data were used to calibrate the logs and determine pay distribution in each zone. By performing a detailed core calibrated log analysis of S_{xo}, S_w and porosity, a detailed analysis was applied to the digitized logs to determine the productivity and the water zones in each interval. The application of porosity/permeability transforms and relative permeability data to each zone yielded flow capacity data for each interval. These data were summed for each layer to be input into the reservoir simulator. A typical example of the input data is exhibited in Table 4. This example depicts the wide variation in the reservoir quality observed from well to well.

Early in the analysis of the sidewall core data, the full core data, and the digitized logs, it became evident that an accurate method of predicting oil productive zones was necessary. Following the sidewall core methodology used to identify pay zones, a method was devised which identified pay zones using core calibrated log analysis. This analysis requires the following steps:

1. Obtain an accurate history of the resistivity of the mud filtrate (R_{mf}) while drilling the pay zones. Obtain accurate R_{mf} values for the mud used while logging. Correct the R_{mf} values to bottomhole temperature using Arp's Equation:

$$\mathbf{R_{mfcorr} = R_{mf@75^{\circ}F} \times (75^{\circ}+7)/(T_{amb}+7+((depth/100\ ft) \times T_{gradient\ per\ 100\ ft}))} \qquad (3)$$

2. Correct porosity values using the cross-plot vs. core porosity transform.

3. Calculate a residual oil saturation (S_{xo}) using the R_{mfcorr} and ϕ_{corr} values in the equation

$$\mathbf{S_{xo} = 1-((F_r \times R_{mfcorr})/R_{XOMSFL})^{.5}} \qquad \mathbf{F_r = 0.81/\phi^2} \qquad (4)$$

4. Calculate an S_{xo} value for each interval in the digitized logs, and sort out the intervals with S_{xo} values greater than the residual oil values in the cores. Since intervals with low or no residual oil saturation have a low probability of being oil productive and intervals with high residual oil saturations have a high probability of being oil productive, this is the first sorting step in the process of productive zone determination. These intervals are potential productive zones and can be processed with other criteria to arrive at an accurate determination of the productive zones.

5. Because of the thin-bed nature of the Delaware Formation, the Deep Resistivity Log is influenced by the zones on either side of a productive zone; this averaging of approximately three feet of zone and invasion leads to low Rt measurements. Low Rt values yield high S_w calculations and pessimistic interpretations of potential productive zones. To compensate for the averaging of thinly bedded reservoirs by the deep resistivity tool, an adjustment factor is used to multiply the observed Rt value by this correction factor to obtain a corrected Rt value (Rt_{corr}). This correction factor can be obtained by two methods: (1) by using Tornado Charts for thin-bed reservoirs, or (2) if a known productive zone is available and the S_w is known, it can be used to calibrate the calculations by finding the correction factor which yields S_w calculations which match actual production and test data. The most often used correction factor at Nash Draw Pool is 1.1, when this correction is multiplied by the Rt value, this yields a Rt value 10% higher than measured. By applying a S_w cutoff of less than 60% to the prospective intervals, only intervals which have favorable relative permeability values will be included in the sample of potentially productive zones.

6. The next sorting criteria is the gamma ray (GR) value from the logging suite. By eliminating intervals with GR values greater than 70 API units, shales and shaley sands are eliminated from consideration as productive zones. Shaley sands have low permeabilities and are seldom productive.

7. The relative permeability data and the permeability/porosity relationships indicate that porosity values less than 11% yield permeabilities below the level that is productive.

Therefore, only zones with a corrected porosity of 11% or greater are included in the final set of intervals which are projected to be productive.

8. Using S_w, ϕ_{CORR}, and other reservoir parameters, an original-oil-in-place (OOIP) value can be calculated for each interval on the digitized log. The OOIP value cutoff is a value greater than 300 bbl/ac-ft.

An example of the final output of the core-calibrated log analysis is shown in **Figure 9**.

In summary, the following sorting guidelines, given in Table 5, were used on the Nash Draw Pool wells to determine productive zones.

Special core analysis included wettability, capillary pressure, relative permeability, thin sections, X-ray diffraction, and Scanning Electron Microscope (SEM) studies. The data indicate a water-wet zone with slightly higher clay content in the "K" Zone. Data used to characterize these zones are presented in the following figures: capillary pressure data (**Fig. 10**), wettability data (Table 6), and water-oil relative permeability (**Fig. 11**).

Special Fluid Swelling Tests (Core #2)
Instead of obtaining a second full-core as planned in the original statement of work, additional reservoir fluid swelling tests were performed to determine possible injectant parameters. Lean gas, carbon dioxide, and nitrogen were studied as possible injection fluids for a pressure maintenance project. From the fluids tested, carbon dioxide exhibits the most favorable characteristics, and separator gas exhibits satisfactory results. Nitrogen has limited solubility in the Nash Draw Pool crude oil and exhibits only approximately half of the oil viscosity reduction of CO_2 and separator gas. These data are summarized in **Figure 12**.

Reservoir Mapping
Production, transmissibility, capillary pressure data, and geological interpretations were combined to arrive at reservoir maps which honor the available data. It was necessary to perform a detailed correlation of the sands in the basal Brushy Canyon sands in order to better understand the lateral and vertical distribution of the reservoirs. Detailed correlations also facilitate a more accurate geological model for use in the reservoir simulation phase of the study. The data were compiled into a spreadsheet for ease of use among all members of the project team. Well data were compiled for each of the wells within and directly adjacent to the Nash Draw Pool for the purposes of constructing the maps listed in Table 7 for the initial structural and stratigraphic model.

The structure and isopach maps have been loaded into Landmark's Stratamodel program. A preliminary 3-D geological layer model has been developed. All surface intersections in the multi-layered model have been eliminated by fine tuning the relationships of the structural surfaces using isopach maps. The model was constructed from the bottom up using the Bone Spring surface as the basal surface.

The sandstone reservoirs of the basal Brushy Canyon sequence lie above the Bone Spring Formation **(Fig. 13)**. The top of the Bone Spring is marked by a regionally persistent limestone varying from 50 to 100 feet in thickness. This surface provides an excellent regional mapping horizon. **Figure 14** is a structure map contoured on the top of the Bone Spring Limestone. Regional dip is to the east - southeast in the area of the Nash Draw Pool. It should be noted that the current structural dip results from an overprint of post-depositional tilting. This overprint is reflected in the reservoir rocks of the Delaware Formation and impacts the trapping mechanism in the sands.

Subsequent to the deposition of the Bone Spring, the Delaware Basin began to fill with a thick sequence of clastic deposits. The deposits consist mainly of sandstone and siltstones with lesser amounts of shale. The environment of deposition is generally considered to be deep water density currents. The materials were deposited episodically through shelf by-pass systems along the shelf-edge margin. In a turbidite scheme, the sands would be considered to be in a distal facies in the Nash area. **Figure 15** is a structure map contoured on top of the basal Brushy Canyon "L" Sand. In general, the dip mirrors that of the underlying Bone Spring Formation. Though the top of the "L" sand can be easily correlated and mapped from well to well, the sands cannot be categorized as blanket type sands from the standpoint of reservoir continuity. Detailed mapping has revealed the complex nature of these sands. Mapping the reservoir engineering data along with the geological data supports the complexity of the reservoirs as well.

Each of the three primary reservoir sands in the study were mapped using a variety of parameters. In the Nash Draw Pool, there appears to be three primary depositional fairways in the "L" sand in which the better reservoir quality rock has been developed **(Fig. 16)**. Net porosity maps combined with log derived net pay and capillary pressure data have been integrated and seem to support this interpretation. **Figure 17** is an isopressure map for the "L" sand. These data represent the height above free water in each of the wells based upon capillary pressure calculations. Comparing this map to **Figure 16**, there appears to be a correlation between pressure distribution and the distribution of sand in the lobes of the "L" sand complex. If these sands were more uniform or laterally continuous, then we would expect to see a more gradational and uniform change in pressure following the east-to-west change in structural dip. The pressure distribution along with the geological interpretation suggests that these reservoirs are more compartmentalized than initially believed. This methodology will be followed for the initial simulations. This model was adopted, in part, because we must have some constraints to the limits of the reservoir for controlling the volumes of fluid held in a particular area and, in part, because corroborating seismic and engineering data, points us in that direction. The "K" sand has been laterally segregated into two primary depositional lobes **(Fig. 18)** in the same manner as the "L" sand.

Further evidence for the complexity of the reservoirs can be seen by examining the logs and core data from the wells. These data show that each of the three primary sands, the "K", "K-2", and "L" sands, are actually composites of stacked "micro" reservoirs. **Figure 13** is a portion of the Litho Density-Compensated Neutron Porosity log from Well No. 15. The interval shown covers the basal Brushy Canyon "K", "K-2", and "L" sands which are the three principle reservoirs. This is the high resolution pass that gives the most detailed look at the reservoir. Of particular note is the highly

laminated, thin-bedded character of the sands. Close examination of each of the gross intervals shows the composite nature of the reservoirs.

Detailed examination of the whole core from Well No. 23 under ultra-violet light shows that these individual "micro" reservoirs appear to be segregated vertically. Hydrocarbon fluorescence is vertically discontinuous from sand lense to sand lense. Each "micro" reservoir may be wet, oil-bearing, or have what appears to be an oil-water contact. They seem to vary from 1 to 4 ft in thickness. This idea of "micro" reservoirs provides insight to explain the difficulty in obtaining a water-free completion in the basal Brushy Canyon sand in the Nash Draw Pool. The obvious next concerns are the factors that control the distribution of the water and oil in these sands and the procedures necessary to quantitatively determine OOIP and expected reserves.

SEM Study

In the SEM study for this project, detailed petrographic, scanning electron microscopy, and x-ray diffraction analyses were performed on thin-section samples from Well Nos.15 and 23. The sands were generally very fine-grained to silt-sized with variable pore geometries. The petrographic analysis of sidewall cores from Well Nos. 15 and 23 described the sands as follows: silty, very fine to fine grained, feldspathic to feldspathic lithic sandstones, angular to subrounded, low to moderate sphericity, and polymictic quartz. Various diagenetic effects are present including quartz and calcite overgrowths, authigenic chlorite, pore-bridging illite, mixed layer illite/smectite, and detrital kaolinite. All of these components work to influence the porosity and permeability of these reservoirs in a negative way. Table 8 shows the composition of the sands in Well No. 23 based upon whole-rock x-ray diffraction analysis. Examples of porosity and permeability occlusion can be seen in **Figures 19, 20, and 21**.

A common concern in Delaware sands has always been the clays content. Fieldwide, consistently higher water saturations are calculated in the "K" sand than in the "L" sand. According to the x-ray diffraction clay analysis, there is a 1 to 2 percent by volume increase of boxwork chlorite filling the pores in the "K" sand than is present in the "L" sand, at least in Well Nos. 15 and 23. The morphology of the chlorite clays is such that they have a very high surface area upon which to bind water. A higher initial, irreducible, water saturation (Sw_{ir}) would have prohibited migration of oil into the already crowded pore spaces. If this relationship exists between the "K" and "L" sands in other wells in the field, then that could explain the low OOIP in the "K" sand.

There has been much conjecture as to why Well No. 23 is such a poor producer as compared to other wells in the field. There is evidence in Well Nos. 15 and 23 that there was a significant loss of critical reservoir porosity and permeability in Well No. 23 as compared to Well No. 15. The porosity and permeability in samples from Well No. 23 are significantly reduced due to framework grain collapse or compaction-dissolution that significantly reduces already small and asymmetrical shaped pore spaces and pore throats. Additional occlusion of the "compressed" pore throats and spaces by various clays, quartz, and carbonates cements also occurs.

Delaware Data

Data from wells in the E. Loving Pool, the Texaco, and the Maralo fields offsetting the Nash Draw Pool have been obtained and analyzed. For example, structure maps and cumulative oil, gas, and water production for the E. Loving Pool is shown in **Figure 22.** Data from all three fields were analyzed and compared to data from the Nash Draw Pool. Core data correlate very well in the "L" Zone, but there is less agreement in the data from the "K" and "K-2" Zones. These data are presented in **Figure 5**.

Quantification

An initial ten layer geological model has been developed for the basal Brushy Canyon sands in order to develop a more detailed reservoir model for simulation. The "K" and "L" sands were divided into four sub-units **(Fig. 23)**. The sands were correlated laterally from well to well in the Nash Unit. Gross isopach, net porosity isopach, and log derived net pay maps were constructed for each of the sub-units of the "K" and "L" sands as well as the "K-2" and "J" sands. The maps were contoured to conform to the overall gross interval isopach maps for the respective pay zones that were used to construct the geological model. Reservoir attributes such as porosity, relative permeability, and oil and water saturations will be distributed vertically and laterally throughout the layers in the simulation model.

Calibration

Using core and log data, each well was calibrated to match production, net pay, and transmissibility. By calculating a kh/m value for each interval, production rates and cumulative production was allocated to each interval. The transmissibility for each layer will be used as input into the reservoir simulation model along with saturation data to determine the producing characteristics of each layer. **Figure 24** shows the transmissibility values used to establish production from the various zones for 14 of the 15 wells in the Nash Draw Pool.

III. SEISMIC ACQUISITION

Compile Seismic Data

A search of available data including and surrounding the Nash Draw Pool yielded no 2-D seismic data. Just prior to the 3-D shoot in May 1996, Texaco performed a 3-D seismic survey south of the Nash Unit. While these data were not available for review, some important parameters were confirmed.

Vertical Wavetest and Vertical Seismic Profile Acquisition

A vertical seismic wavetest and two vertical seismic profiles (VSPs) were recorded in Well No. 25 to aid the characterization of the Nash Draw Pool reservoir system. A single Litton 315 vibrator was positioned at selected surface-source stations to generate these data. Each vibrator weighed 40,000 lbs and was operated at an 80-percent drive level to produce a 32,000-lb ground force during each recorded sweep.

The vibrator stationed 255 ft southeast of the well generated vertical wavetest data during the downward trip of the geophone module and produced a zero-offset VSP image on the upward trip. The vibrator stationed 2,178 ft north of the well generated a far-offset VSP image during the upward

movement of the well geophone. During the downward trip, vertical wavetest data were recorded with the downhole geophone locked at depth increments of 1,000 ft, starting at a depth of 2,000 ft and extending to 7,000 ft. During the upward trip of the borehole geophone, VSP receiver stations were spaced 50 ft apart and covered a vertical aperture extending from 7,100 to 3,000 ft.

Vertical Wavetest

Because no seismic data have been recorded across the Nash Draw Pool, a vertical seismic wavetest was completed in Well No. 25 to determine (1) which vibrator operating parameters produce optimum seismic wavefields for illuminating the reservoir systems between depths of 6,500 and 7,000 ft, and (2) what types of cultural noises exist in the Nash Draw Pool area that can interfere with and deteriorate 3-D seismic reflection signals. These wavetest data were generated by coupling a wall-locked, 3-component geophone to the formation at successive depth stations of 2,000, 3,000, 4,000, 5,000, 6,000, and 7,000 ft in Well No. 25 and recording a series of four wavefields produced with different vibrator operating parameters at each of these depth stations. The specific vibrator parameters that were tested are tabulated in Table 9.

The critical seismic wavefield property that is defined by a vertical wavetest is the signal bandwidth contained in the downgoing seismic wavelet at critical stratigraphic depths. At the Nash Draw Pool, it is particularly important to know which seismic source parameters create the greatest signal bandwidth in the illuminating wavelet that reaches the thin-bed reservoirs at a depth of 7,000 ft. Each of the tested frequency sweeps listed, spans 3.5 octaves, which is an ideal spectral bandwidth for thin-bed detection if all of the frequency components remain in the wavelet during the two-way trip to the target and back to the surface.

The spectra at 3,000 ft define the signal character of the wavelets as they exit from the shallow salt and anhydrite layering and enter the clastic portion of the stratigraphic section. The spectra at 7,000 ft illustrate the signal properties of the wavelets as they interact with the thin-bedded "J", "K", "K-2", and "L" reservoirs.

A key finding of this vertical wavetest is that high-quality seismic data can be recorded at the Nash Draw Pool. Essentially all of the signal components of each test wavelet survived the downward trip to the targeted stratigraphy at a depth of 7,000 ft. This conclusion is demonstrated by the fact that the amplitudes of the sweep frequencies are at least 12 dB (a factor of 16) greater than the noise amplitudes of the frequencies outside of the vibrator sweep band. Since these test wavelets were generated by a single vibrator, the more robust wavelets—which will be produced by the 4-vibrator array that is to be used for the 3-D seismic survey across the Nash Draw Pool—should result in good quality, wideband reflection data.

Based on these vertical wavetest results, the vibrators used to produce the Nash Draw Pool 3-D seismic data were designed to be operated in a linear, 6-120 Hz sweep mode. This sweep range is an extra wide, 4.25 octave signal bandwidth, which should provide excellent thin-bed resolution if the frequency components are not adversely attenuated by the surface receiver arrays used in the 3-D grid or by the 3-D data processing procedures. A linear sweep is preferred over a nonlinear sweep because the spectra show that a linear sweep causes the low-frequency components to have

amplitudes that are about 6 dB (a factor of 4) greater than the low-frequency components of a nonlinear sweep.

Background Noise

Considerable potash and salt mining activity occurs around the Nash Draw Pool. Some of this mining is done as deep as 1,500 ft, and one underground excavation (panel face) extends underneath the north edge of the Nash Draw Pool. The seismic noise created by continuous mining machines, blasting, and mine vehicles—all of which are located at various depths around Nash Draw Pool—can conceivably be large enough to overwhelm the seismic reflection signals produced by surface vibrators. One purpose of the vertical wavetest done in Well No. 25 was to numerically measure the magnitude and spectral character of this cultural noise.

The Nash Draw Pool covers Sections 11, 12, 13, and 14 in Township 23S and Range 29E, and Sections 7 and 18 in Township 23S and Range 30E. Discussions with IMC Global, a local mining company, verified that a mine work area, or panel, extends underneath Section 12. Fortunately, IMC Global plans to do no mining activity at this location during 1996, so this potentially severe noise source will not affect the Nash Draw Pool 3-D seismic data. The nearest active mine is in Section 5 at a depth of 600 ft. The noise sources at this location involve underground blasting along panel faces during two 30-minute time periods each day as well as considerable underground vehicular traffic. The nearest continuous mining machines are working at a depth of 500 ft about 3 miles north of the Nash Draw Pool. Each machine has a large number of carbide bits secured to a heavy, metal cylinder, 10 ft long and 3 ft in diameter, that continuously rotates to dig material away from the panel face of that mine. These machines run 8 to 10 hours per day and, while operating, should generate a high level of background noise within the seismic signal band. One objective of the vertical wavetest was to determine if any of these remote noise sources interfere with seismic signals inside the Nash Draw Pool.

Measurements of the background noise were made in Well No. 25 at depths of 2,000, 3,000, and 7,000 ft and compared to the signal strength produced by a single Litton 315 vibrator. The signal-to-noise measurement made at a depth of 2,000 ft is the most definitive because this downhole receiver station is the shortest straight-line distance to the mining noise and because that receiver station is in the same salt/anhydrite layer as the mining activity. These data document that the amplitude of the background noise is approximately 17 to 26 dB (a factor of 50 to 400) less than the amplitude of the vibrator signal. Consequently, the mining activity around Nash Draw Pool should not adversely affect the vibroseis-generated 3-D seismic data acquired there. This conclusion is further substantiated by the VSP data that were acquired in Well No. 25 immediately following this vertical wavetest.

VSP Acquisition

Two vertical seismic profiles were recorded in Well No. 25. One Litton 315 vibrator was positioned 255 ft southeast of the well (127° azimuth) to produce zero-offset VSP data, and a second Litton 315 vibrator was stationed 2,178 ft north of the well (349° azimuth) to create a far-offset VSP. Four vibrator sweeps were summed from the zero-offset vibrator; six sweeps were summed from the far-offset source. Each vibrator had Advance II electronics and produced a phase-locked ground

force of 32,000 lbs. A linear, 12s, 8 to 96 Hz sweep was used for the VSP imaging. A gimbaled, 3-component, 10 Hz, LRS 1300 geophone tool was locked to the formation to record the downhole data. Receiver stations started at a depth of 7,100 ft and were spaced at 50-ft intervals up to a depth of 3,000 ft. Above 3,000 ft, checkshots were recorded at depths of 2,500, 2,000, 1,500, 1,000, and 500 ft from the zero-offset vibrator only.

The zero-offset data and the upgoing reflection wavefield extracted from this zero-offset profile confirm that good quality seismic reflection signals should be acquired over the Nash Draw Pool. Specifically, the stratigraphy associated with the reservoirs near the bottom of Well No. 25 generates measurable and interpretable reflection signals, and reflections generated a considerable distance below the bottom of Well No. 25 are also observed. Equally important, there is no evidence of noise contamination from the nearby mining activity.

This far-offset profile provides the same encouragement as the zero-offset data, thus, it should be possible to record wideband 3-D seismic data over the Nash Draw Pool. These offset VSP data are particularly insightful because the travel paths involved in this far-offset VSP geometry are approximately the same as many of the travel paths that will occur during the 3-D seismic survey. The fact that good-quality reflection data are created by a single 40,000-lb vibrator operating at an 80-percent drive level suggests that particularly good-quality 3-D data will be generated by the array of four 50,000-lb vibrators that will be used for the Nash Draw Pool 3-D data acquisition. The far-offset VSP data verify that reflection signals should be obtained from depths considerably below the bottom of Well No. 25 (that is, deeper than 7,100 ft, KB) and that there should be minimal noise contamination from the surrounding mining activities.

The zero-offset and far-offset images extracted from the VSP data agree at the receiver well. The zero-offset image has to be shifted up by 8 ms to optimize the waveform character tie, which indicates that the seismic imaging velocities at Nash Draw Pool will be anisotropic, that is, the horizontal velocity (which affects the far-offset VSP image) is greater than the vertical velocity (which controls the zero-offset VSP image). Velocity anisotropy is a common problem in 3-D seismic imaging, and these VSP data results will help 3-D data processors set bounds on the velocities that will be used to stack and migrate 3-D data over Nash Draw Pool. The good waveform character tie between the zero-offset and far-offset VSP images confirms that good-quality VSP data were recorded and that valid VSP data processing procedures were used to create the images.

VSP Data

One advantage of VSP data recording is that the image that is produced can be displayed as either a function of seismic two-way traveltime, so that it can be correlated with surface-recorded 3-D seismic data, or as a function of stratigraphic depth to better correlate with wireline-measured log and core data. The Nash Draw Pool far-offset VSP image is in a depth format to illustrate this latter VSP imaging option. Also shown in this display is the velocity-layer model that was used to calculate the reflection point coordinates that create the far-offset VSP image. This velocity layering was constructed from the zero-offset VSP data and shows that there is a significant velocity inversion at 3,000 ft where the high-velocity salt and anhydrite section converts to a lower velocity clastic section. Because there is no significant structural dip down to the base of Well No. 25 (~7,100

ft, KB), a horizontally-layered velocity model could be used to calculate the subsurface coordinates of each VSP reflection point.

The VSP reflection events shown above 7,100 ft are correctly positioned in depth because the downhole geophone actually occupied the depth stations that span these reflectors, thus a rigorous time-to-depth relationship can be defined that allows the VSP image between 3,000 and 7,100 ft to be expressed either in traveltime coordinates or in depth coordinates. The reflection depths below 7,100 ft are approximations because no geophone reached those depths to define how to equate seismic traveltime to stratigraphic depth. Below 7,100 ft, the seismic P-wave velocity is assumed to have a constant value of 17,000 ft/s, and this assumption is only an approximation of the correct velocity behavior below the bottom of Well No. 25. Still, the far-offset data show that a wavefield from a single 40,000-lb vibrator can image reflectors that appear to originate more than 4,000 ft below the deepest VSP receiver, which means that the reflectors can be assumed to be 11,000 ft deep, or deeper. The deepest event should be at a depth of 11,000 ft or more.

By measuring the vertical distance spanned between successive peaks (or successive troughs) of the VSP image, an interpreter can determine the magnitude of the dominant wavelength that exists in the image at any particular stratigraphic depth. Even though the seismic wavefield contains a wide spectrum of wavelengths, it is the dominant wavelength that controls the vertical resolution of the data, and by definition, the dominant wavelength is that distance between successive reflection peaks (or successive troughs) in the final image that is available for interpretation. Examination shows that at the targeted "J", "K", "K-2", and "L" reservoirs just above 7,000 ft, the dominant wavelength is about 140 ft. Stratigraphic units having a thickness greater than one-fourth of this wavelength (that is, units that are 35 ft thick or more) can be resolved with these VSP data, meaning that a distinct reflection peak and/or trough will occur at the top and base of the unit. Units that are thinner than 35 ft cannot be resolved in this particular VSP image, but they can be detected and mapped. The term detection means that even though there is not a distinct reflection peak or trough at the top and base of the unit, the presence of the unit still creates a measurable and detectable change in the reflection waveform.

Efforts will be made to shorten the dominant wavelength in the 3-D seismic data by expanding the vibrator sweep from 8-96 Hz (as in the VSP image) to 6-120 Hz. This change from a 3.5 octave to a 4.25 octave sweep range should shorten the dominant wavelength from 140 ft to about 120 ft and aid thin-bed resolution.

The log-interpreted depths of the tops of the "J", "K", "K-2", and "L" reservoirs in Well No. 25 are 6598, 6639, 6737, and 6765 ft, respectively, where all depths are measured relative to KB. Two of these reservoirs, "K" and "L", are of particular interest in Well No. 25 because the "K" reservoir is well developed, but the L reservoir is not. The depth positions of the "K" and "L" reservoirs are labeled in the VSP image in **Figure 25**, together with the position of the Bone Spring Limestone that is immediately below the "L" Sandstone.

An important insight provided by these VSP data is that the closely spaced "K" and "L" reservoirs are defined as separate seismic features when the illuminating wavelet has a bandwidth of at least

8-96 Hz. The VSP image shows that the "K" reservoir creates a reasonably strong reflection peak at Well No. 25, where as the "L" reservoir generates a weaker reflection trough. Seismic modeling will be required to establish if there is a definitive correlation between reservoir properties of the "K" and "L" units and seismic reflection amplitude. However, seismic modeling at Nash Draw Pool is handicapped because no sonic logs are available for calculating synthetic seismograms.

The reflection character of both the "K" and "L" events, (**Fig. 25**), as it appears at the well (the right most trace of the image), changes significantly about 100 ft north of the well (the 5th and 6th trace from the right side of the VSP image), which implies that some type of variation in the reservoir system occurs at this location. Again, seismic modeling, or the careful integration of geologic control with 3-D seismic interpretation, will be required to establish the stratigraphic and rock-property messages implied by such variations in seismic facies. The VSP image also shows that the reflection trough associated with the "L" reservoir has a slightly greater amplitude (brightens) at location A, about 200 to 300 ft north of the well, and that at location B about 500 to 650 ft north of the well, where the amplitudes of both the "K" reflection peak and the "L" reflection trough become noticeably stronger. These reflection amplitude variations are direct indicators of stratigraphic changes, or facies changes, or both, within the "K", "K-2", and "L" reservoir systems. The interpretation challenge is to establish a definitive correlation between areal distributions of these variations in seismic reflection character and areal maps of geologic and engineering properties of the reservoirs. These variations in the reflection amplitude of the VSP image are an early indication that considerable changes in 3-D seismic reflection attributes will occur across this heterogeneous reservoir system.

The far-offset VSP data were processed so that the stacking bins used in the image construction had a horizontal width of only 20 ft. Consequently, the trace spacing is 20 ft. Much of the lateral variation in reflection waveform character that occurs in this image is due to the fact that the VSP stacking bins (that is, the trace spacings in the image) have a small width. The stacking bins that were to be created in the original 3-D seismic geometry that was sent out for bids covered an area measuring 110 x 110-ft. In such a geometry, each 3-D seismic trace would thus have been equivalent to the trace that would be created by summing five adjacent traces in the VSP image. In the 3-D image resulting from this acquisition geometry, the stratigraphy extending 870 ft north of Well No. 25 would be defined by only eight traces; whereas, that same stratigraphy is defined by forty-four traces in the VSP image.

One important result of this initial VSP imaging effort is that it revealed that smaller stacking bins would have to be created in the 3-D seismic data volume if the 3-D data are to show lateral changes in the reservoir of the size seen in the VSP images. Consequently, as a result of the VSP work, the Nash Draw Pool 3-D seismic grid has been redesigned to produce acquisition bins measuring 55 x 110-ft. During data processing, a trace interpolation will be done in the source line direction to create interpretation bins measuring 55 x 55-ft.

3-D Seismic Data Acquisition at Nash Draw Pool

Dawson Geophysical began deploying receiver lines across Nash Draw Pool on May 29, 1996. Wavetesting was done on May 30, and 3-D data recording started May 31. A total of 917 source points were recorded to create a 3-D coverage across an area of 7.875-mi^2. A high production rate of 160 source points per day was achieved as the result of thorough pre-planning, an efficient 43-man work crew, and state-of-the-art seismic equipment.

All equipment that Dawson Geophysical used in the Nash Draw program was less than one year old and well maintained. Dawson supplied nine excellent vibrators, which allowed two 4-vibrator source arrays to be in the field with one vibrator in a standby, backup status. By using two vibrator arrays and a backup unit, there was no lost production time due to stuck vehicles, flat tires, lengthy drive-around time to get to the next source line, or electronic/mechanical breakdowns. The two vibrator arrays operated on source lines that were usually separated a distance of one mile or more.

All of the vibrators were state-of-the-art Mertz Model 18DH623 units with Pelton Advance II electronic control. Four of the vibrators had been in service for 12 months (a short operating life for a vibrator), and these four units represented the oldest equipment that Dawson used at Nash Draw Pool. Each Model 18HD623 vibrator had a total weight of 58,000 lbs, a hold-down weight of 52,500 lbs, and was operated at an 80-percent drive level to apply 42,000 lbs of ground force during each recorded sweep. Because all of the vibrators were in good mechanical condition and had Advance II electronics, they phase-locked to the specified ground-force sweep-signal with great fidelity.

Ideally, 3-D seismic data should be recorded using regular spacings between source lines and receiver lines. However, the large salt lake in the north-central portion of Nash Draw Pool had a significant impact on the 3-D acquisition geometry and caused the source-receiver grid to assume the irregular configuration. An archeological team found that this lake area was surrounded by numerous ancient camp sites and that several of these archeological sites were traversed by one or more source or receiver lines of the original survey grid. The archeological search was confined to strips that extended 50 ft in both directions away from each surveyed source and receiver line, which accounted for all of the areas where seismic vehicle traffic might occur.

While in the field, the archeological team prepared hand-drawn sketches that showed the size and shape of the area encompassed by each cultural site and the locations of key artifacts found within the boundary of each site. In general, receiver lines were not altered by any of the archeological constraints because cable trucks could drive around each relic site while field personnel deployed the data transmission cable and geophone strings by walking through the area, which was a permissible intrusion. In contrast, source lines were affected by the archeological sites, and several source stations had to be moved or abandoned to prevent vibrators from driving over any relics. The final source-receiver line geometry that was used, once all of the archeological constraints were imposed, is shown in **Figure 26.**

Various surface constraints forced three different source array geometries to be used during the recording of the Nash Draw Pool 3-D data. An important requirement of the pre-survey wavetesting was to determine if any one of these three distinct geometries created wavefields that exhibited any kind of fundamental difference in signal quality or frequency bandwidth. The preferred source array that was employed at approximately 90 percent of the source stations was four vibrators that were

positioned inline with the pads separated 55 ft. For sweep 1, the pad of vibrator 2 was 5 ft ahead of the source flag. All four vibrators moved forward 9 ft for each successive sweep, causing the pad of vibrator 3 to be 5 ft short of the source flag for sweep 6, the last sweep recorded at each source station. After sweep 6 was recorded, there were 24 inline pad imprints, spaced 9 ft apart, spanning a distance of 220 ft, and symmetrically distributed about the source flag. The summation of six sweeps with this array geometry created a wavefield equivalent to that which would have been created by one sweep of 24 inline vibrators symmetrically distributed about the source flag with the pads separated by 9 ft.

An important step of the pre-survey planning was a closeup, on-site inspection of almost all of the 917 surveyed source stations. This inspection showed that there were several source stations where surface conditions and/or cultural constraints would not allow an inline moveup of vibrators as required by the preferred source array geometry. The purpose of the pre-survey wavetesting was to determine what types of source array geometries should be used at these restricted sites.

Because conditions at some source stations would not allow much vibrator movement, two additional source geometries were tested. These alternate source arrays required that the vibrators position themselves inline with, and symmetrically disposed about, the source flag, with the pads 55 ft apart, and that the vibrators remain stationary for all six sweeps. This source option is a good approximation of the preferred moveup concept previously described.

The third source geometry was a fixed box pattern. In this geometry, four vibrators were positioned in a square, box-like distribution about the source flag with the pads separated a distance of 35 to 55 ft. Less than 10 percent of the source stations required that the vibrators be positioned in either a linear, no-moveup geometry or a box geometry.

Wavetest records generated by these three source arrays and the source-receiver geometry used to record the test records established that any one of the three source arrays could be substituted for the other and not significantly alter the basic character of the seismic wavefield. Because of this wavetesting effort, there was no justification for moving any of the non-standard source stations to new coordinates where the basic inline moveup array could be implemented or to expend any effort to modify surface conditions at these non-standard stations.

The seismic acquisition at Nash Draw Pool began at the east side of the 3-D grid and progressed westward. The fundamental recording geometry was a 10-line swath. In a 10-line recording swath, there are five active receiver lines to the left of the source station that is being recorded and five active receiver lines to the right. Once the six easternmost receiver lines were deployed (lines 501 through 506), the data acquisition began with the two sets of vibrators successively occupying all of the source stations between line 501 and line 502. This 6-line recording swath created the western half of the desired 10-line swath. One set of vibrators worked the northern source stations along this source strip between lines 501 and 502; the second vibrator array worked the source stations in the southern half of the source strip.

When the vibrators moved west to occupy the source stations between receiver lines 502 and 503, a seventh receiver line (507) was added to the recording swath. When the vibrators occupied source stations between receiver lines 503 and 504, an eighth receiver line (508) was added to the swath. The first, full 10-line recording swath was achieved when the vibrators progressed westward far enough to generate data at the source stations between receiver lines 505 and 506.

The Nash Draw Pool 3-D seismic data were recorded using an I/O System 2 acquisition system. Commonly, this system is referred to as a 2000-channel recorder (actually 2016 channels). However, this large 2000-channel capacity is available only if the data sampling rate is 4 ms. Because the Nash Draw program was designed so that the reflection signals would have frequency components up to 100 Hz, a sample rate of 2 ms was used. This increased data sampling requirement reduced the system capacity to 1008 data channels.

A complete north-south receiver line across the Nash Draw Pool contained 108 receiver stations (108 stations x 110 ft = 11,880 ft). Consequently, a 10-line recording swath slightly exceeded the I/O System 2 limit of 1008 channels if all ten lines in the swath contained the full complement of receiver stations, which would create a total of 1080 data channels. Because the receiver lines in the central portion of the grid were shortened due to the presence of the salt lake, most of the 10-line swaths used at Nash Draw Pool were able to utilize the full north-south extent of all receiver lines within the swath and still not exceed the 1008-channel limit, because one or more of these short receiver lines was usually incorporated into each recording swath. When a swath did have more than 1008 receiver stations, an appropriate number of receiver groups were omitted at the extreme north and south ends of a few lines to reduce the number of active receiver stations to 1008.

The efficiency of the Nash Draw Pool seismic data acquisition was exhibited in the following example. Two vibrator source arrays working within a source strip in the central part of the Nash Draw project were on source lines that were one mile apart. The south vibrator array was at the indicated source station on source line 249; the north vibrators were at the source station identified on source line 225. The two vibrators were working inside the same north-south strip of source stations, specifically those source stations between receiver lines 513 and 514. However, it was not required that the vibrators always be in the same north-south strip of source stations. For example, the north vibrators could be at source stations between receiver lines 514 and 515 and the south vibrators at source points between receiver lines 513 and 514, which would require that two different 10-line recording swaths be used. The I/O System 2 software would automatically and quickly activate the correct-10-line swath for each vibrator group whenever the active source station was identified. By using two vibrator arrays and a versatile I/O System 2 recorder, the Nash Draw Pool 3-D data were recorded, correlated, and plotted at a rate of 3½ to 4 minutes per source station, resulting in a high production rate of 160 source stations (on average) per 10-hour day.

Data from a total of 917 source stations were acquired during the Nash Draw Pool 3-D program. These reflection data were recorded by a multi-line recording swath (usually a 10-line swath), creating a seismic display of 700 to 1000 traces for each of these 917 source stations. Each of these

field records was plotted approximately one minute after the data were recorded, and these plots were examined to confirm data quality, identify noise problems, and verify system performance.

The small display scales allow only the general features of the data to be seen; much more detailed reflection character could be examined in the large-scale plots that were made onsite with the field recorder. Expanded views of single-line records illustrate the general signal-to-noise character of the field data. These records illustrate how good-quality vibroseis data can overwhelm typical cultural noises that exist in a producing oil/gas field. The worst noise sources that were encountered inside the Nash Draw Pool 3-D survey area were a large, cross-county gas compressor station near receiver line 507 and the pump-jack motor at Well No. 24, this motor being almost directly atop receiver line 514. The vibroseis correlation process, when coupled with the robust reflection wavefields generated by an array of four Mertz 18HD623 vibrators, overwhelms the noise and produces high-quality reflection responses for approximately 2 seconds after the first-break arrivals. The noise from the compressor station and the pump-jack motor builds back to a high level after 2 seconds because only weak reflection signals occur at these long traveltimes. The resulting signal-to-noise ratio in these field records was quite high considering how close these noise sources were to receiver lines 507 and 514. Specifically, Well No. 24 was only 40 ft from receiver line 514, and the compressor station was only 200 ft from line 507.

The third dominant cultural noise inside the Nash Draw Pool 3-D grid was the heavily traveled county road. Receiver line 507 was deployed immediately next to this rough, gravel road; the geophones being less than 10 ft from the edge of the road bed. Numerous large tank trucks and a variety of other vehicles traveled the road daily, yet that vehicle traffic never seriously deteriorated the signal-to-noise character of the data recorded by line 507 or any other nearby receiver line.

The key requirement for a successful implementation of 3-D seismic data into a reservoir characterization project is to ensure that good-quality seismic field records are provided to the processing shop that is to produce the 3-D image of the reservoir system. That critical first-step requirement has been accomplished at Nash Draw Pool because the 3-D field data exhibit a high signal-to-noise ratio and a broad frequency bandwidth that should provide a migrated image having frequencies from 10 to about 100 Hz.

The fundamental objective of the processing sequence that was applied to the Nash Draw Pool 3-D seismic data was to create accurate 3-D images of the thin-bed Brushy Canyon reservoirs systems that need to be characterized. A secondary objective was to create data files at various stages of the processing sequence that can be made publicly available during the technology transfer phase of the project.

Spectral balancing (or spectral enhancement, as some seismic processors refer to the technique) was perhaps the most important prestack computation done to improve the interpretive value of the Nash Draw Pool 3-D seismic data. Spectral balancing is done quite early in the processing sequence, and is a demanding computational procedure. Lengthy computation time results because the process is a prestack calculation that is applied on an individual field trace by field trace basis to every data sample of every field record. In the case of the Nash Draw Pool 3-D data, the spectral balancing

computation required 30 hours of continuous runtime on a Sun SPARC 10, which is a significant demand on computer resources. The objectives of spectral balancing are to cause all of the traces of every field record to have equivalent frequency spectra, and for these spectra to exhibit a reasonably flat response over the widest possible bandwidth without introducing unacceptable noise into the data. A hypothetical example of the concept where the amplitudes of all of the frequency components of the wideband spectrum shown in the top display are altered so that the energy content is uniformly distributed across the complete frequency range of the data; that is, the bottom spectrum is balanced across the complete signal bandwidth after the spectral enhancement process is completed. Spectral balancing is done in successive, narrow, frequency passbands such as those indicated by the twelve frequency intervals, the computation is not done in the frequency domain as one might assume, but is implemented in the time domain following the procedural path(s).

Analysis of the Nash Draw Pool seismic field records showed that the reflection signal amplitudes diminished above 100 Hz, even though the vibroseis sweep extended to 120 Hz. Consequently, spectral balancing was not done to frequencies above 100 Hz so that excessive noise would not be introduced into the data. The specific filters used to spectrally balance the Nash Draw Pool data had a passband width of 10 Hz and rolloff widths of 4 Hz at both the low end and the high end. A linear rejection of 12 dB occurred across the 4-Hz-wide low-cut and high-cut bands. The first full-pass frequency was set at 10 Hz, and the low-end rolloff for this filter extended to the starting frequency (6 Hz) of the vibroseis sweep. At the low end of filter 1, the linear cutoff design attenuated the 8-Hz component by 6 dB and the components from 0 to 6 Hz by 12 dB. At the high end, the 22-Hz component was suppressed by 6 dB and the components from 24 to 120 Hz were reduced by 12 dB.

In some spectral balancing computations, the full-pass portions of adjacent filters are allowed to overlap, but for the Nash Draw Pool data, the full-pass portion of each filter was defined so that it did not overlap the full-pass portion of adjacent filters. The filters did overlap in 50-percent of their linear rejection bands. One appealing feature of this spectral balancing technique is that the procedure tends to be rather forgiving as to how the overlap regions of adjacent filters are designed.

The full-pass portion of the sixth, and last, bandpass filter in the spectral balance suite extended from 80 to 90 Hz. For this filter, the 78-Hz component of the data was attenuated by 6 dB and the components from 0 to 76 Hz were attenuated by 12 dB. At the high end, the 92-Hz component was suppressed by 6 dB, and the components from 94 to 120 Hz were suppressed by 12 dB.

This filter suite resulted in computation loop A being executed six times for each data trace of every Nash Draw Pool record. Because the Nash Draw Pool data were sampled at 2 ms and the record length was 3 s, computation loop B generated 1,500 trace amplitude scaling factors, one for each data sample of the trace being processed, during each execution of computation loop A.

Spectral balancing analyses were done on several Nash Draw Pool records to establish appropriate parameters that should be applied to the full 3-D data set. Typical of field records used in this testing, a major part of the data is dominated by high-amplitude, low-frequency ground roll components that overwhelm reflection signals. The objective of the spectral balancing step was to adjust the amplitude contributions of all of the frequency components in the wavefield to the same level so that

broadband reflection signals could compete with the more dominant noises, particularly with the low-frequency ground roll. The appearance of these data after spectral balancing shows that this processing objective was achieved; specifically, the ground roll noise was greatly subdued and the numerous continuous, broadband reflection events extended across the records after the spectral balancing filters were applied to the data.

The spectral enhancement that occurred both inside and outside of this ground roll domain was especially beneficial for thin-bed interpretation. Data windows positioned outside of the influence of the ground roll; spectral analyses were done in these windows to verify how the spectral balancing process altered the energy spectrum of the data in relatively noise-free areas of a typical seismic field record. The spectral distribution of seismic energy in the original field record is limited to the frequency range 6 to 120 Hz, since that was the sweep range of the vibrators that generated the wavefields. However, the energy was not evenly distributed across this frequency range, and the spectrum exhibited undesirable peaks and troughs. After spectral balancing, the spectrum calculated in the same data window had a flatter, more uniform energy distribution. The imaging wavelet associated with this smoother wavefield spectrum will provide a better resolution of the thin-bed reservoirs at Nash Draw Pool than will the wavelet having the more erratic spectrum associated with the raw data.

3-D Seismic Data Processing

The Nash Draw Pool acquisition geometry was structured on the concept of a receiver station spacing of 110 ft and a source station spacing of 220 ft, resulting in acquisition bins that had dimensions of 55 ft in the inline direction and 110 ft in the crossline direction. The objective of the processing was to produce a 3-D image based on 55 x 55 ft bin resolution; however, the data were first sorted into 110 x 110 ft bins for static calculations and velocity analysis.

The ultimate objective of a static calculation is to determine the static corrections that need to be applied to the traces generated at each source station and to determine the static corrections that have to be applied to the traces recorded at each receiver station, to an accuracy that is less than the time sampling of the data, which would be less than 2 ms for the Nash Draw Pool data. The static adjustments converged to this processing objective by reducing to a magnitude of 1 ms or less after only two calculations of surface-consistent residual statics and one calculation of trim statics, which indicates the high signal-to-noise character that existed in the data following spectral balancing.

Stacking velocity analyses were done on every fifth east-west crossline, that is, at intervals of 550 ft across the 3-D grid. Along each of these lines, stacking velocities were determined at every thirtieth common reflection point, or at intervals of 1,650 ft. These velocity determinations were done twice, once after the first residual statics calculation and once following the final trim statics calculation.

This 550 x 1,650 ft spatial sampling of the stacking velocity field was interpolated to produce a velocity function in every 110 x 110 ft bin across the 3-D grid, with a velocity value being defined at vertical time intervals of 50 ms in each of these functions.

Workstation inspection of the stacking velocity cube verified that no spurious velocities existed and that the calculated velocities were a realistic depiction of the lithologic sequence that was imaged. Inspection of these section views of the velocity data shows that in the lateral direction, the stacking velocities varied by only a modest amount, which meant that post-stack time migration would be adequate for correctly imaging the subsurface stratigraphy. The more expensive and more demanding process of prestack depth migration is required only when stacking velocities exhibit a significant lateral variation across the space that is to be imaged. Prestack depth migration was not necessary at Nash Draw Pool because the same laterally smooth velocity behavior was observed on all profiles extracted from the Nash Draw Pool stacking velocity cube.

Poststack time-migration velocities are defined as being some constant multiple of stacking velocities. Typically, a series of time-migrated seismic images are created by using migration velocities that are 80, 90, 100, 110, and 120 percent of the stacking velocities. The correct migration velocity is chosen by visually inspecting these images. Although this procedure for selecting the proper migration velocity is subjective, it produces excellent results. The best choice for migration velocity at Nash Draw Pool was found to be 100-percent of the stacking velocities. Thus, the 3-D migration velocity cube is quite similar to the 3-D stacking velocity cube.

The manner by which seismic reflection amplitude varies with angle of incidence at a target boundary can provide considerable insight into the lithological and pore-fluid properties that exist at that boundary. To allow angle-dependent interpretation to be done at Nash Draw Pool, the 3-D seismic data were processed in a unique way to analyze the thin-bed turbidite reservoirs within the Nash Draw Pool. Specifically, the data were processed to create a full-angle volume that contained all trace offsets, a near-angle volume that contained traces with only small offsets, and a far-angle volume that contained traces having only large offsets. By using all three seismic images in the reservoir interpretation, there is an increased probability that lateral facies changes and variations in reservoir pore fluid can be detected.

To create these three seismic data volumes, it was necessary to define the manner by which the incidence angle of the illuminating wavefield varied with depth as the surface-generated seismic wavefields traveled downward to the deepest reservoirs at a depth of 7,000 ft (approximately). The objective of this wavefield analysis was to establish an empirical relationship between the incidence angle at any depth and the offset distance between the source and receiver involved in that particular reflection raypath. This incidence angle behavior was then used to sort the 3-D data according to offset so that only near-angle, far-angle, or full-angle traces were involved in the imaging process.

To calculate the variation of incidence angle with depth, it was necessary to first create an accurate velocity-layer model for the Nash Draw Pool stratigraphy using the velocity information provided by the VSP data recorded in Well No. 25. The VSP-based velocity structure determined at Well No. 25 generated the 2-D layer model of Nash Draw Pool stratigraphy that was constructed and used for the required raypath calculations.

This 2-D velocity layer model was assumed to be accurate for the entire Nash Draw Pool, an assumption which is supported by the laterally consistent velocity behavior illustrated by the seismic

data. The subsurface raypath behavior for any combination of source-receiver offsets within the Nash Draw Pool 3-D grid can thus be calculated using this single earth model. By analyzing a large suite of these raypaths, the incidence angles at which the seismic wavefields impinged upon each layer boundary was determined. The results of these raypath calculations shows the relationship between incidence angle and source-receiver offset as a function of vertical two-way traveltime. The incidence angles defined by this suite of functions were used to segregate the 3-D field traces into subsets of near-angle traces and far-angle traces, and these traces produced the full-angle, near-angle, and far-angle image volumes.

Ever since seismic data first began to be recorded, geophysicists have relied on the lateral coherency between traces to make important processing decisions, such as determining static corrections and choosing stacking velocities, and to interpret the geological significance of reflection events. In 1995, Amoco described a technology referred to as a coherency cube which has attracted considerable attention throughout the industry. This coherency cube technology numerically quantifies the lateral trace coherency that interpreters use to make geologic decisions and displays these coherency numbers in an easily understandable format. To ensure that the latest seismic technology was used in evaluating the Nash Draw reservoirs, all of the 3-D seismic data volumes created during the data processing sequence were converted to coherency cubes.

The parameter that is calculated to create a coherency cube is termed semblance in the geophysical literature, although the term multichannel coherence is sometimes used. For a set of M seismic traces, the semblance S (or lateral coherency) exhibited by the traces at time sample k is defined as:

$$S(k) = \frac{\sum_{j=k-\frac{N}{2}}^{k+\frac{N}{2}} \left[\sum_{i=1}^{M} f_{ij} \right]^2}{M \sum_{j=k-\frac{N}{2}}^{k+\frac{N}{2}} \sum_{i=1}^{M} \left(f_{ij} \right)^2} \qquad (5)$$

where f_{ij} is data sample j for trace i, and N is the length of the data window over which the coherency is measured. If the M traces in Equation 1 are identical, the semblance S is unity. If some of the M traces have a different waveshape within the analysis window, the value of S is less than unity. The lateral coherency decreases as the amount of waveshape variation increases among the M traces. Continuous reflection events with a consistent reflection waveshape create high values of S. In contrast, S diminishes at faults and stratigraphic pinchouts because these geologic conditions create variable reflection waveshapes over a span of several adjacent traces. The importance of a coherency cube is that a 3-D volume of these S values allows structural and stratigraphic discontinuities to be numerically defined and displayed; these geologic features being defined by continuous, narrow trends of minimum coherency (S) values. The coherency cubes that were created in this processing strategy should help interpret the lateral continuity of the Nash Draw Pool thin-bed reservoirs.

Several different types of 3-D data volumes were built at various stages of the Nash Draw Pool seismic processing sequence (Table 10). Some of these volumes had internal stacking bins measuring 110 x 110-ft; others consisted of 55 x 55-ft bins. The volumes based on 55 x 55-ft bins contain four times as many data traces as the volumes built from 110 x 110-ft bins and thus require four times as much disk space when loaded into interpretation workstations. Note that these storage requirements are based on the assumptions that the data exist as 32-bit data words and that the trace length is 3 seconds. The storage requirements can be reduced if the trace length is reduced to 2 seconds. The Brushy Canyon reservoirs are positioned at 1 second (approximately) and would not be affected by such a decimation.

Preliminary amplitude maps are shown in **Figures 27 and 28.** High reflection amplitudes occur at the better producing wells and low reflection amplitudes occur at the poorer producers, so seismic amplitude attributes appear to be quite valuable for identifying productive reservoir intervals.

Summary of First Year Geophysical Activities

Considerable geophysical activity occurred in year one of the Nash Draw field study. The critical component of the geophysical data base that had to be generated for the reservoir characterization effort in year one was a high-quality 3-D seismic survey over the Nash Draw Pool. However, to properly prepare and plan for this 3-D seismic effort, a vertical seismic wavetest had to first be done in the centrally located Well No. 25. These vertical wavetest data characterized the seismic noise induced by surrounding subsurface mining and defined the optimum vibroseis parameters that should be used to generate 3-D seismic wavefields. Concurrent with this wavetest, vertical seismic profile data were also recorded in Well No. 25 to establish a precise depth-to-time conversion function for interpreting the 3-D seismic data and to produce a first-look seismic image of the targeted thin-bed "K" and "L" turbidite reservoir. These VSP data were instrumental in setting the size of the stacking bins used in the subsequent 3-D seismic program.

Using the information provided by this vertical wavetest and vertical seismic profile, a 3-D seismic survey was designed and implemented. The recorded data were of quite high quality due to the extensive pre-survey testing and planning. The rigorous processing sequence that was applied to the 3-D field records produced a valuable image volume of the heterogeneous turbidite reservoirs that are the focus of the Nash Draw study.

The interpretation of the 3-D seismic image was initiated late in year one. Structure, isochron, and seismic attribute maps have been produced. Seismic amplitude attributes appear to be quite valuable for identifying productive reservoir facies, with high reflection amplitudes occurring at the better producing wells and low reflection amplitudes at the poorer producers.

The geophysical activity that will occur in year two will focus on optimizing the interpretation of the thin-bed reservoirs in the Nash Draw Pool, defining compartment sizes and shapes for reservoir simulation studies, and preparing technology transfer products. State-of-the art investigations that will be pursued include: (1) comparisons of near-trace and far-trace 3-D image volumes to determine if fluid-sensitive amplitude effects exist in the 3-D data, (2) inversion studies that will produce pseudo sonic and density logs from the 3-D seismic data, (3) reflection waveform continuity investigations that should identify subtle reservoir compartment boundaries, and (4) geostatistical correlations between seismic attributes and reservoir properties.

Technology transfer efforts will concentrate on writing technical papers that will be submitted to international, peer-reviewed geophysical journals and on creating a 3-D seismic short course that will be offered at two locations, Roswell, NM and Midland, TX. Consideration is also being given to creating a public 3-D seismic data set that can be used to train and educate operators in the use of 3-D seismic data for reservoir characterization purposes.

Seismic data are currently being processed, and results will be made available in subsequent reports covering the Nash Draw project.

IV. DATA

Decline Curves

Historical production data are updated monthly to track production characteristics of each well. A "Delaware Model" has been developed and applied to each well to estimate ultimate recoveries and determine deviations from the model. Deviations from the model are analyzed to determine interference, boundaries, and production anomalies. An example of the production curve and model projection is presented in **Figure 29**.

BHP Tests 1, 2 & 3, and Analysis

Bottomhole pressure(BHP) buildup tests were run in Well Nos. 23 and 25. A test is planned for Well No. 12 during the completion, which is in progress. These tests plus tests on Well Nos. 5, 14, 19, and 20 have resulted in reservoir pressure data, permeability data, and frac treatment parameters such as skin and fracture half length, as presented in **Figures 30A and 30B**. Using these data, the pressure history of the reservoir can be input into the simulator, permeability can be verified, and optimum frac treatment design can be evaluated.

Using the BHP analysis, the frac treatment design has been evaluated and the presently used design parameters have been confirmed. The design used to frac treat the Brushy Canyon uses a frac height of approximately 200 feet, which includes the "K", "K-2", and "L" Zones, and a fracture half-length of 400 feet. Using the Delaware Model to predict the ultimate recovery from the wells and an average recovery factor of 12%, the drainage area is estimated to be 50 to 60 acres. This represents

an area approximately 600 feet surrounding the indicated fracture geometry. The drainage area is described as a rectangle approximately 1200 ft wide and 2000 ft long. These assumptions will be further verified using the reservoir simulation model. **Figure 31** depicts the criteria used to evaluate the effectiveness of the stimulation treatments. Larger designs are being considered to extend the frac length, but the concern over frac height growth has curtailed these plans until a quantitative model can be found to predict frac heights with frac lengths of 600 to 800 ft.

E. Loving Analogy—Log Data-Test Data

Sixteen (16) wells in section 14, T23S-R28E were selected as an analogy to the Nash Draw Pool. These wells represent varying structural positions and corresponding production characteristics. Logs have been obtained from each well, structure maps have been constructed, and available core data have been obtained for the wells in the study area. Structure, gross pay thickness, and production are shown in **Figure 32.**

.

A series of preliminary structure and isopach maps have been developed in the analog area using the same criteria that were used in the Nash Draw Pool area. It appears that the rock characteristics in the analog area are similar enough to those in the Nash Draw Pool to allow accurate comparisons of the production data and characteristics of the two areas.

V. SIMULATION

The goal of the simulation component of the Nash Draw Brushy Canyon Reservoir Management Project during this past year has been to develop a numerical simulation model of the pilot area (northeast quarter of Section 13) of the Nash Draw Pool. This model will be used prior to the actual implementation of the pilot to evaluate the technical feasibility and commercial viability of three enhanced recovery processes: waterflooding, lean gas injection, and CO_2 injection.

Reservoir simulation lies at the top of the food chain of reservoir management technology, as was clearly evident from the task diagram of the original PON proposal. It consumes most of the *interpreted* geophysical, petrophysical, geological, and reservoir engineering data described in the previous sections of this report. In turn, it produces forecasts of the expected performance of alternative recovery strategies like the ones cited above.

A revised task diagram—for the activities which have been performed by the geological, engineering, and simulation teams in support of the simulation goal—appears in **Figure 33.** The black boxes represent tasks that are substantially complete. Most of the simulation team effort was focused on the development of a geological model of the Nash Draw Pool which can support simulation. To date, two "generations" of models have been developed. Both are based solely on petrophysical measurements, i.e., they exclude any geophysical input. In the first instance, a full Nash Draw Pool model was developed from the initial geological interpretation available based on logs and cores. The second generation model was based on this data plus newly interpreted pressure transient test data. The integration of the log, core, and pressure transient data led to an interpretation of the Nash Draw Pool with three non-communicating lobes of oil. The pilot area is confined to one of these lobes. This lobe is depicted in **Figure 34.** This figure also illustrates the current interpretations of the major horizons of the Nash Draw Pool. It is anticipated that the inclusion of

geophysical data like seismic amplitude will lead to further refinement of the present model—a third generation model.

Highlights of the major tasks of the simulation effort appear below.

Network/Database Consolidation
A Silicon Graphics Indigo2 workstation with High Impact graphics and a Pentium PC were installed and linked by an ethernet LAN. The Lotus engineering database was installed on the PC and is maintained through the exchange of Zip files between the engineering and simulation teams. The Landmark Graphics Corp. Stratigraphic Geocellular Model (SGM), called "Stratamodel," was installed at the end of April to support the geological modeling activity.

Geological Modeling
The engineering and geology teams performed the following tasks in support of the simulation team efforts:

- Catalog Engineering Data
- Develop Base Maps
- Calibrate Well Logs
- Perform Log Analysis
- Establish Trial Zonations
- Populate Well Attribute Databases
- Develop Surface Facilities Data
- Estimate In-Place Fluid Distributions and Recoverable Hydrocarbons

The simulation team imported digitized maps of the interpreted horizons ("J", "K" with four subzones, "K-2," "L" with four subzones, and the top of the Bone Spring formation) into SGM to create a stratigraphic framework model of the eastern half of the Nash Draw Pool (which contains the oil lobe supporting the pilot). Since the producing zones and subzones are relatively thin, great care had to be exercised to prevent intersections of the horizons. It is also critical that the surfaces tie to the well picks of the lithological markers in the well traces. In general, the most successful approach to this problem was based on the use of gross isopach thickness interpretations building from the structural top of the Bone Springs formation to the structural top of the "J" sand. Unix awk scripts were developed to process the ascii output from GenericCadd®, an inexpensive variant of AutoCad, which was used to digitize the successive generations of geological interpretations provided by the geology team.

The next major step was the development of a well attribute model. This activity was supported by the Lotus engineering database. For each of the following Nash Draw Brushy Canyon Pool wells (Well Nos. 1, 5, 6, 9, 10, 11, 13, 14, 15, 19, 20, 23, 24, 25), the following attributes were imported into the well model:

- neutron porosity, gamma ray

· interpreted porosity and permeability
· perforated interval and fractured interval
· net pay
· water saturation

In some instances, these attributes were available on a foot-by-foot basis for one or more of the producing zones. Not all of the attributes were available for each well. For reservoir simulation, the most important reservoir attributes are fluid conductivity and rock matrix storage capacity. The distribution of these properties throughout the Nash Draw Pool have been based on the well attribute model. SGM distributes these properties deterministically, that is, weighted by the reciprocal of the square of the distance between the location of interest and nearby wells in the reservoir model. **Figure 35** illustrates this for the distribution of porosity calculated in this manner; **Figure 36** illustrates the distribution of permeability. Statistical techniques like kriging (and co-kriging) may be used to distribute these attributes in the third generation model.

From the point of view of reservoir simulation, the geological characterization is complete if it specifies zone structure, hydraulic conductivity and continuity, and storage capacity.

All of these requirements were satisfied by the second generation model. In addition, the distribution of initial water saturation was mapped in three dimensions across the Nash Draw Pool. This is illustrated in **Figure 37.**

Reservoir Simulation

Having completed the supporting geological model, attention is now focused on the generation of a reservoir simulation model for the pilot area. It is envisioned that a single well in the pilot area will be converted to injector status to test the efficacy of injecting water, lean gas (immiscible), and/or CO_2 (immiscible or miscible) to promote additional oil recovery and help maintain reservoir pressure. The following tasks are required to complete the pilot simulation phase:

· possible scale-up of lithological units
· interpolation of geological attributes on simulation grid
· validation of pilot simulation model
· design and execution of prediction cases

A simulation grid is being designed which will be centered around the potential injector, but will include the net pay of the oil lobe containing the pilot area. The scale-up task will be done in Stratamodel. The present geological model has on the order of 10 million cells. The several hundred layers of this model will be reduced to no more than 10 for the simulation model. The PVT and rock property data needed for the simulation (not a part of the geological model) has been processed, and scripts are being written to convert the production data in the Lotus engineering database into simulator input format. It is anticipated that the four tasks described above will be completed by December 31, 1996.

VI. PILOT AREA

To expedite the final unitization of the Nash Draw Pool, some small interest owners have been bought out and interests consolidated. To estimate the value of these interests, a decline curve analysis was used to estimate the value of the interests.

The pilot area has been proposed around Well No.1, as shown on the map in **Figure 38**. The spacing in this part of the field is very close and interference has been observed between the Well Nos. 1, 6, 14, 5, 9, and 10. Preliminary calculations of water injection rates, **Figure 39,** indicates that injection rates would be 150 to 200 barrels of water per day (BWPD), too low to obtain response in a reasonable length of time. Pressure maintenance will be accomplished with a low viscosity injectant that can be injected at sufficiently high rates to effect response in a timeframe adequate for project economic success.

Detailed flow unit maps have been prepared in the pilot area. Each of the sub-units of the three main sands previously mentioned has been mapped individually. Maps prepared for each sub-unit are isopach maps for log-derived net pay and gross sub-unit isopach maps. These maps have been included in the initial geologic model for the simulation study of the pilot area.

VII. TECHNOLOGY TRANSFER

The transfer of technical information generated during the course of this project is one of the prime objectives of the project. Toward this objective, Strata has participated in many meetings and workshops to promote the dissemination of information generated during the first year of the project. A summary of these activities is outlined as follows:

Partners Meeting, February 1996

A meeting of the partners in the Nash Draw Pool was held on February 23-24, 1996 with twenty (20) participants in attendance. The project status was discussed, and plans for the remainder of the year were outlined.

Poster Session Midland, Texas, May 1996

Strata participated in the workshop titled: "Improving Production from Shallow Shelf Carbonate (Class II) Reservoirs," held at the Center for Economic Diversification in Midland, Texas on May 15-16, 1996. A poster session was presented outlining the goals and preliminary findings of the Nash Draw Project.

DOE Outreach Meeting, July 1996

A poster was presented at the DOE Outreach Program meeting in Roswell, NM, on July 25 and 26, 1996. Several area producers attended the meeting, and there was considerable interest in the activities being conducted at the Nash Draw Pool.

Liaison & Technical Committee Meeting, August 1996

A liaison and technical committee meeting was held on August 16, 1996. There were fourteen (14) participants including Nash Draw Pool partners, BLM representatives, OCD representatives and

industry group representatives. The status of the project was discussed and findings to date were presented for review.

Characterization Workshop, August 1996
A workshop sponsored by the Petroleum Recovery Research Center at New Mexico Tech, titled "Integration of Advanced Reservoir Characterization Techniques" was held in Roswell, NM, on August 22 and 23, 1996. Strata Production Company presented an update of the status and findings at the Nash Draw Pool Project.

FRAC Design Workshop, September 1996
A conference titled: "Stimulation Design and Monitoring -Delaware Mountain Group Formations" was held on September 19, 1996 at the New Mexico Junior College in Hobbs, New Mexico. Sponsors of the Conference included the PRRC and the Petroleum Technology Transfer Council. Strata presented the findings and conclusions of the fracture stimulation design and evaluation scenario used to determine effectiveness of the stimulation program.

Internet Home Page
An Internet homepage went online in September 1996, as part of the PRRC's homepage. The page is located at http://baervan.nmt.edu/prrc/homepage.html. At this page go to "Research Divisions", then "Reservoir Evaluation and Advanced Computational Technologies (REACT)" and then go to "DOE CLASS III PON Slope Basin Reservoir Characterization: Nash Draw Field." After reviewing the homepage, click on "NASH DRAW" to view project and field data. This site will be updated as new information becomes available.

CONCLUSIONS

All sections of the statement of work have been completed or are in progress. The simulation work and planning for the pilot area are slightly behind schedule because of delays in obtaining software licenses. Conclusions drawn during the first year of the Nash Draw Pool project are summarized below.

The primary concerns at Nash Draw Pool are: (1) the low primary oil recovery of 10% or less, (2) a steep oil production decline rate, and (3) rapidly increasing gas-oil ratios. Initial reservoir pressure is just above the bubble point pressure and declines to below the bubble point after a few months of production. With the solution gas drive reservoir, oil production declines approximately 50% in the first year and gas/oil ratios increase dramatically. These concerns point out the importance of considering various reservoir management strategies to maximize the economic recovery of oil at Nash Draw Pool.

Production at the Nash Draw Pool is from the basal Brushy Canyon slope basin sandstone. The structure trend at the Nash Draw Pool is N-S to NE-SW, and there were at least three depositional events. The reservoir consists of complex sands - a series of stacked micro-sands, vertical permeability is extremely low, and horizontal permeability is poor to good. The main producing

intervals of the Brushy Canyon formation are the "K" and "L" sands. These sands have multiple lobes, and both sands can be divided in four sub-units.

Mineralogy of the "K" and "L" sands are similar. Both zones contain some clays - illite and chlorite. The "K" sand has up to 2% more chlorite which occludes permeabilties and may have influenced higher initial water saturation in the "K" sand. Overall, the "K" sand has a higher water saturation than the "L" sand.

A major problem in analyzing the Nash Draw Pool reservoir is to distinguish productive pay from non-productive intervals. Therefore, a procedure for establishing net pay was developed. By using the full-core analysis to calibrate log calculations, a procedure was developed to identify the zones that are oil-productive. The procedure is based on the premise that zones with residual oil saturation have a high probability of being productive and zones with no residual oil saturation have a low probability of being productive. By calibrating the Micro Lateral Log to calculate a residual oil saturation value for each one-half foot interval from the digitized log, potential pay zones were identified. By applying porosity correction transforms, setting gamma ray and porosity limits, and calibration of resistivity values, a more accurate determination of the productive intervals was made. With corrected porosity values, water saturations, and net heights, a volumetric calculation was performed to estimate the original-oil-in-place. A comparison of volumetric analysis and decline-curve analysis indicated close agreement.

A corresponding calculation was performed to determine the zones that are water productive and the volume of water present. This analysis showed that the "L" zone has minor amounts of interbedded water, the "K-2" has many water zones, and the "K" has highly interbedded oil and water zones. The "L" has high oil saturation (greater than 50%), and the "K-2" has high oil saturations when productive zones are present. The "K" zone has lower average permeability which corresponds to higher capillary pressure and higher water saturations, with S_w in the range of 50% to 60%. Water saturations in the "L" sand average in the high 40s.

After identifying net pay intervals in each zone, relative permeability was calculated using the relative permeability data derived from the full-core analysis. By summing the transmissibility (kh/i) values for each oil and water zone, an estimate of the oil-water cut could be calculated for each interval. These values were used to allocate production from each of the three zones.

Capillary pressure data and height above the 100% water saturation were calculated for each well. Mapping these values versus structure indicates there may be multiple sand pods with different characteristics. These data, coupled with the 3-D seismic interpretation, should help identify depositional pods and their orientation.

Vertical seismic profiling was done in one of the newly drilled data acquisition wells to get calibration and frequency set for the 3-D seismic shoot that subsequently was done in May and June of this year. The 3-D data is currently being processed. Three levels of information are expected: (1) boundaries, (2) depositional direction, and (3) information on individual channels or separate zones. The quality of the seismic data was good, and resolution of 15 to 20 ft appears to be possible.

Activities of the modeling/simulation team during the first year of the project resulted in two generations of geological models for Nash Draw Pool. The typical model-building steps were: (1) start with a geological interpretation (map form) and petrophysical database, (2) digitize the maps, (3) build a stratagraphic framework, (4) build a well attribute model (e.g. porosity, permeability, water saturation, fracture characteristics), and (5) interpolate reservoir attributes between wells (porosity, permeability, and initial water saturation). To date, a detailed reservoir description of the pilot area has been made, and current efforts are concentrating on defining the reservoir volume which supports the pilot area wells. In the next quarter, a preliminary evaluation of enhanced recovery options will be made for the pilot area, and by the end of 1996 the next generation geological model will include 3-D seismic input and greater use of statistical methods.

During the first year of the project, several presentations were made to transfer results from the Nash Draw Pool project. An Internet-based Web site was developed, and the document at this site will be updated as new information becomes available.

Table 1. General Characteristics of the Nash Draw Delaware Field, Eddy County, New Mexico.

Discovery Date	1992
Trapping Mechanism	Stratigraphic Trap
Current Number of Wells	15
Current Production	490 BOPD + 2.4 MMCFGPD + 500 BWPD
Reservoir Depth	6600 to 7000 ft
Pay Thickness—K & L Sandstones	20 to 50 ft
Reservoir Porosity	12 to 20%
Reservoir Permeability	0.2 to 6 md
Initial Reservoir Pressure	2963 psi
Bubble Point Pressure	2677 psi
Drive Mechanism	Solution Gas Drive
Oil Gravity	42.4° API
Primary Recovery Factor	10 to 15% oil in place
Estimated Oil in Place	25 to 50 MMbbl
Reserves, Primary Recovery	2.5 to 5 MMbbl

Table 2. Permeability/Porosity Correlations.

Flow Unit	Sidewall	Core	Full	Core
Variable	a	b	a	b
"K"	0.164915	2.25338	0.207675	2.8858
"K-2"	0.186535	2.06872	0.315038	3.69966
"L"	0.179787	2.45666	0.231250	3.06330

Table 3. Results of Drilling First Year Data Wells.

Well	Location	Initial Rate BOPD	Initial Rate MCFGD	Initial Rate BWPD
Nash Draw No. 12	12O-T23S-R29E	Completing		
Nash Draw No. 23	13D-T23S-R29E	112	281	574
Nash Draw No. 24	14H-T23S-R29E	140	392	187
Nash Draw No. 25	14I-T23S-R29E	41	155	274

Table 4. Saturation and Flow Capacity Data for Simulation Input.

Simulator Input Data by Layers—Nash #25								
	Oil Zones					Water Zones		
Zone	Net Feet Prod. Oil	Avg. Oil Water Sat. %	Avg. Oil Porosity %	Avg. Oil Perm. to Water Kro–md	Avg Oil Zone Perm. to Water Krw–oil	Net Feet Prod. Water	Avg. Water Porosity %	Avg. Water Perm Krw–md
J	6.00	55.00	11.23	0.0104	0.0043	8.50	10.29	0.4074
Ka	2.50	55.00	12.13	0.0141	0.0055	4.00	10.59	0.4455
Kb	2.50	55.00	11.30	0.0092	0.0039	4.50	9.88	0.2632
Kc	4.50	55.00	12.31	0.0177	0.0068	7.50	11.57	0.7821
Kd	5.00	55.00	12.26	0.0154	0.0060	4.50	10.70	0.4848
K-2	2.50	55.00	12.13	0.0000	0.0314	2.50	13.20	2.0259
La	0.50	45.00	10.01	0.0421	0.0136	4.00	9.07	0.1371
Lb	0.00	0.00	0.00	0.0000	0.0000	0.00	0.00	0.0000
Lc	0.00	0.00	0.00	0.0000	0.0000	2.00	8.72	0.1020
Ld	2.00	45.00	10.60	0.0596	0.0174	3.50	8.82	0.1092

Simulator Input Data by Layers—Nash #15								
	Oil Zones					Water Zones		
Zone	Net Feet Prod. Oil	Avg. Oil Water Sat. %	Avg. Oil Porosity %	Avg. Oil Perm. to Water Kro–md	Avg Oil Zone Perm. to Water Krw–oil	Net Feet Prod. Water	Avg. Water Porosity %	Avg. Water Perm Krw–md
J	7.00	51.32	12.46	0.757	0.0015	14.50	10.17	0.0733
Ka	0.00	0.00	0.00	0.0000	0.0000	3.50	10.06	0.0252
Kb	0.00	0.00	0.00	0.0000	0.0000	6.50	10.59	0.0598
Kc	5.00	56.76	13.18	0.0108	0.0038	9.50	10.38	0.0862
Kd	4.00	57.20	12.12	0.0050	0.0019	10.50	10.61	0.0849
K-2	3.00	53.44	16.40	0.0032	0.9761	11.50	12.11	3.2079
La	1.00	44.94	12.38	0.0865	0.0147	0.00	0.00	0.0000
Lb	4.00	38.59	12.50	0.1510	0.0019	0.00	0.00	0.0000
Lc	12.00	40.46	14.25	0.5492	0.0028	0.00	0.00	0.0000
Ld	11.00	40.23	13.68	0.4288	0.0254	0.00	0.00	0.0000

Table 5. Productive-zone Sorting Guides.

Steps	**1**	**2**	**3**	**4**	**5**
Sorting Criteria	Sxo	Sw - Rt_{corr}	G.R.	ϕ_{corr}	OOIP
Ranges	>Core Sxo	<60%	<70	>11%	>300 BO/ac-ft

Table 6. Wettability of Sample 38A.

Wettability	
Depth	6682.6 ft
Permeability to air	0.925 md
Porosity	0.137
Initial water saturation	0.461
Effective permeability to oil @ SWI	0.364 md

Imbibition of Oil	
Spontaneous inhibition, fraction	0.000
Dynamic inhibition, fraction	0.540
Total imbibed, fraction	0.540

Imbibition of Water	
Spontaneous inhibition, fraction	0.167
Dynamic inhibition, fraction	0.172
Total imbibed, fraction	0.340

Wettability Indices	
Amott Wettability Index to oil	0.000
Amott Wettability Index to water	0.492
Amott-Harvey Wettability Index	0.492

Table 7. Stratigraphic Model Parameters.

"J" Sand	Structural Datum Top/"J" Sand Structural Datum Base/"J" Sand Gross Thickness Isopach Maps Net Porosity Isopach Maps ϕ*h Isopach Maps	
"K" Sand	Structural Datum Top/"K" Sand Structural Datum Base/"K" Sand Gross Thickness Isopach Maps Net Porosity Isopach Maps ϕ*h Isopach Maps Sw Distribution Capillary Pressure Distribution	Gross Isopach Maps: K_a,K_b,K_c,K_d Net Pay Isopach Maps: K_a,K_b,K_c,K_d
"K-2" Sand	Structural Datum Top/"K-2" Sand Structural Datum Base/"K-2" Sand Gross Thickness Isopach Maps Net Porosity Isopach Maps Net Pay Isopach Maps ϕ*h Isopach Maps Sw Distribution Capillary Pressure Distribution	
"L" Sand	Structural Datum Top/"L" Sand Structural Datum Base/"L" Sand Gross Isopach Thickness Maps Net Porosity Isopach Maps ϕ*h Isopach Maps Sw Distribution Capillary Pressure Distribution	Gross Isopach Maps: L_a,L_b,L_c,L_d Net Pay Isopach Maps: L_a,L_b,L_c,L_d
Bone Spring Lime	Structural Datum Top/Bone Spring Limestone	

Table 8. Table Showing Mineralogic Composition of Samples from Whole Core in Nash Unit No. 23 Well.

Whole Rock Mineralogy	Sample Depth											
	6652.7	**6664.6**	**6666.5**	**6681.5**	**6692.6**	**6711.1**	**6735.2**	**6738.6**	**6742.2**	**6785.8**	**6787.8**	**6816.1**
Quartz	66.6%	58.6%	55.2%	62.1%	56.2%	53.9%	56.6%	59.8%	57.9%	60.0%	56.5%	55.9%
K-Feldspar	10.0%	8.1%	9.3%	8.0%	9.7%	11.0%	11.2%	9.6%	9.1%	10.3%	8.4%	8.6%
Plagioclase Feldspar	11.4%	21.2%	26.4%	23.4%	22.9%	24.9%	21.4%	23.2%	25.0%	21.6%	26.0%	21.2%
Calcite	3.6%	5.1%	1.7%	1.4%	3.6%	2.6%	4.6%	1.0%	2.0%	2.3%	1.0%	8.2%
Ankerite	0.0%	0.2%	0.3%	0.0%	0.3%	0.2%	1.6%	0.6%	0.1%	0.1%	0.3%	0.6%
Siderite	0.3%	0.1%	0.1%	0.0%	0.0%	0.2%	0.2%	0.2%	0.2%	0.2%	0.2%	0.2%
Pyrite	0.4%	0.1%	0.2%	0.2%	0.5%	0.5%	0.5%	0.9%	0.5%	0.3%	0.4%	0.7%
Chlorite-Authigenic, Isopachous	4.1%	3.9%	3.9%	2.9%	4.1%	3.0%	0.9%	1.3%	2.2%	2.1%	2.5%	1.4%
Illite-Authigenic, Pore Bridging	2.4%	1.7%	2.1%	1.1%	1.4%	2.0%	2.0%	2.7%	1.8%	2.2%	3.4%	2.2%
Illite/Smectite (I/S)-Authigenic	0.6%	0.6%	0.5%	0.6%	0.9%	1.3%	0.8%	0.8%	0.8%	0.6%	0.8%	0.9%
Kaolinite-Detritial	0.6%	0.3%	0.3%	0.2%	0.5%	0.3%	0.1%	0.1%	2.0%	0.2%	0.4%	0.2%
Total Whole Rock %	100%	100%	100%	100%	100%	100%	100%	100%	100%	100%	100%	100%
Clay Minerals ≥ 4μ												
Sample Depth	**6652.7**	**6664.6**	**6666.5**	**6681.5**	**6692.6**	**6711.1**	**6735.2**	**6738.6**	**6742.2**	**6785.8**	**6787.8**	**6816.1**
Chlorite-Authigenic, Isopachous	4.1%	3.9%	3.9%	1.1%	4.1%	3.0%	0.9%	1.3%	2.2%	2.1%	2.5%	1.4%
Illite	2.4%	1.7%	2.1%	0.6%	1.4%	2.0%	2.0%	2.7%	1.8%	2.2%	3.4%	2.2%
Illite-Smectite (I/S)	0.6%	0.6%	0.5%	0.2%	0.9%	1.3%	0.8%	0.8%	0.8%	0.6%	0.8%	0.9%
Kaolinite	0.6%	0.3%	0.3%	100%	0.5%	0.3%	0.1%	0.1%	2.0%	0.2%	0.4%	0.2%
TOTAL Whole Rock %	8.0%	7.0%	7.0%	5%	7%	7%	4%	5%	7%	5%	7%	5%

Table 9. Vibrator Test Parameters.

Wavefield	Sweep Frequencies	Sweep Rate	Sweep Length	Sweeps Summed
1	8-96Hz	Linear	12 s	4
2	8-96 Hz	3 dB/octave	12 s	4
3	10-120 Hz	Linear	12 s	4
4	10-120 Hz	3 dB/octave	12 s	4

Table 10. Storage Requirements for Nash Draw 3-D Seismic Data Volumes.

	Number of north-south lines	Number of east-west lines	Number of data traces	Files size* (megabytes)
55 x 55	336	216	72576	452
110 x 110	168	108	18144	113

*32-bit data words, 2 ms sample rate, and 3 s trace length.

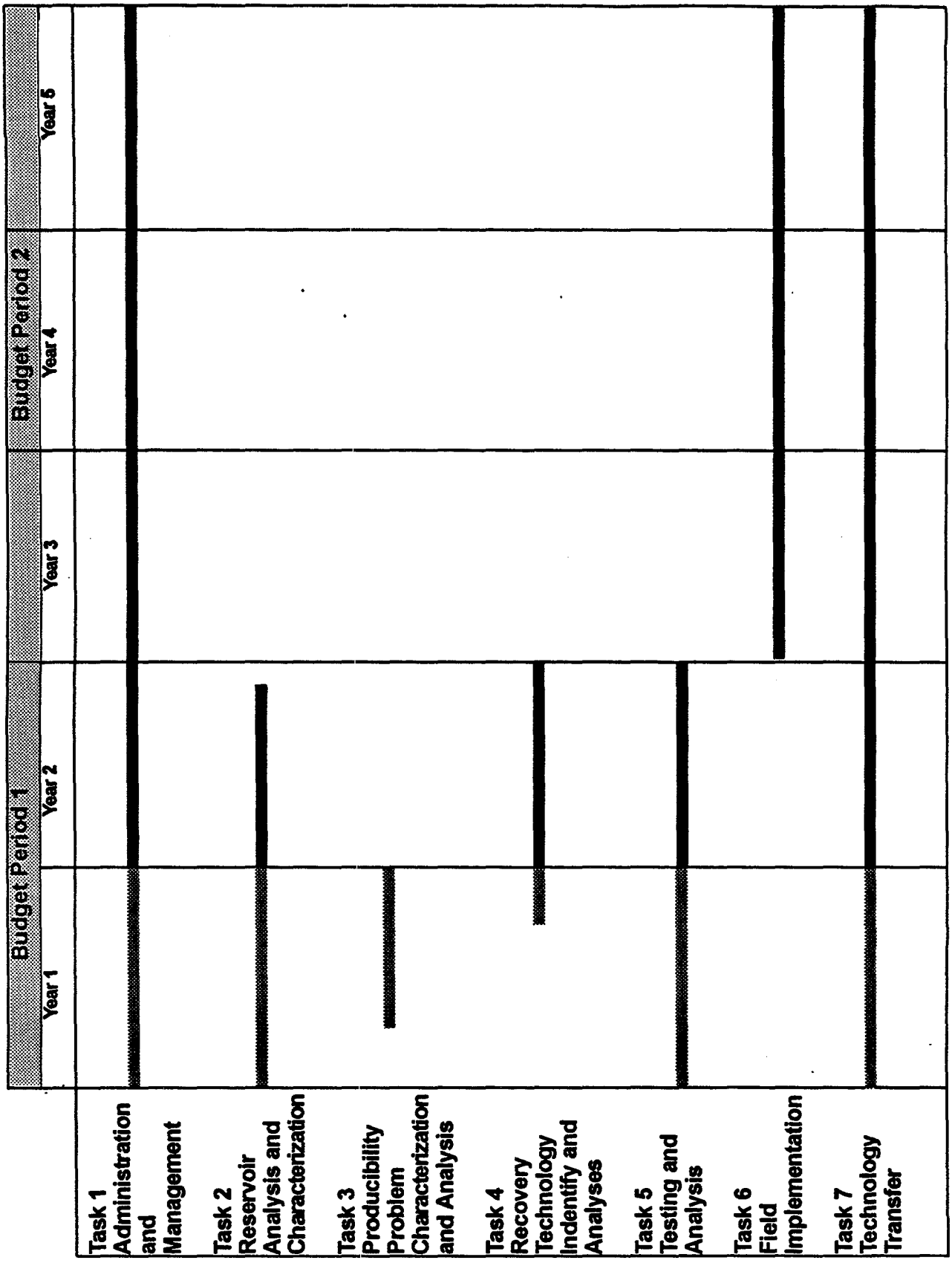

Figure 1. Milestone chart for the Nash Draw DOE Class III PON.

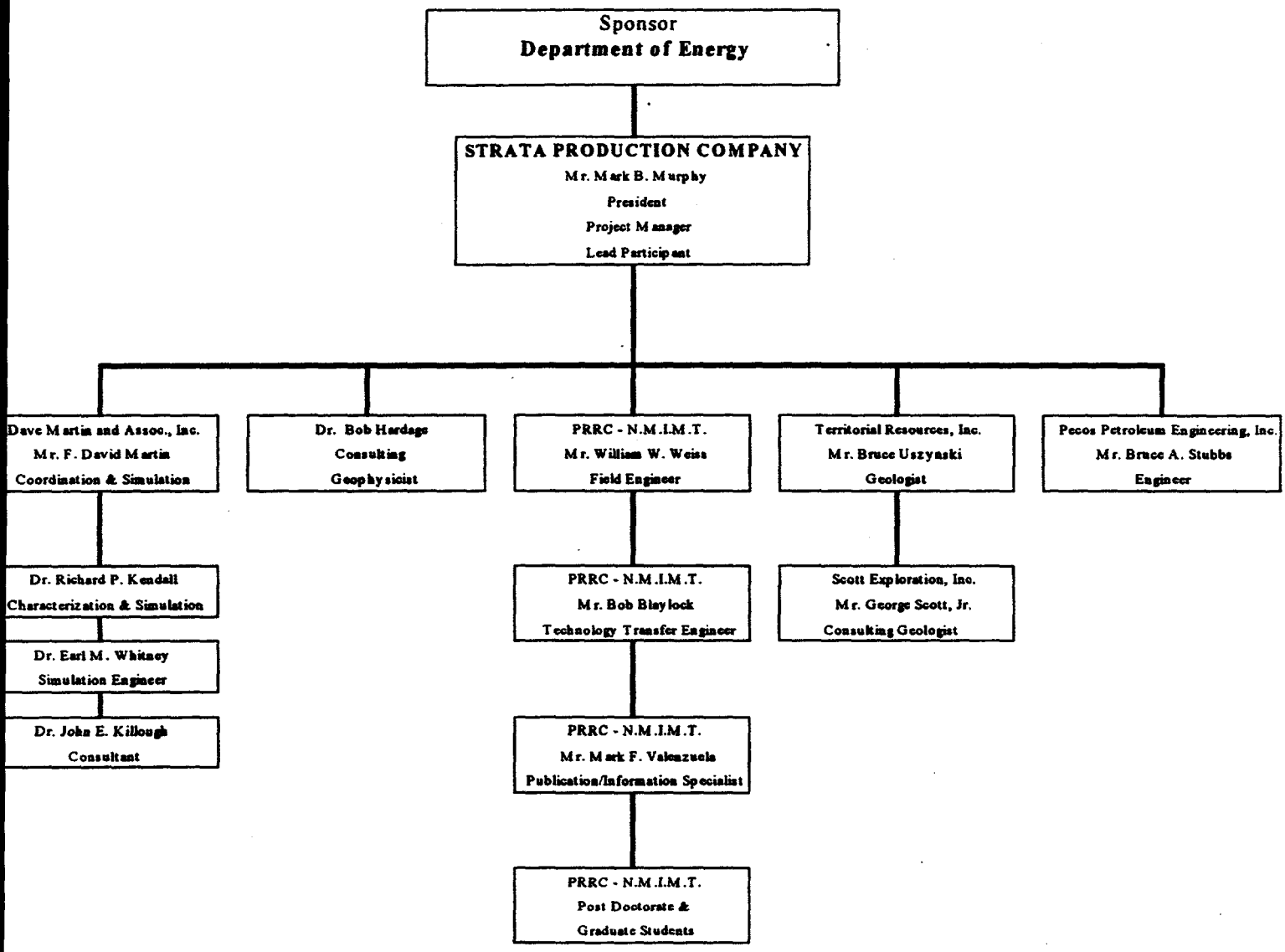

Figure 2. Organizational Chart for Nash Draw DOE Class III PON.

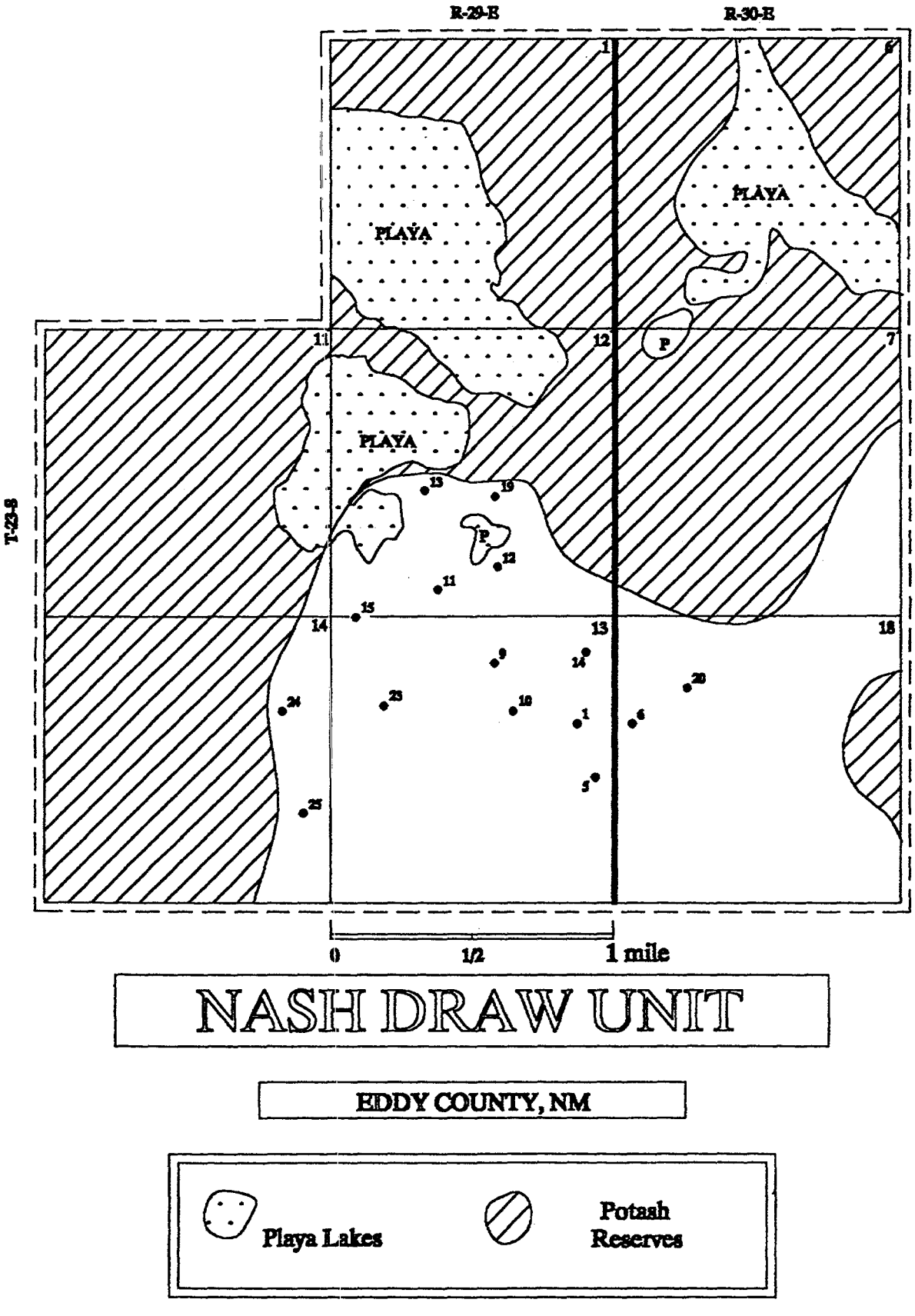

Figure 3. Location of Wells in the Nash Draw Pool.

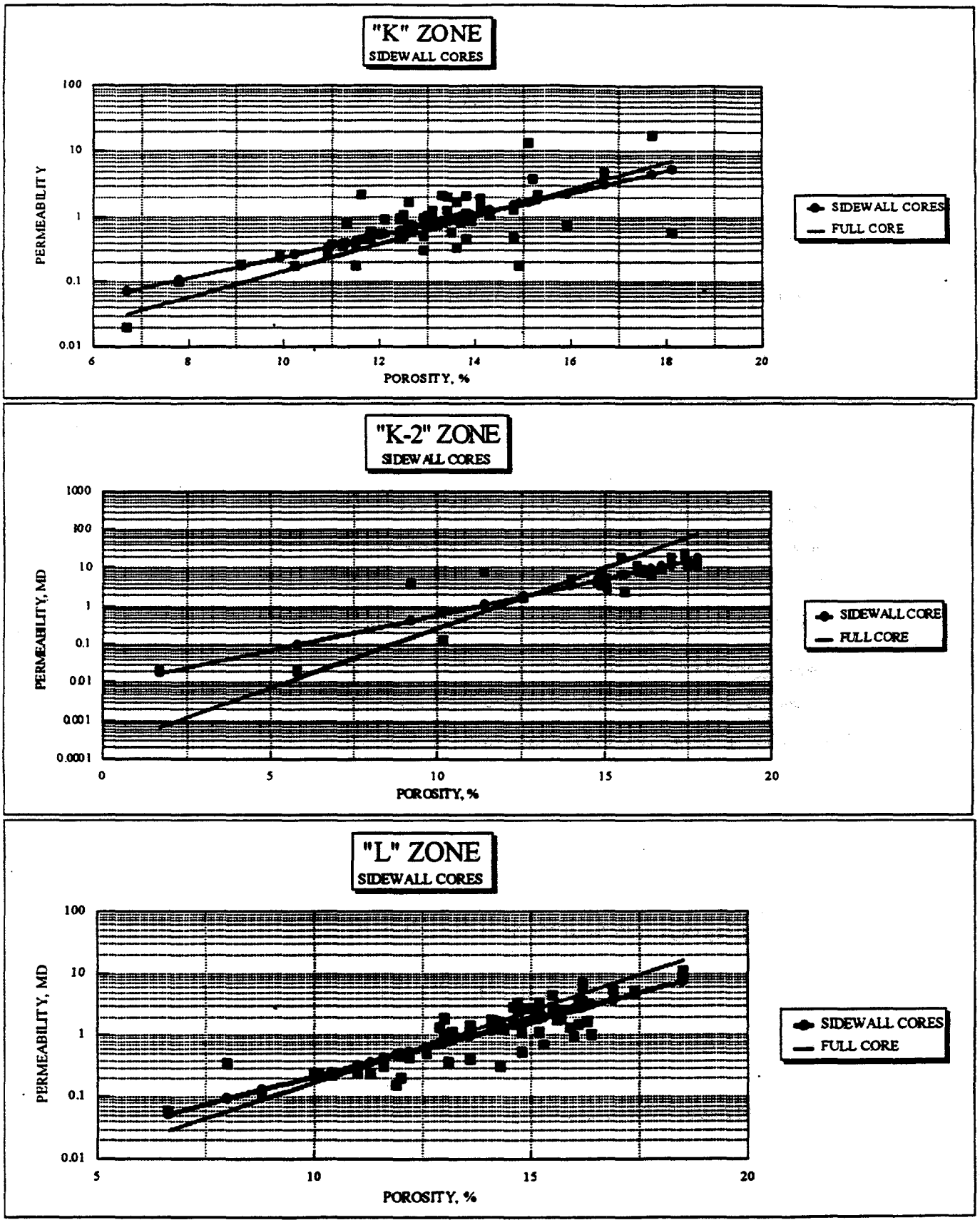

Figure 4. Sidewall core data versus full core data.

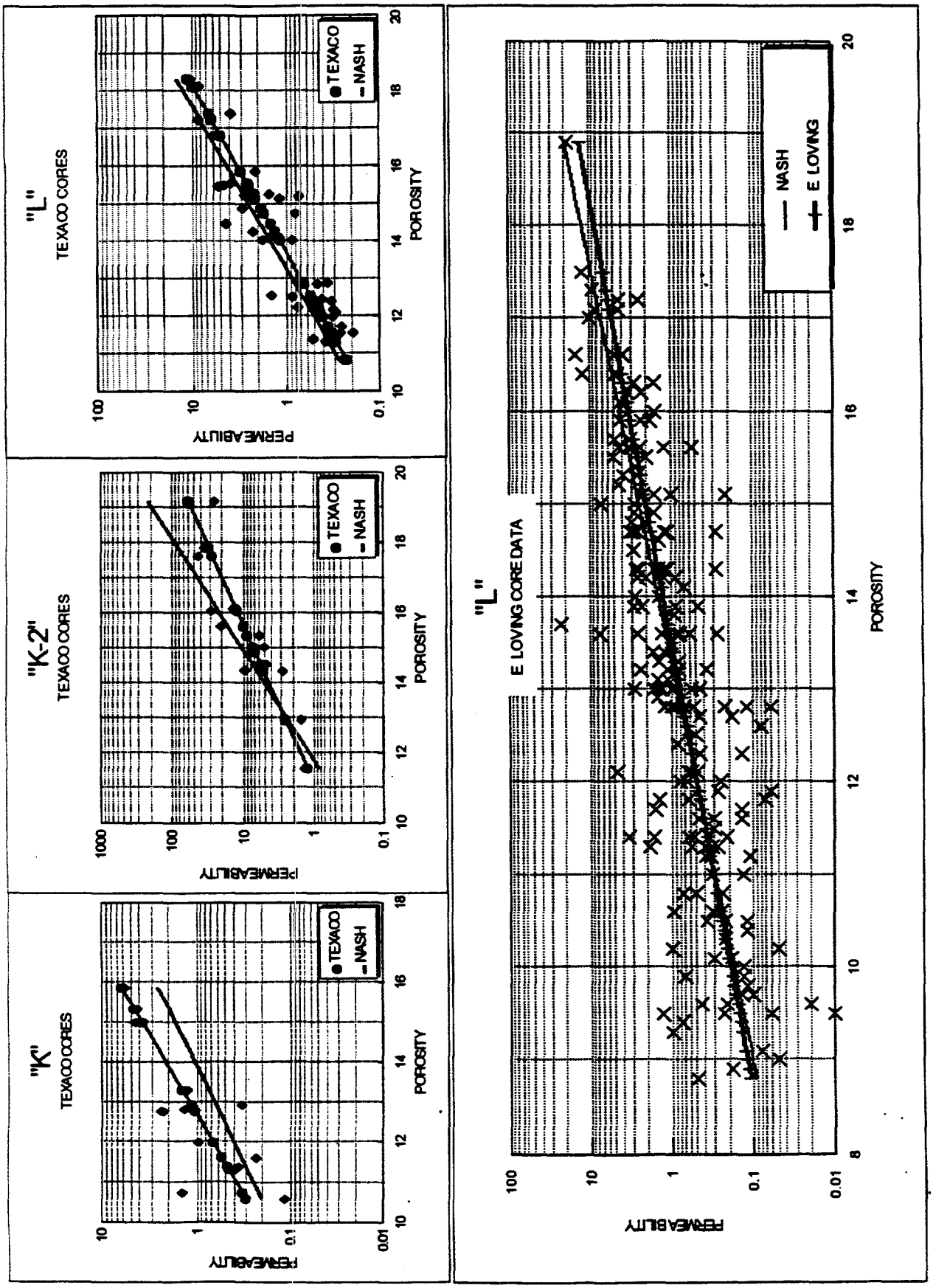

Figure 5. Analog core data versus Nash Draw core data.

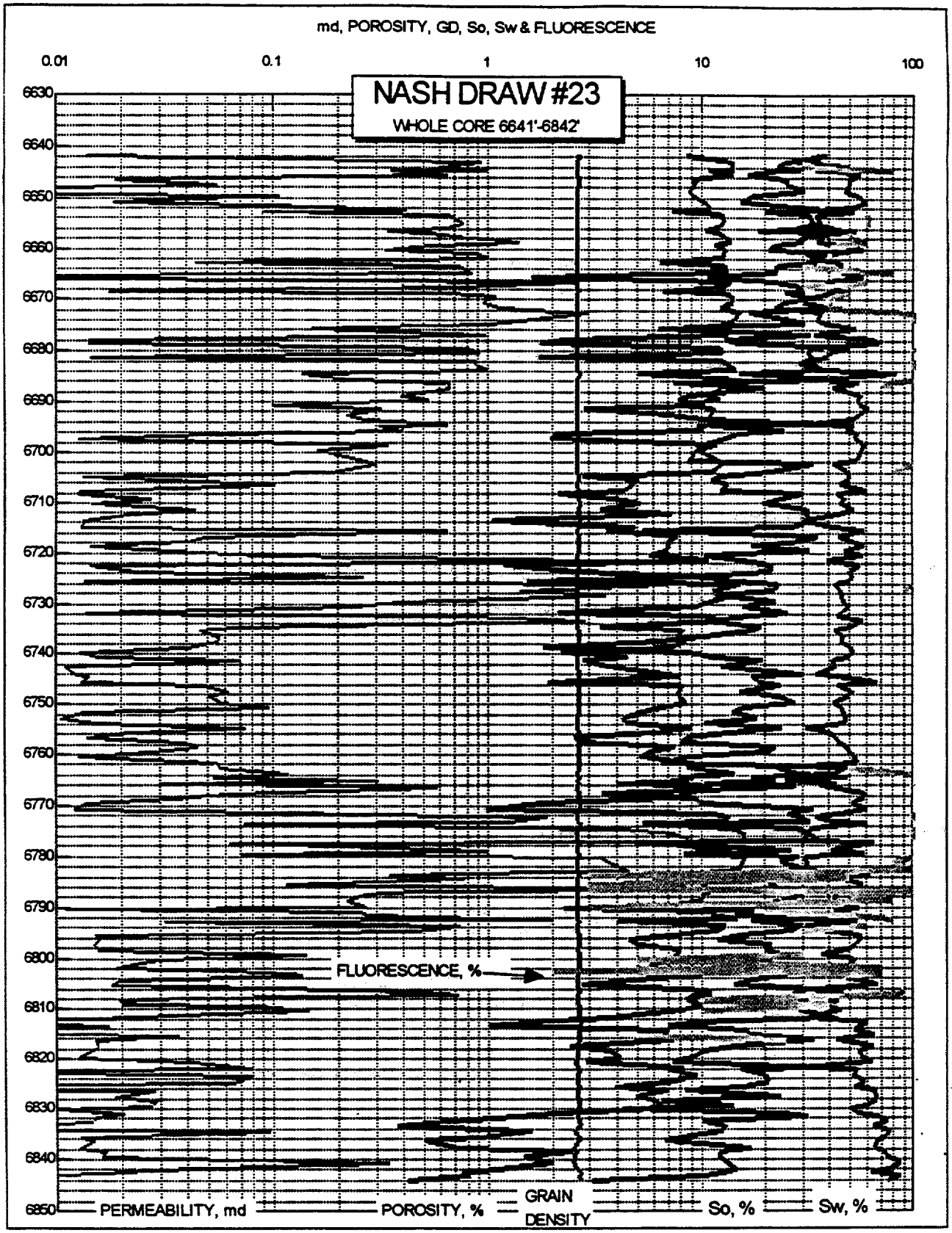

Figure 6. Nash Draw Pool Well No. 23 full core analysis.

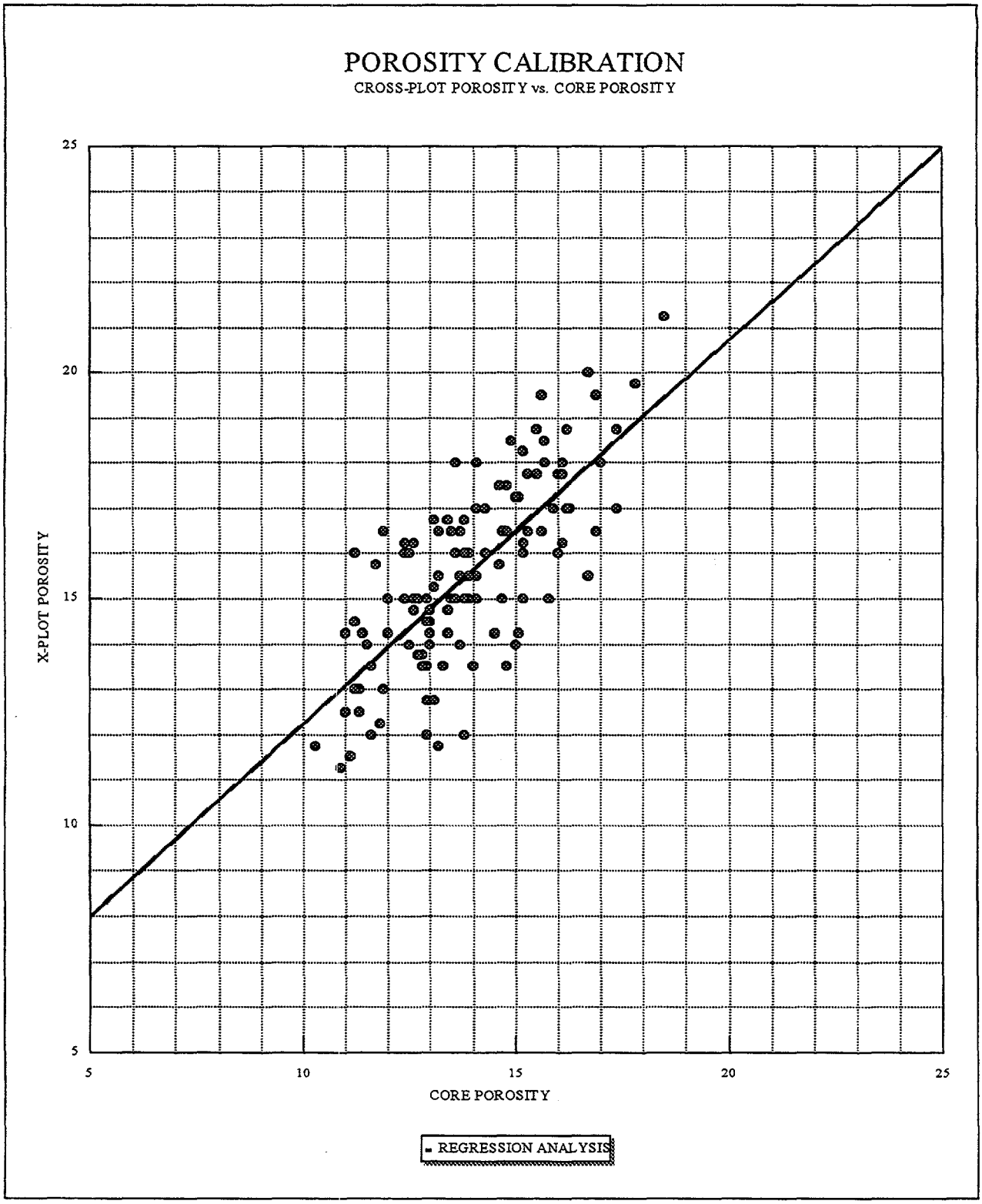

Figure 7. Core porosity versus cross-plot porosity.

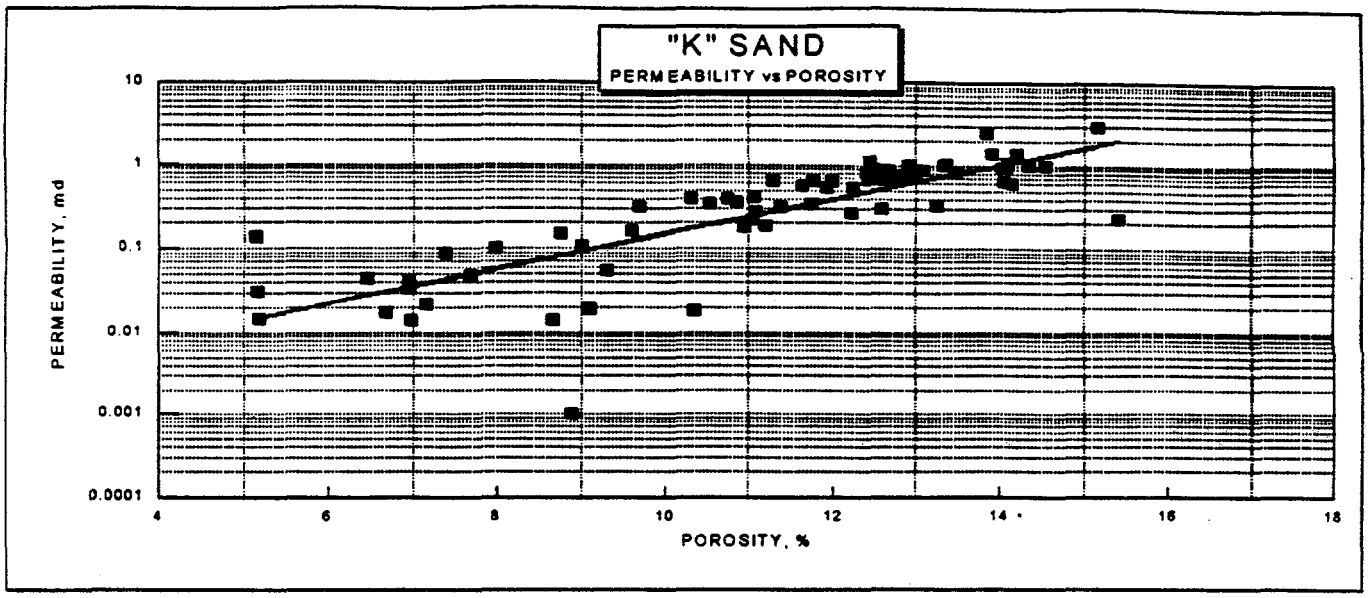

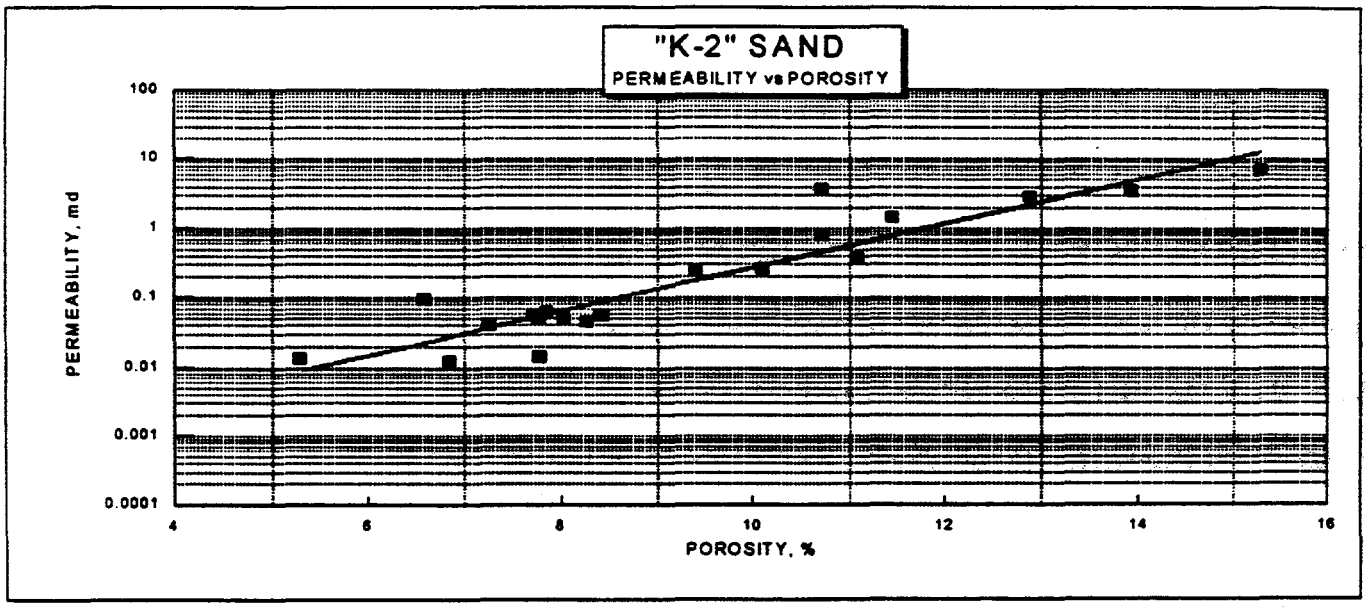

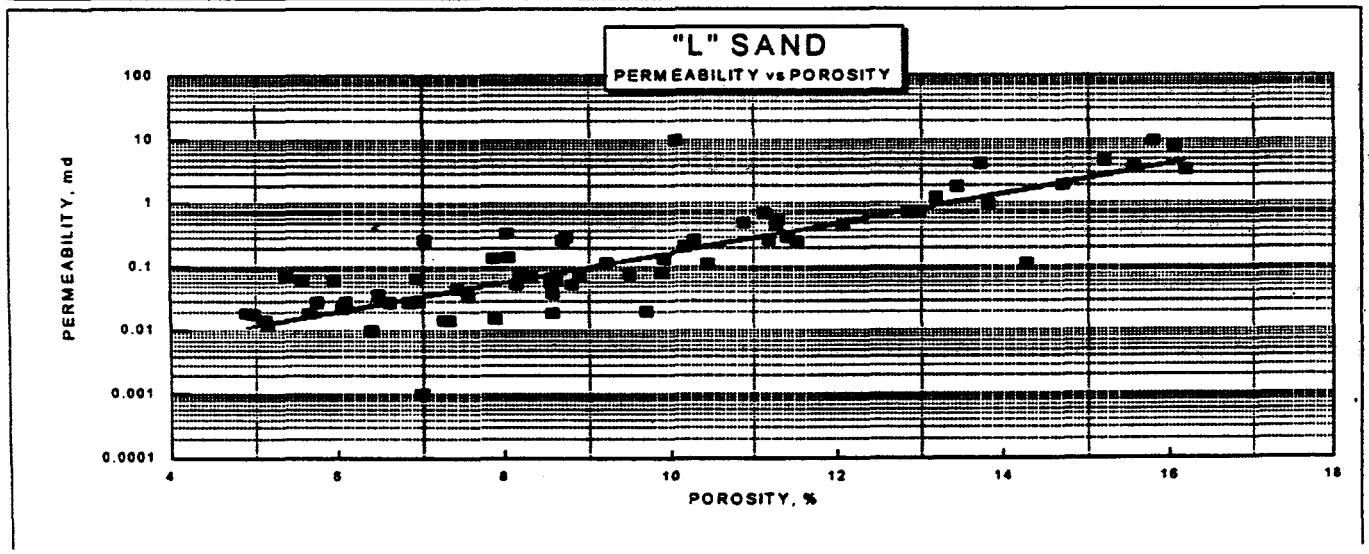

Figure 8. Full core porosity versus permeability relationships.

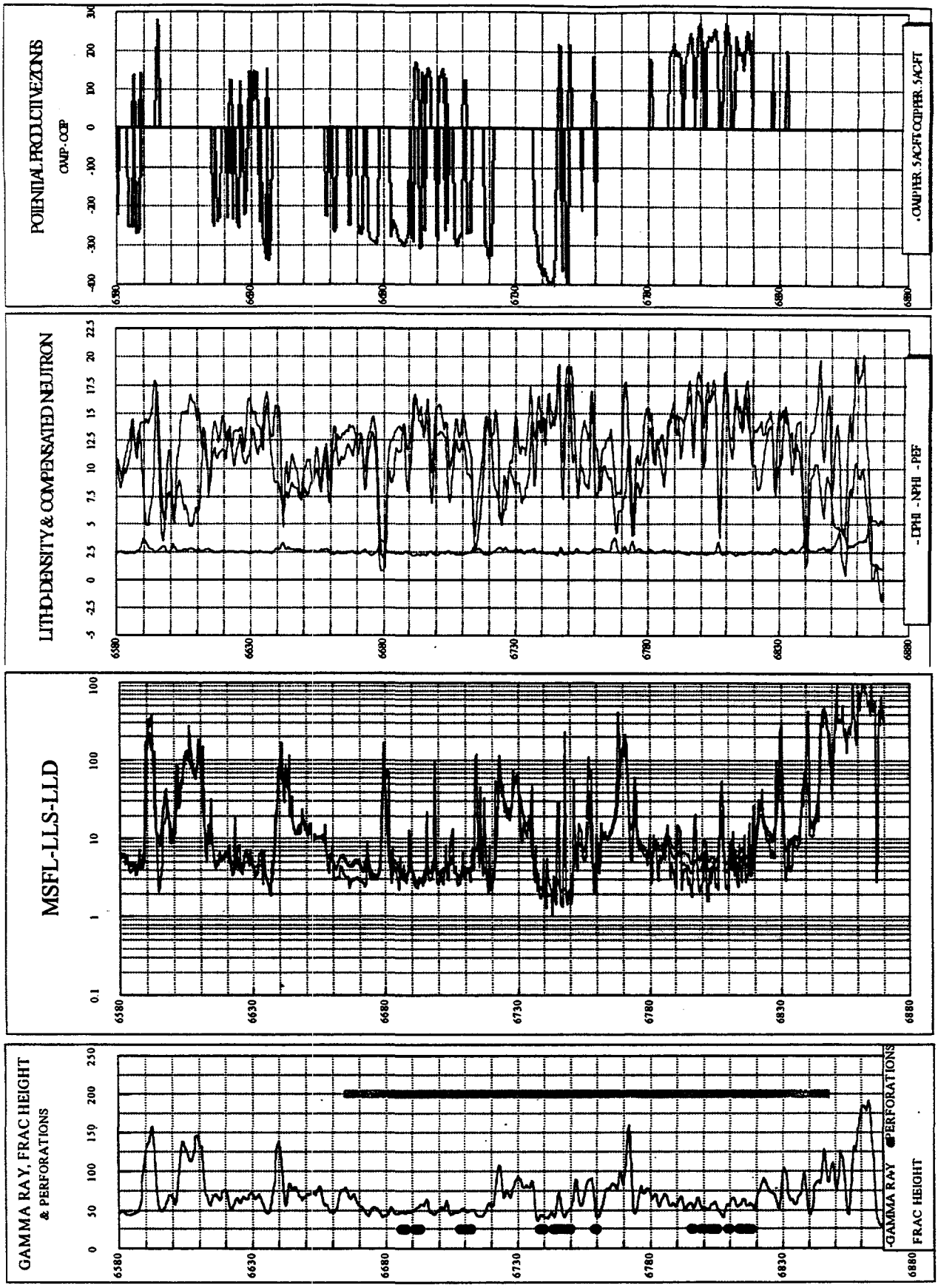

Figure 9. Digitized logs and core calibrated log calculations.

CAPILLARY PRESSURE
GAS-WATER SYSTEM

CAPILLARY PRESSURE, PSI:				2	5	10	20	40	70	100	150	250	400
SAMPLE NO.	DEPTH FEET	KLINKENBERG PERMEABILITY MD.	POROSITY FRACTION	INLET-FACE WATER SATURATION, FRACTION PORE VOLUME									
38	6682.9	0.824	0.156	0.96	0.951	0.944	0.931	0.47	0.355	0.297	0.242	0.187	0.148
151	6791.4	3.18	0.165	0.975	0.965	0.949	0.52	0.385	0.304	0.261	0.219	0.173	0.136
38-"J"	INTERFACIAL TENSION=	72	DYNES/CM	0.0638409	0.159602	0.3192044	0.6384087	1.276817	2.23443	3.192044	4.788065	7.980109	12.76817
151-"J"				0.1219464	0.304866	0.6097321	1.2194643	2.438929	4.268125	6.097321	9.145982	15.2433	24.38929

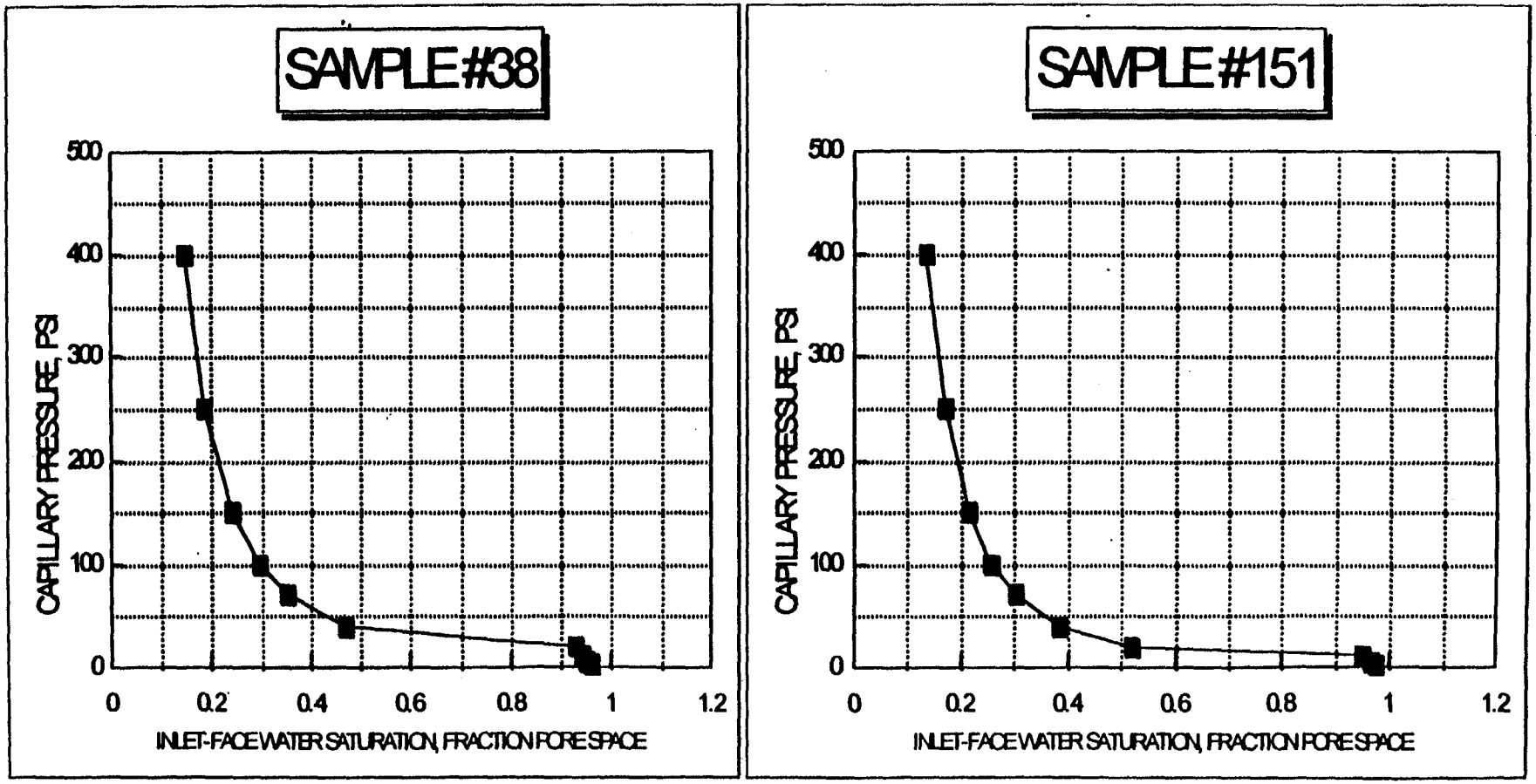

Figure 10. Capillary pressure data.

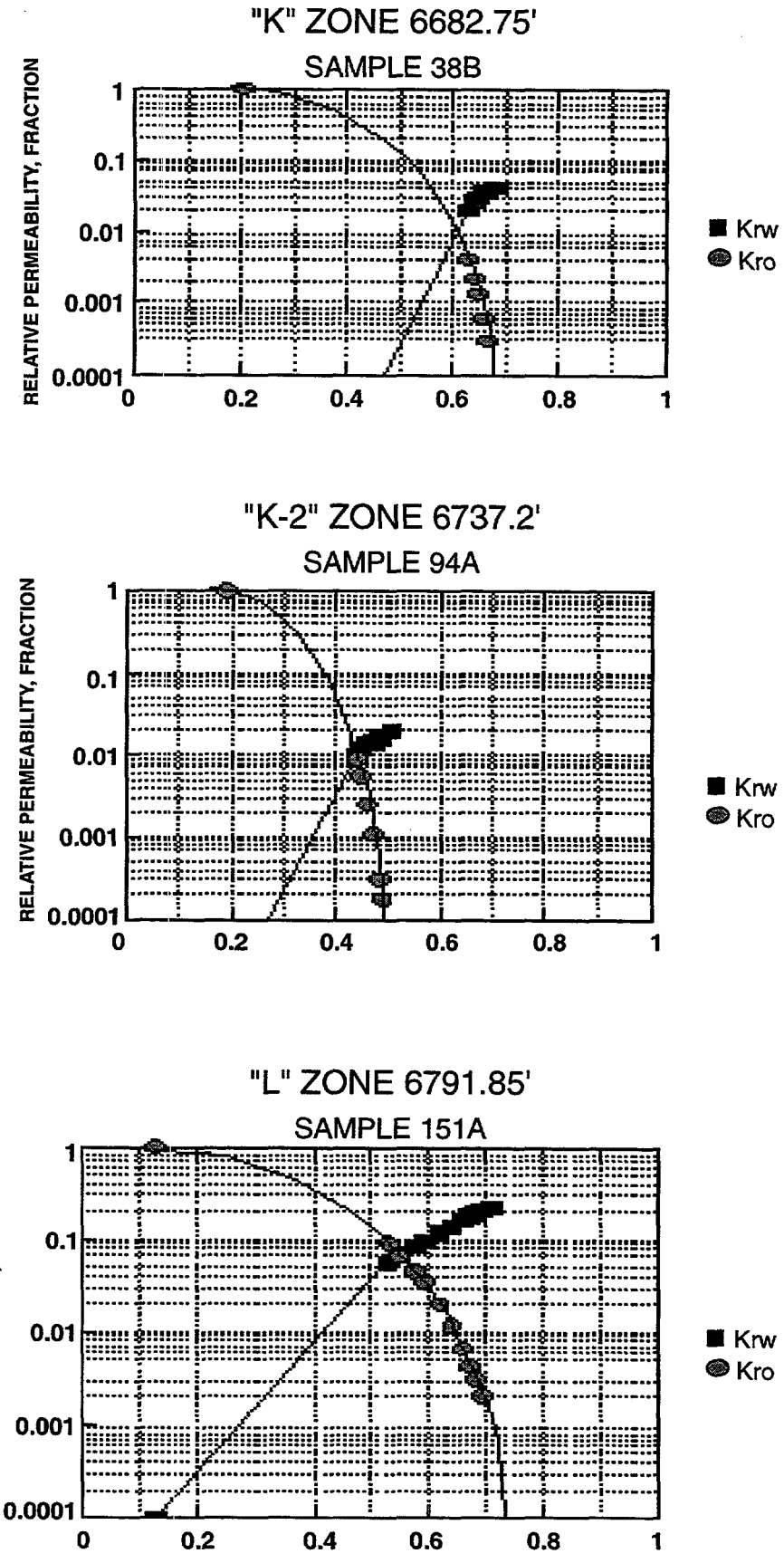

Fig. 11. Water-oil relative permeabilities.

Mixture Psat psig	NITROGEN GOR Injected scf/bbl	Viscosity cp	Relative Volume	Mixture Psat psig	CARBON DIOXIDE GOR Injected scf/bbl	Viscosity cp	Relative Volume	Mixture Psat psig	SEPARATOR GAS GOR Injected scf/bbl	Viscosity cp	Relative Volume
Orig. 1477	0	0.684	1.0000	Orig. 1477	0	0.684	1.0000	Orig. 1477	0	0.684	1.0000
1667	2.23		1.0041	1638	130		1.0455	1830	113		1.0672
1844	4.32		1.0102	1772	256		1.0744	1981	156		1.0777
2015	6.32	0.653	1.0178	1911	426	0.354	1.1180	2165	196	0.439	1.1025

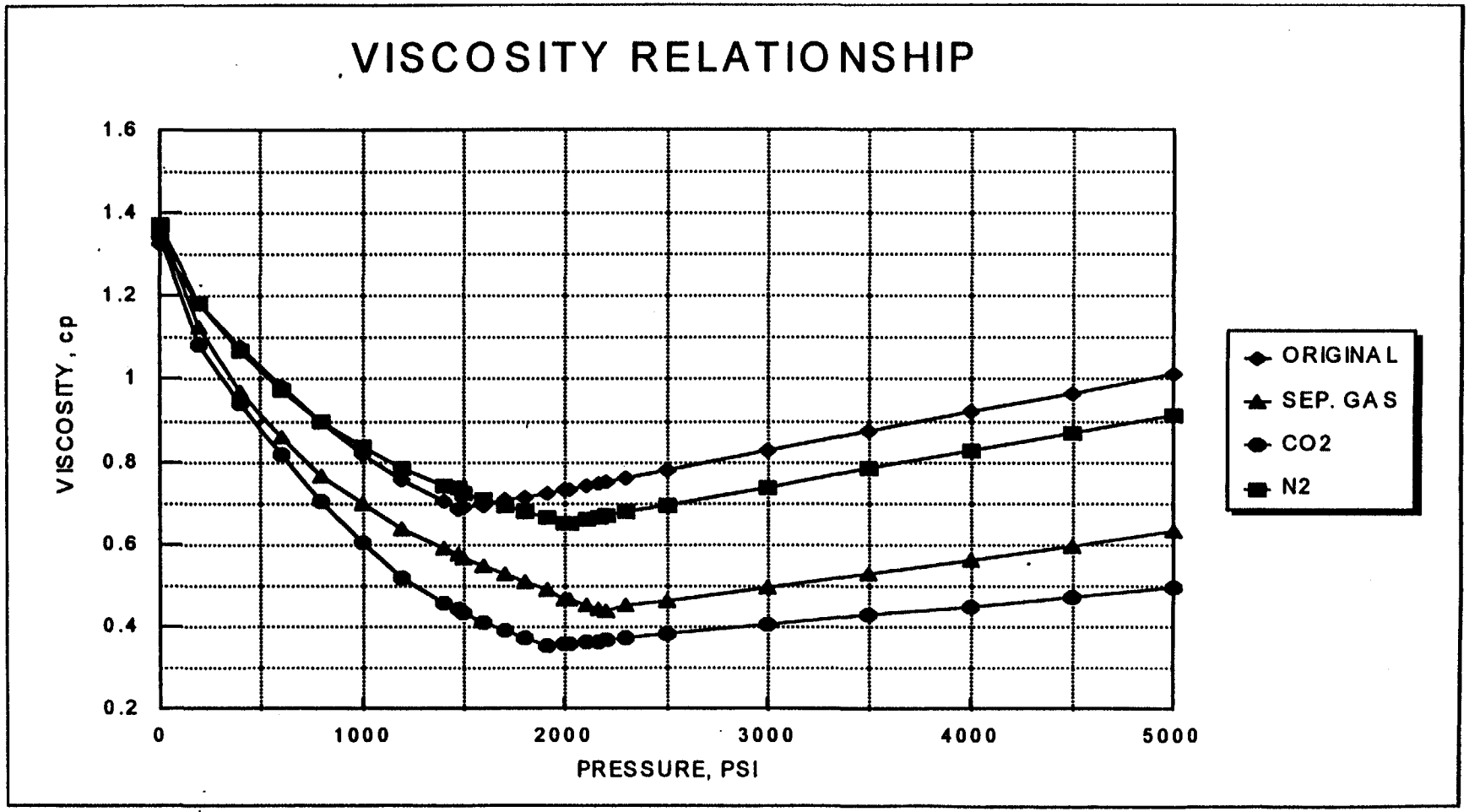

Figure 12. Fluid swelling and solubility test results.

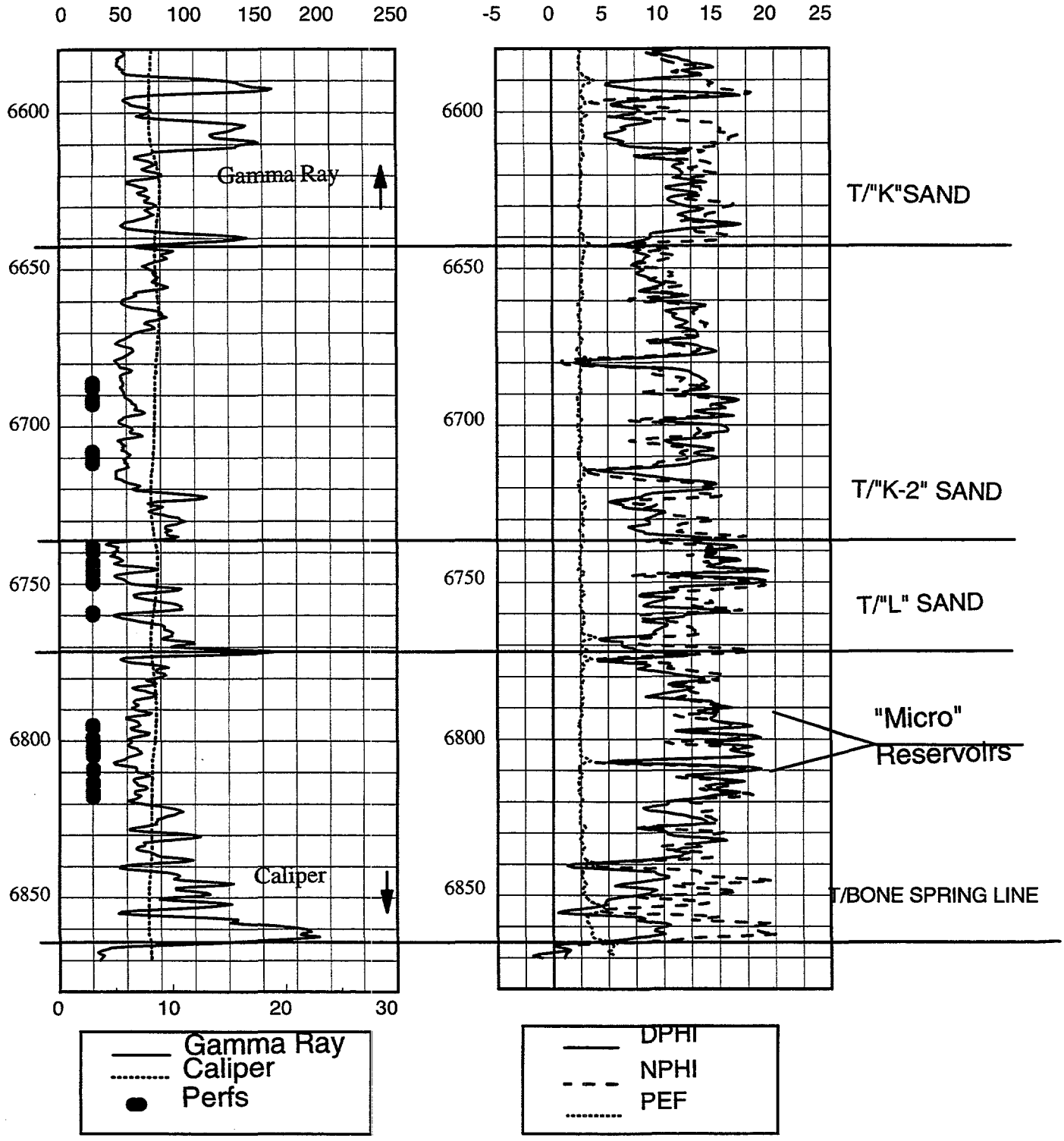

Figure 13. Basal Brushy Canyon sands showing stacking of thin, multiple reservoir packages. Each sand is composed of stacked "micro" reservoirs with vertical permeability barriers.

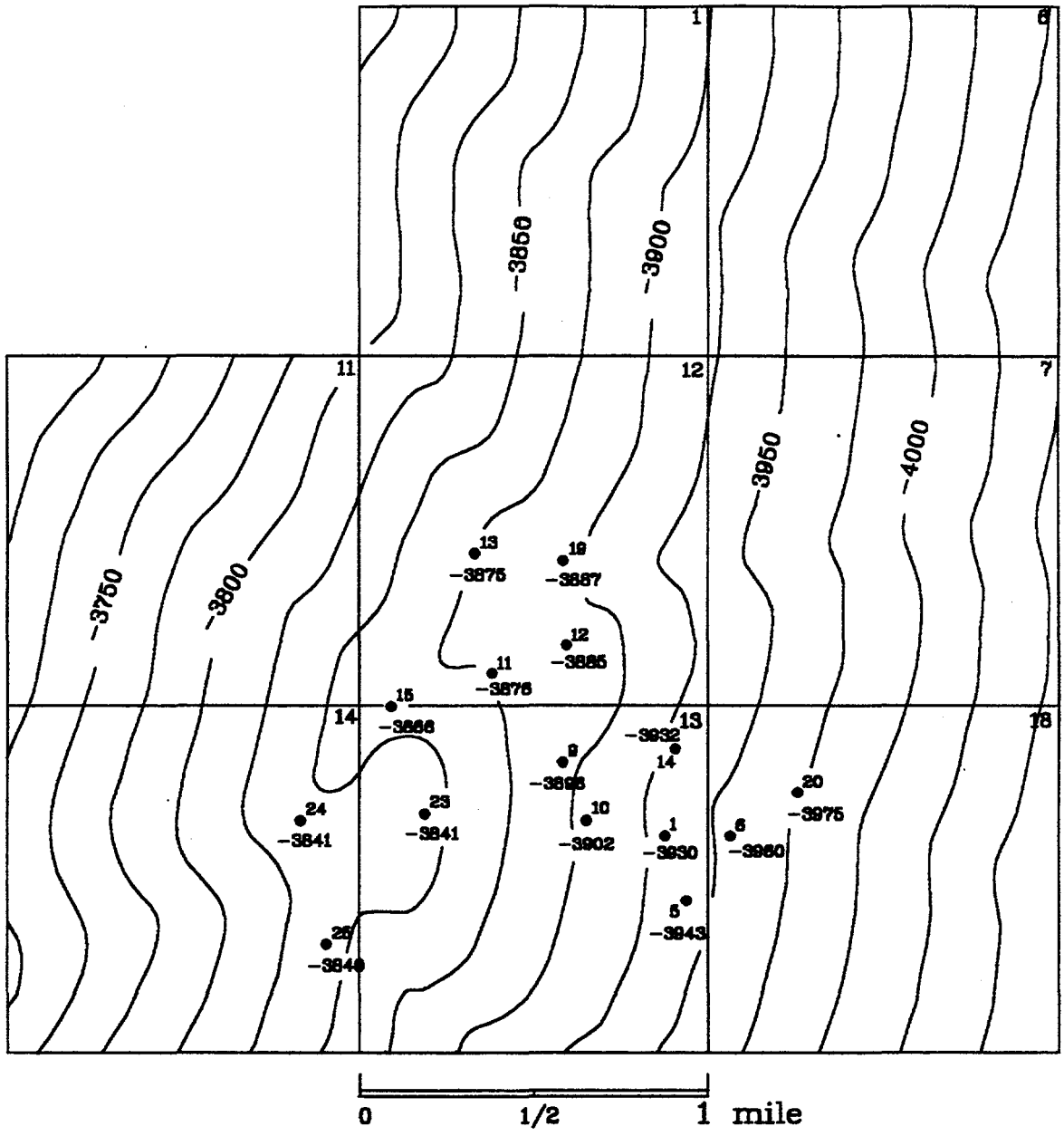

NASH DRAW UNIT

EDDY COUNTY, NEW MEXICO

STRUCTURE MAP
TOP/ BONE SPRING LIME

CONTOUR INTERVAL: 25 FEET

GEOLOGIST: R. USZYNSKI

Figure 14. Structure map top - Bone Spring Limestone.

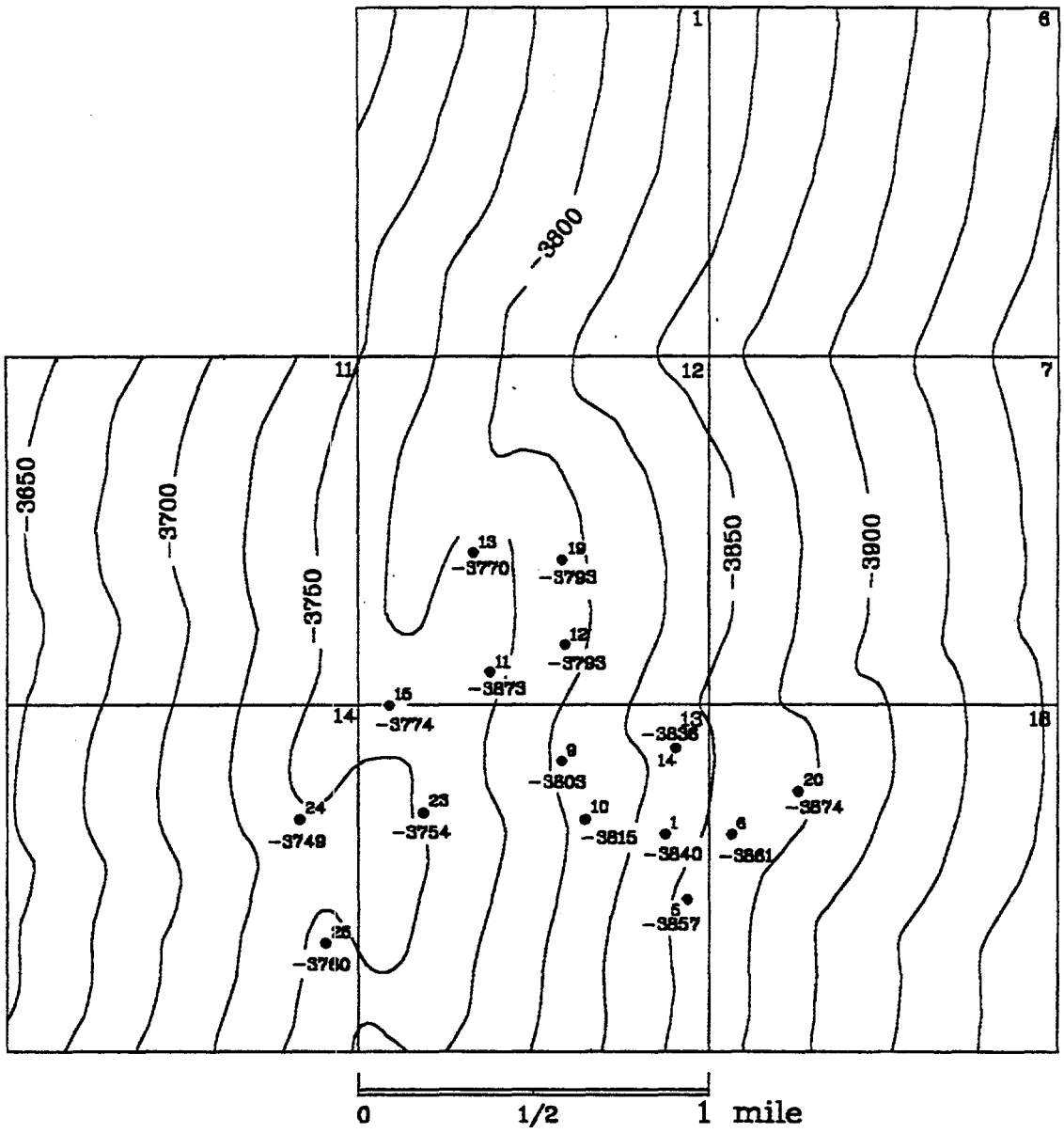

NASH DRAW UNIT

EDDY COUNTY, NEW MEXICO

STRUCTURE MAP

TOP/ " L " SAND

CONTOUR INTERVAL: 25 FEET

GEOLOGIST: B. USZYNSKI

Figure 15. Structure map - Top "L" Sand.

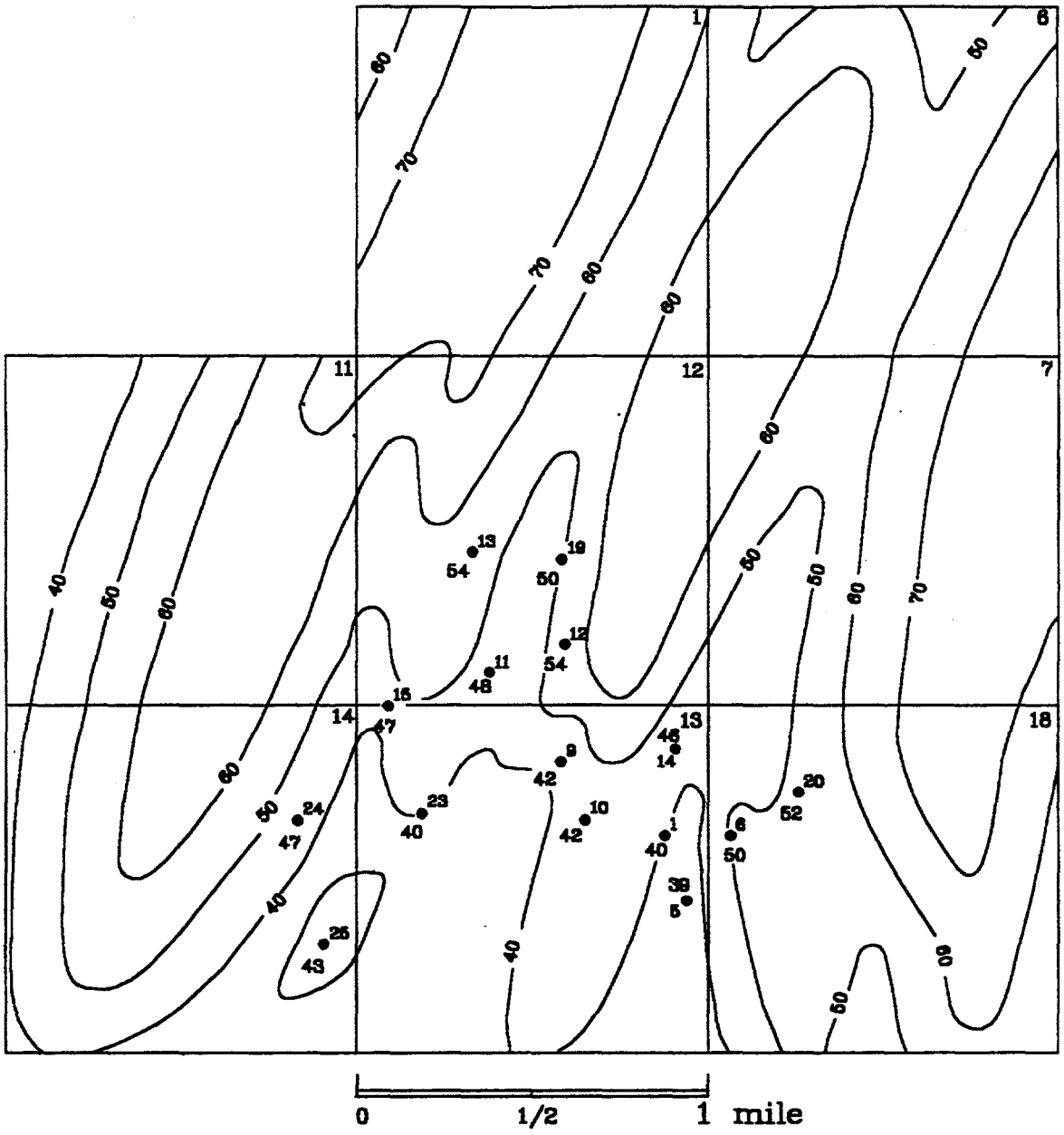

NASH DRAW UNIT

EDDY COUNTY, NEW MEXICO

INTERVAL ISOPACH MAP
BASAL BRUSHY CANYON "L" SAND

CONTOUR INTERVAL:

GEOLOGIST: R. USRYNSKI

Figure 16. Interval isopach map - Basal Brushy Canyon "L" Sand.

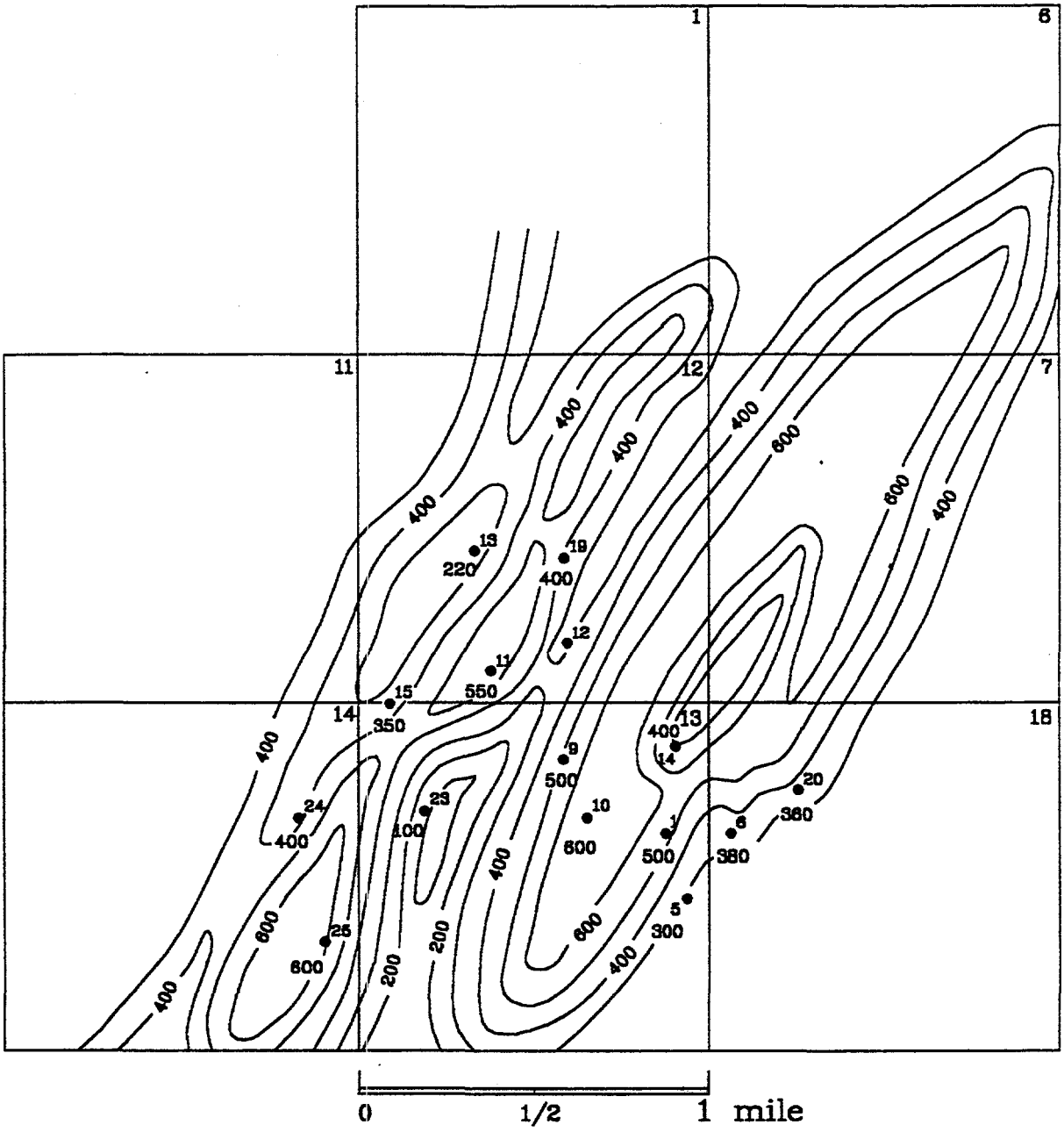

NASH DRAW UNIT

EDDY COUNTY, NEW MEXICO

ISOPRESSURE MAP – "L" SAND

HEIGHT ABOVE FREE WATER – Hcp

CONTOUR INTERVAL: 100 FEET

GEOLOGIST: B. USZYNSKI

Figure 17. Isopressure map - "L" Sand.

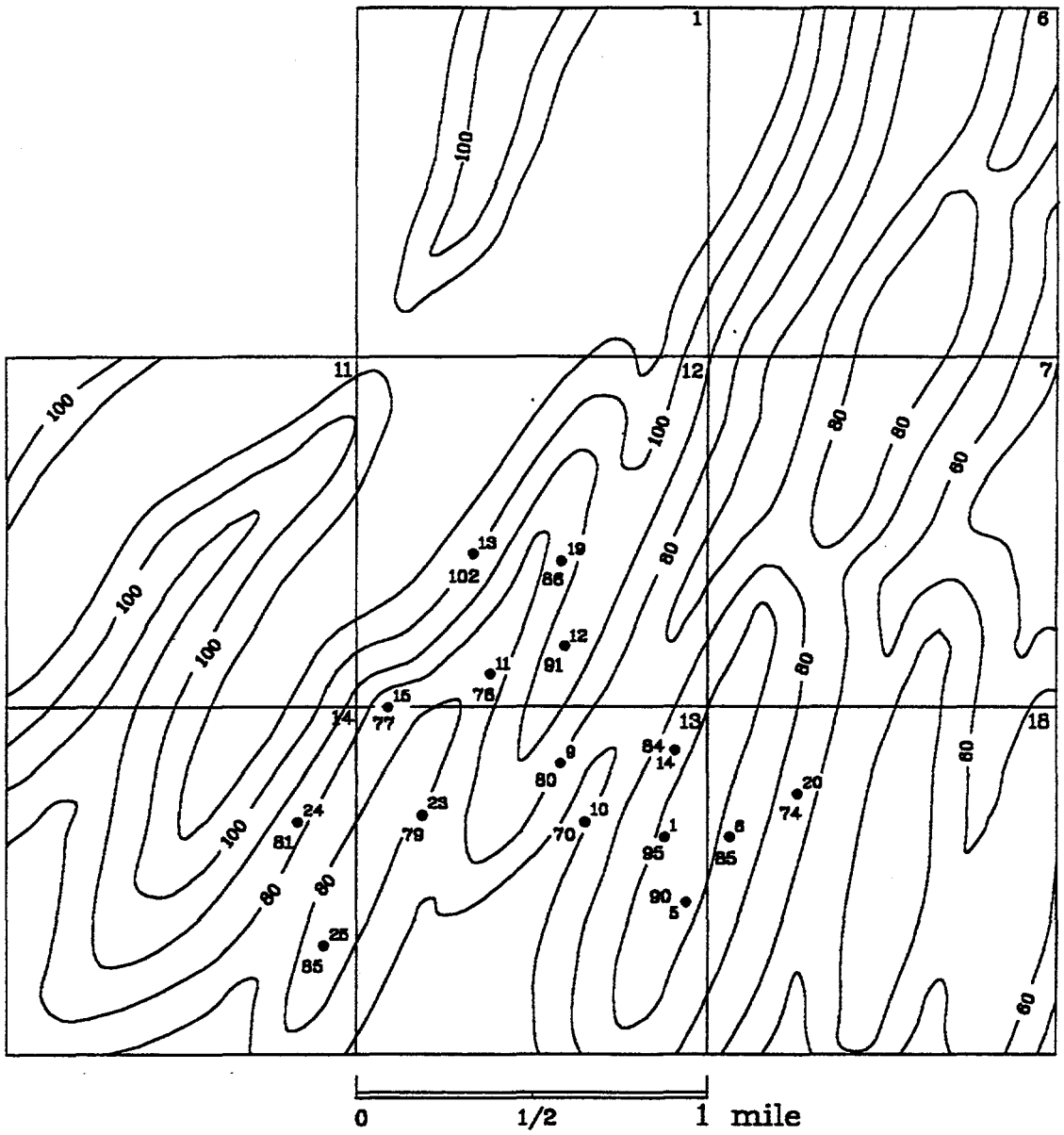

NASH DRAW UNIT

EDDY COUNTY, NEW MEWIXO

INTERVAL ISOPACH MAP

BASAL BRUSHY CANYON "K" SAND

CONTOUR INTERVAL: GEOLOGIST: R. USZYNSKI

Figure 18. Interval isopach map - Basal Brushy Canyon "K" Sand.

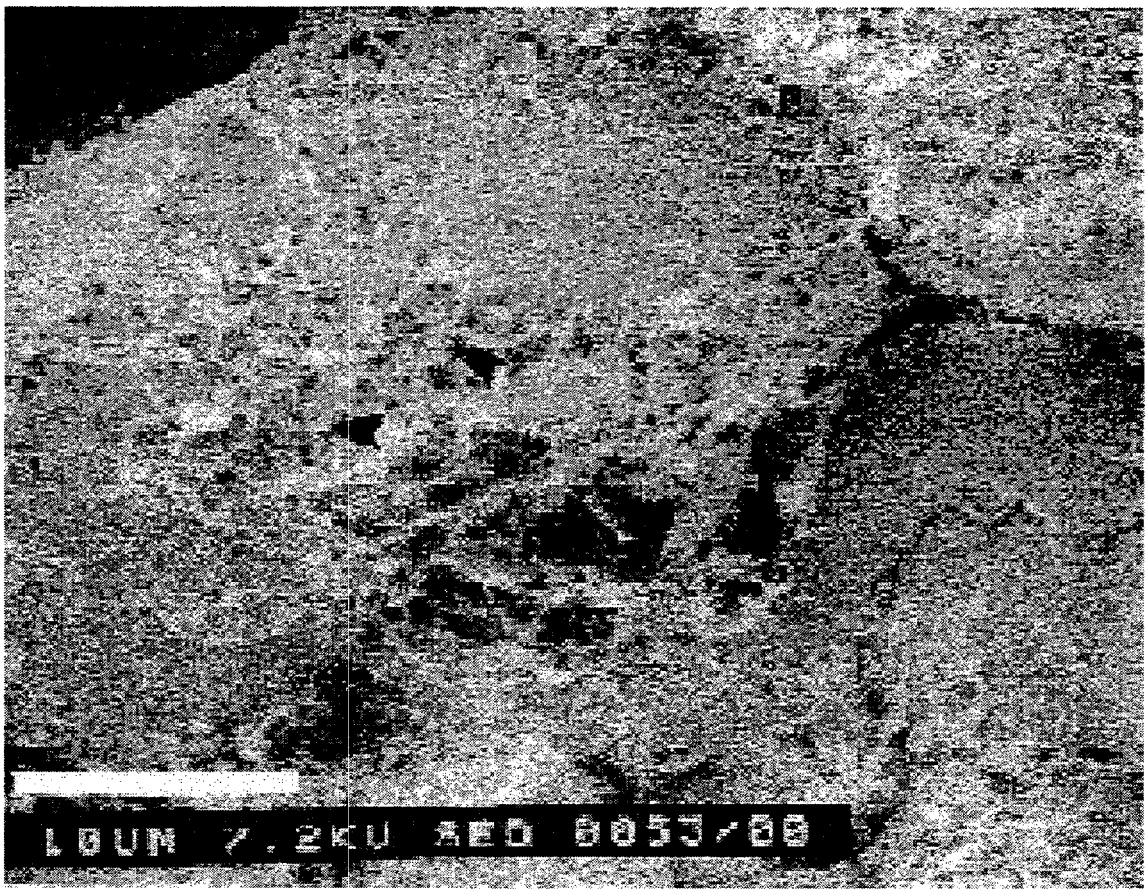

Figure 19. Detailed view of boxwork chlorite and fibrous illite cements occluding porosity. Length of scale: 50 microns. Sample 6652.7.

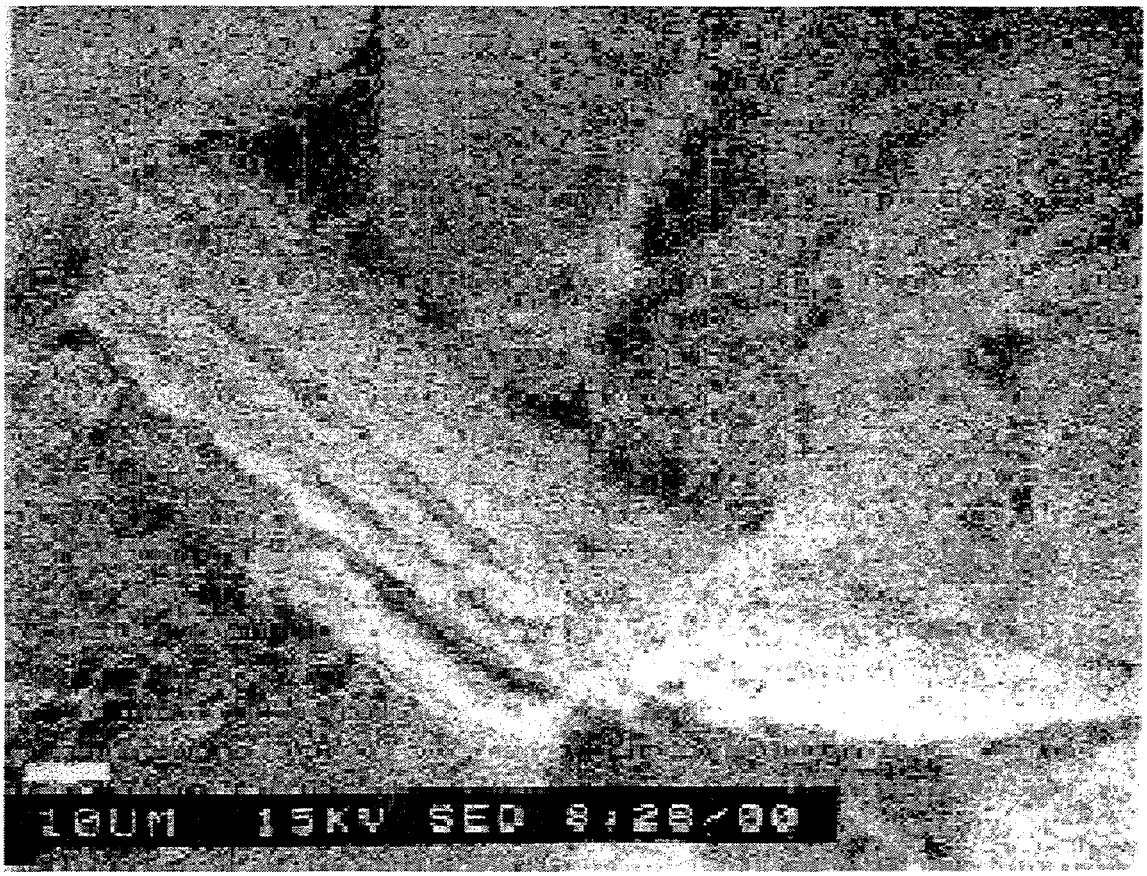

Figure 20. Interparticle porosity occluded by chlorite cement (center-right at top of photo). Note also the partially dissolved feldspar grains with microporosity (left-center). Length of scale: 20 microns. Sample 6692.6.

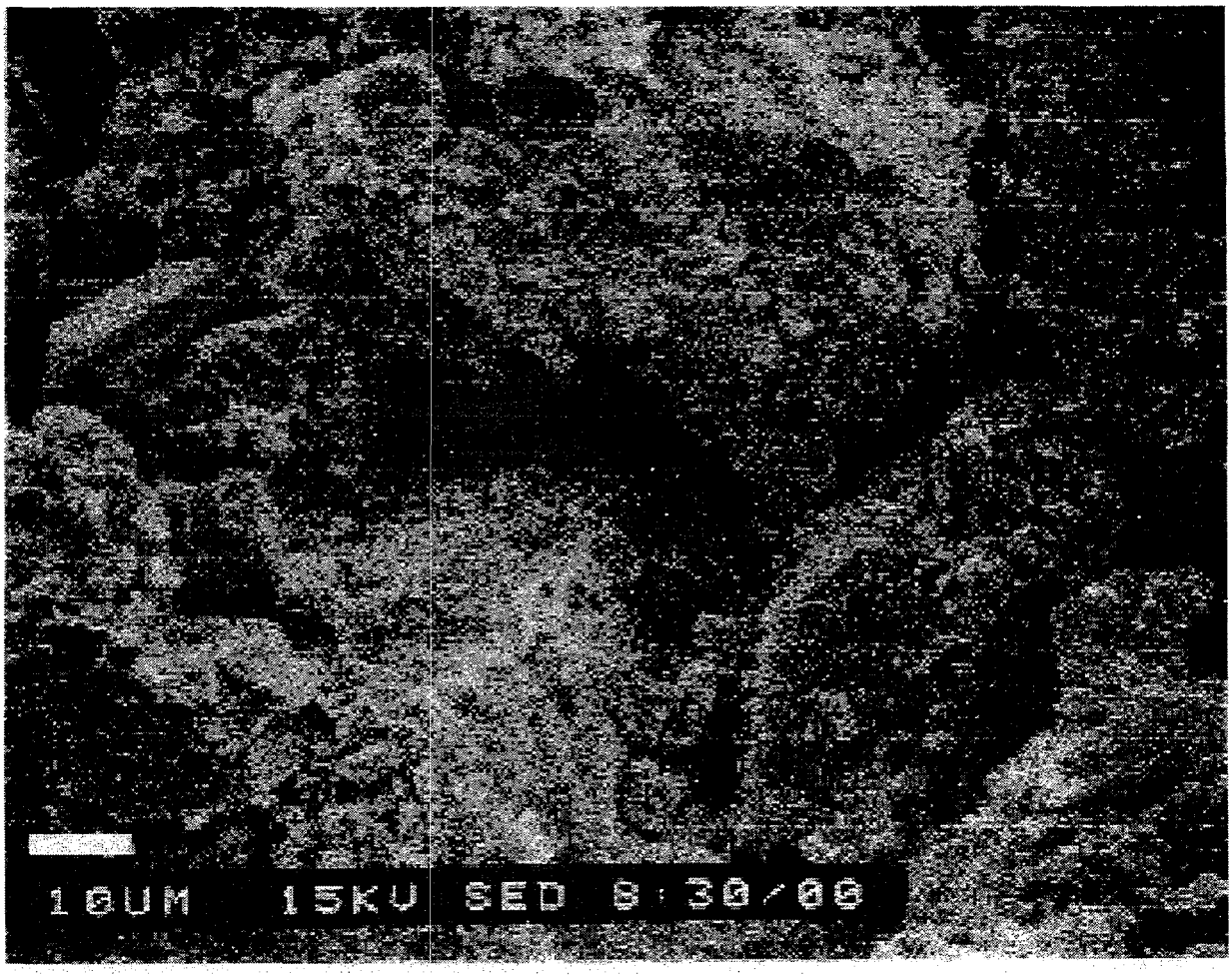

Figure 21. Small pores with abundant fine crystalline interparticle quartz cement partially occluding pores. Length of scale: 30 microns. Sample 6816.1.

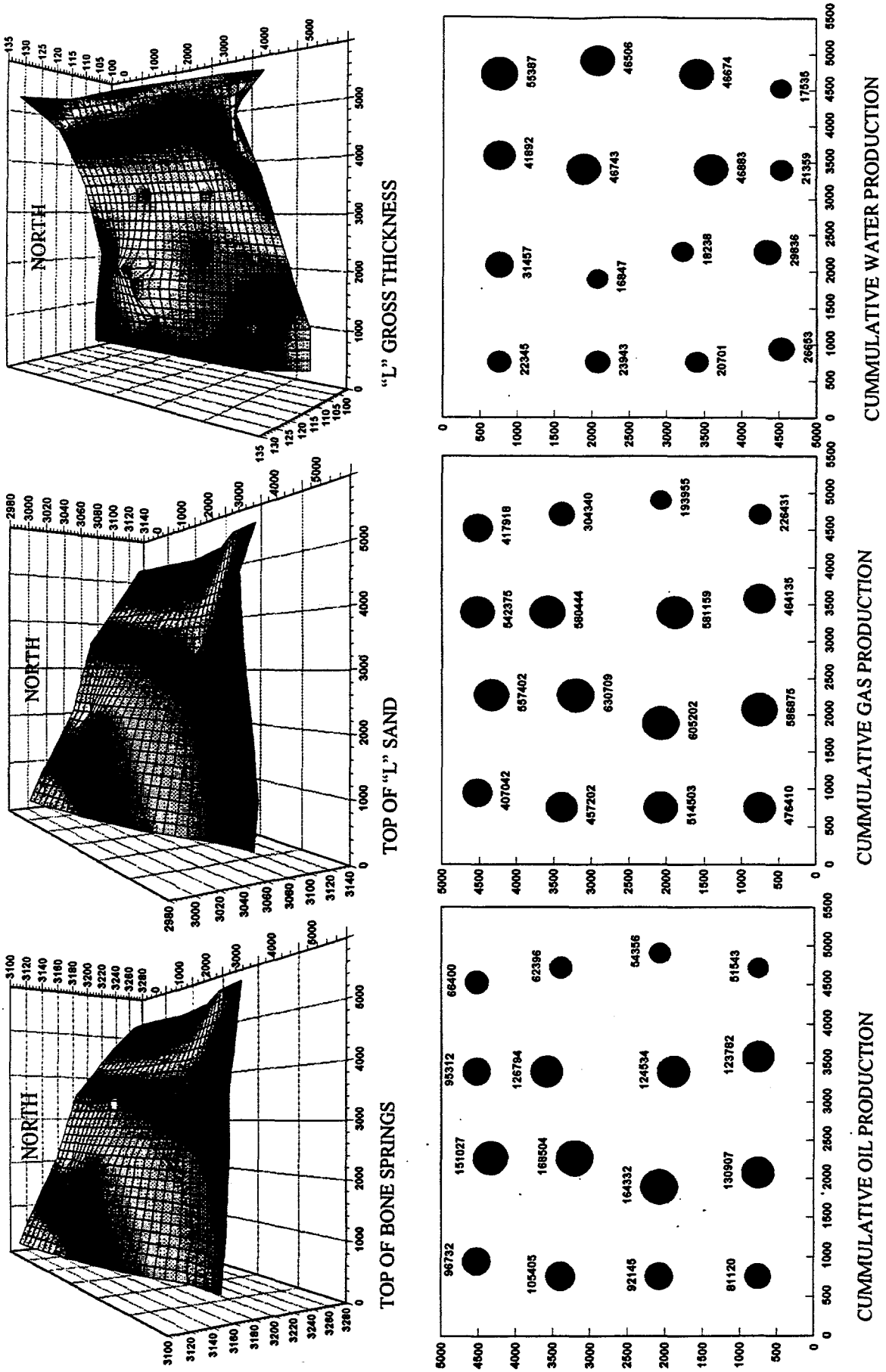

Figure 22. Analog area section 14, T23S - R28E.

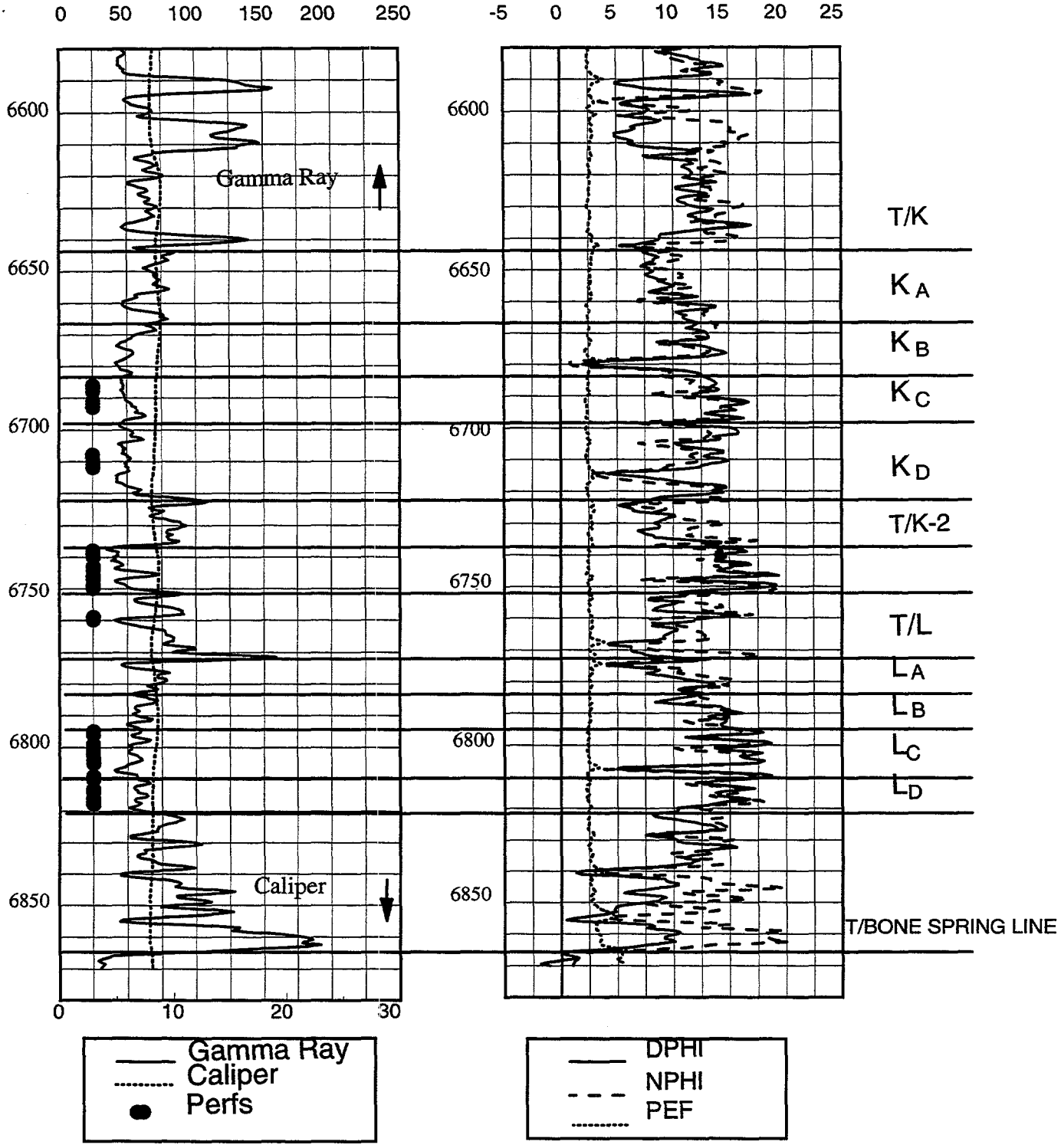

Figure 23. Subdivision of reservoir sands for initial distribution of reservoir attributes for simulation.

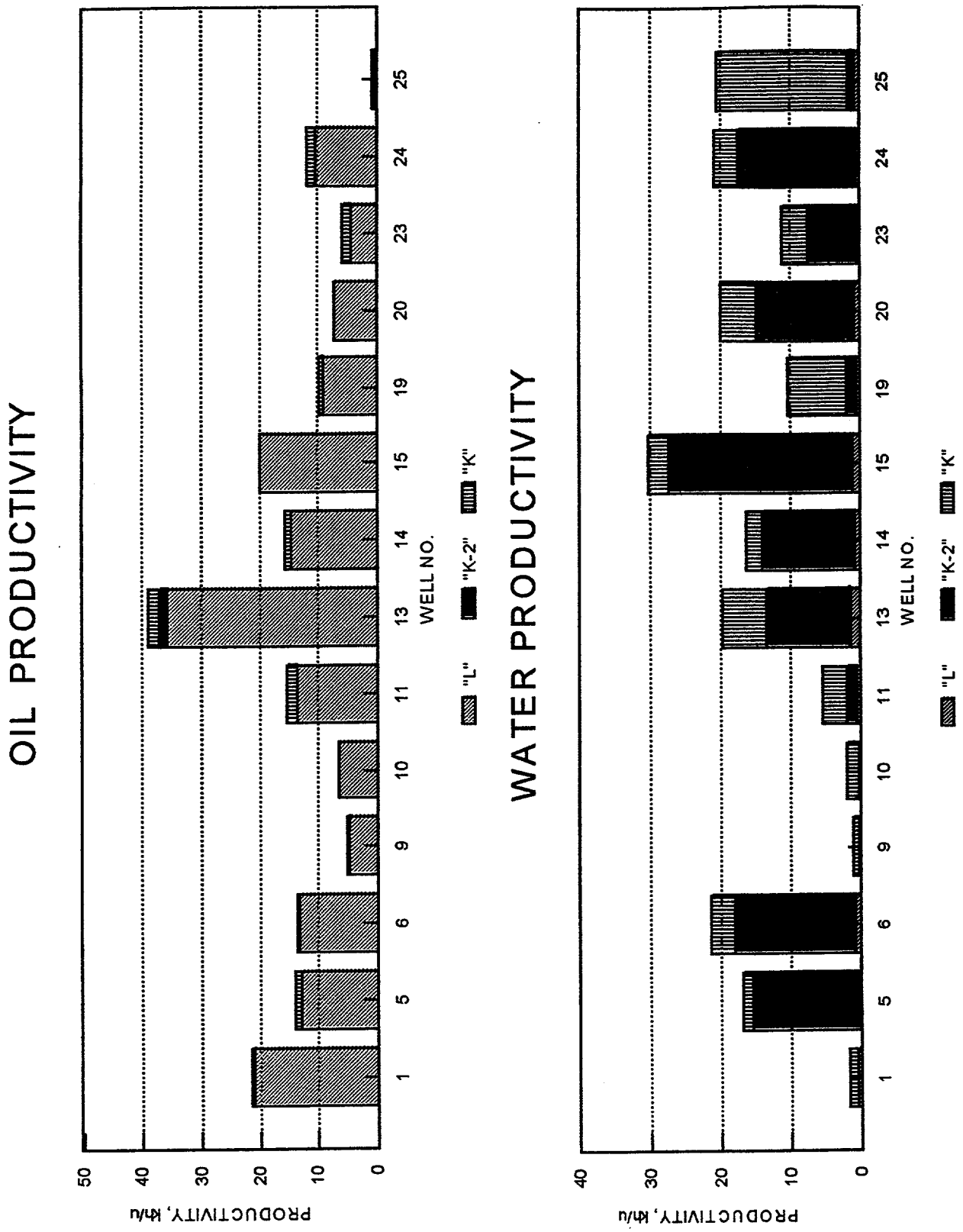

Figure 24. Productivity values used for production allocations.

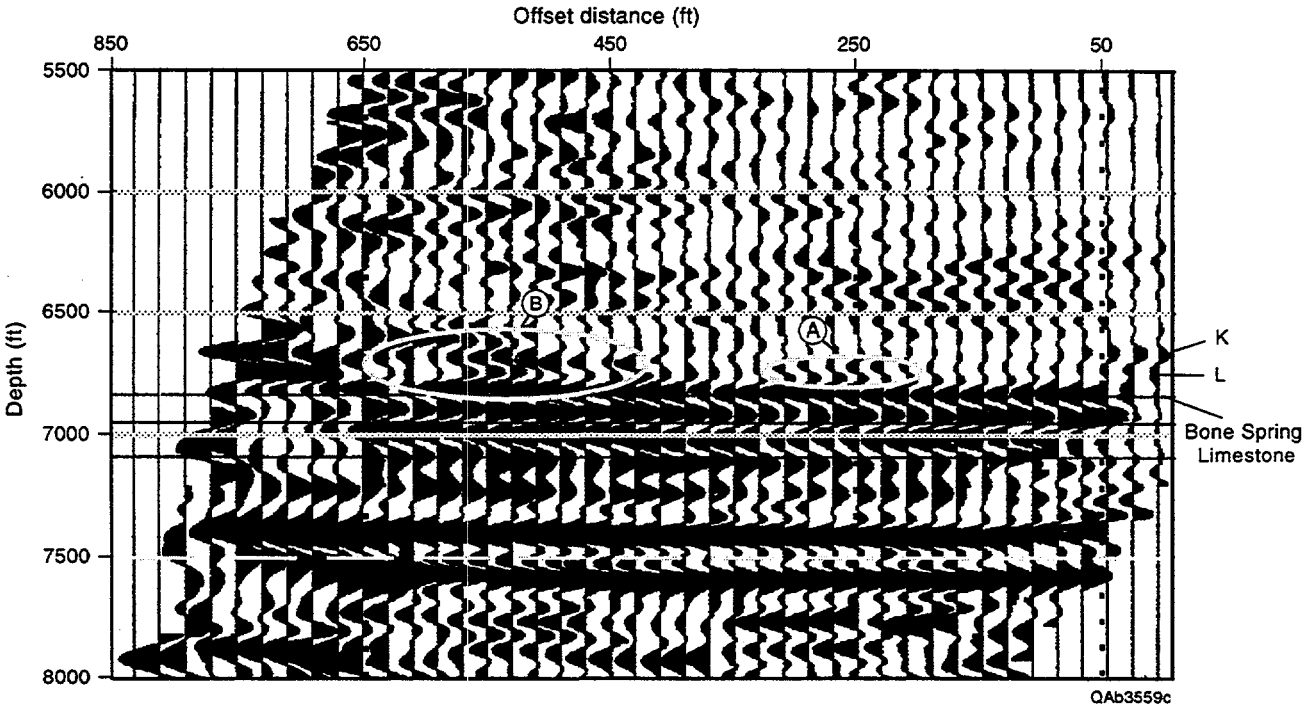

Figure 25. VSP image showing wavelet peak in "K" sand and wavelet trough in "L" sand.

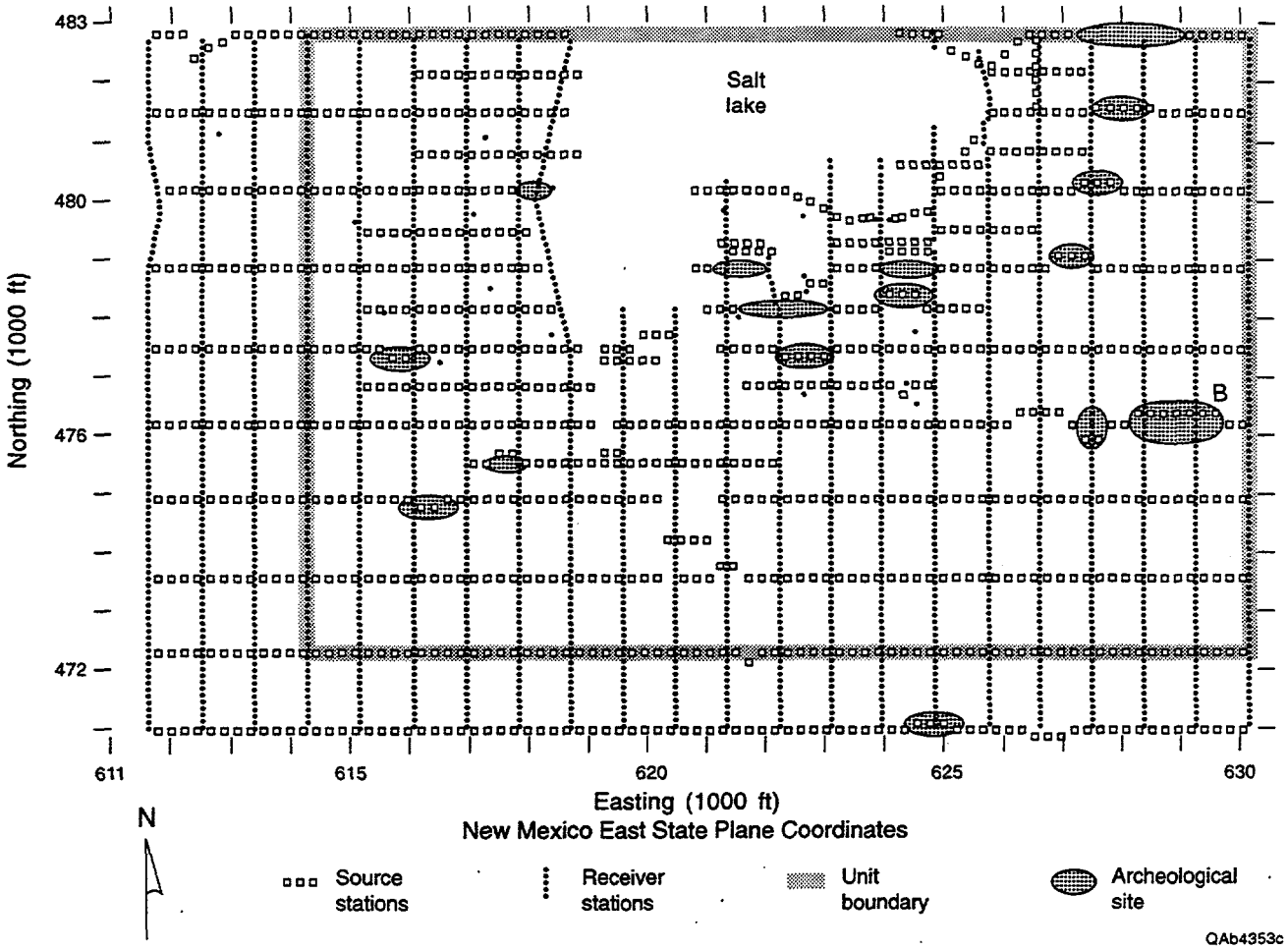

Figure 26. Final 3-D seismic geometry used at Nash Draw.

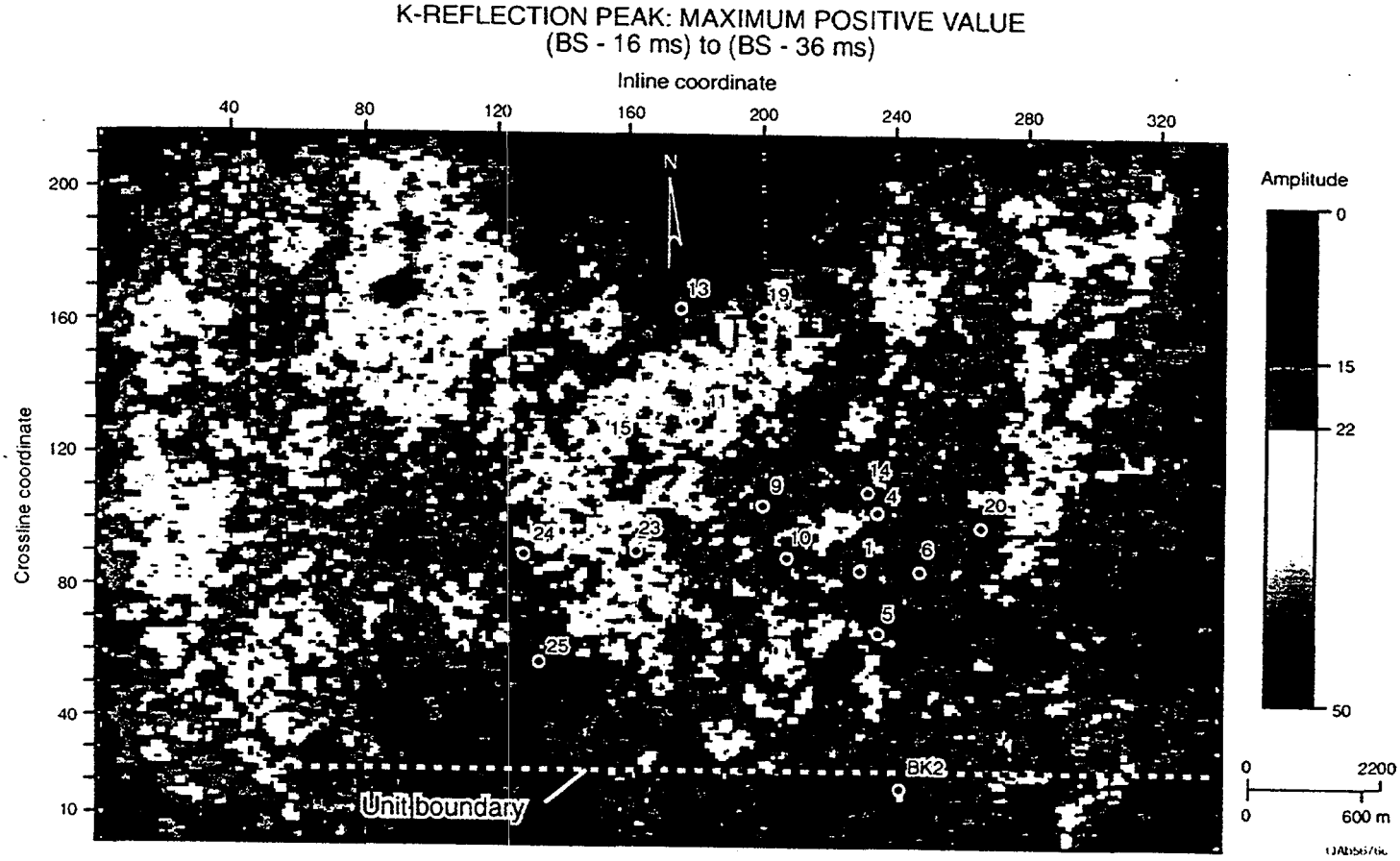

Figure 27. Preliminary Seismic Amplitude Map for "K" Sand at Nash Draw.

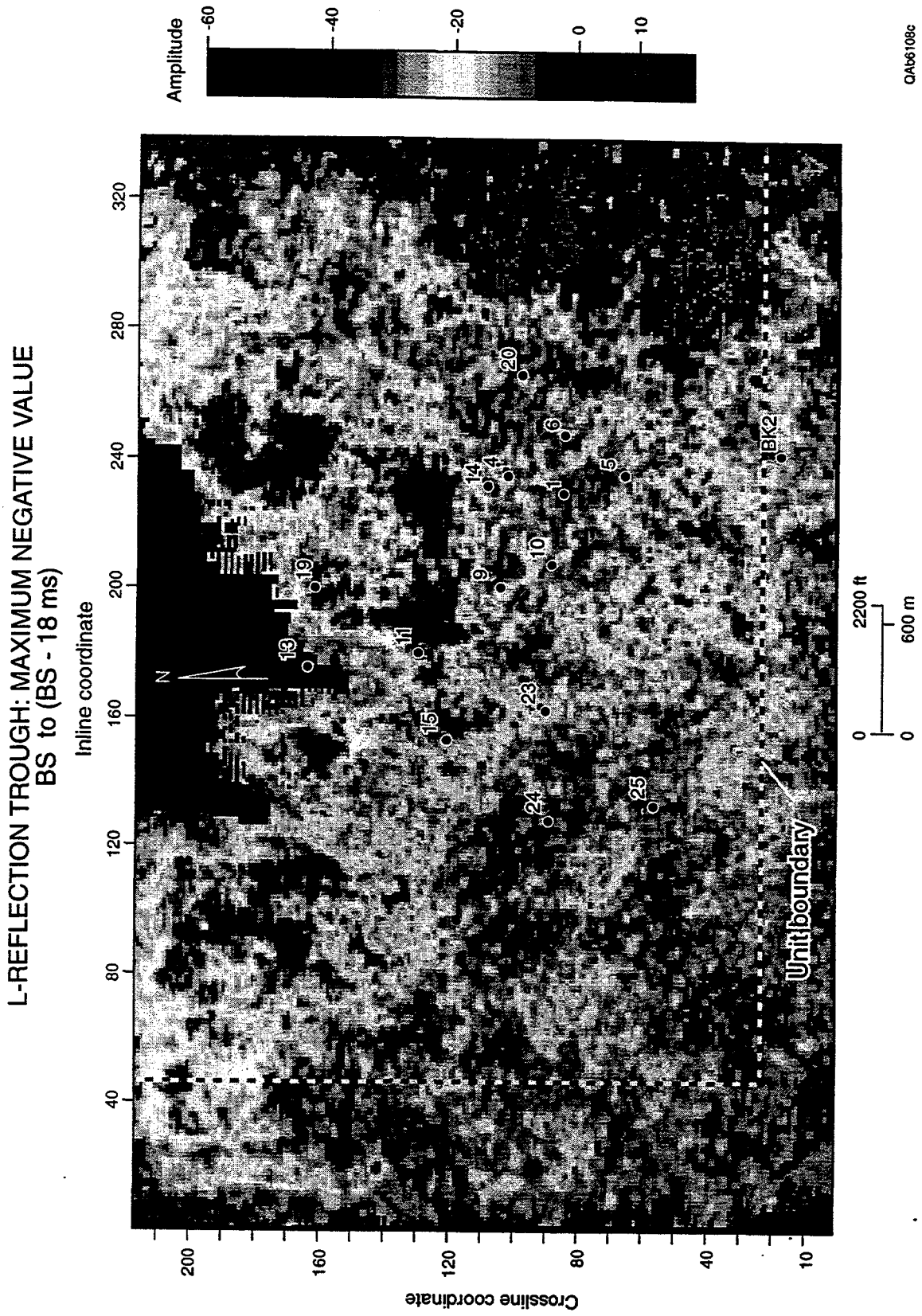

Figure 28. Preliminary Seismic Amplitude Map for "L" Sand at Nash Draw.

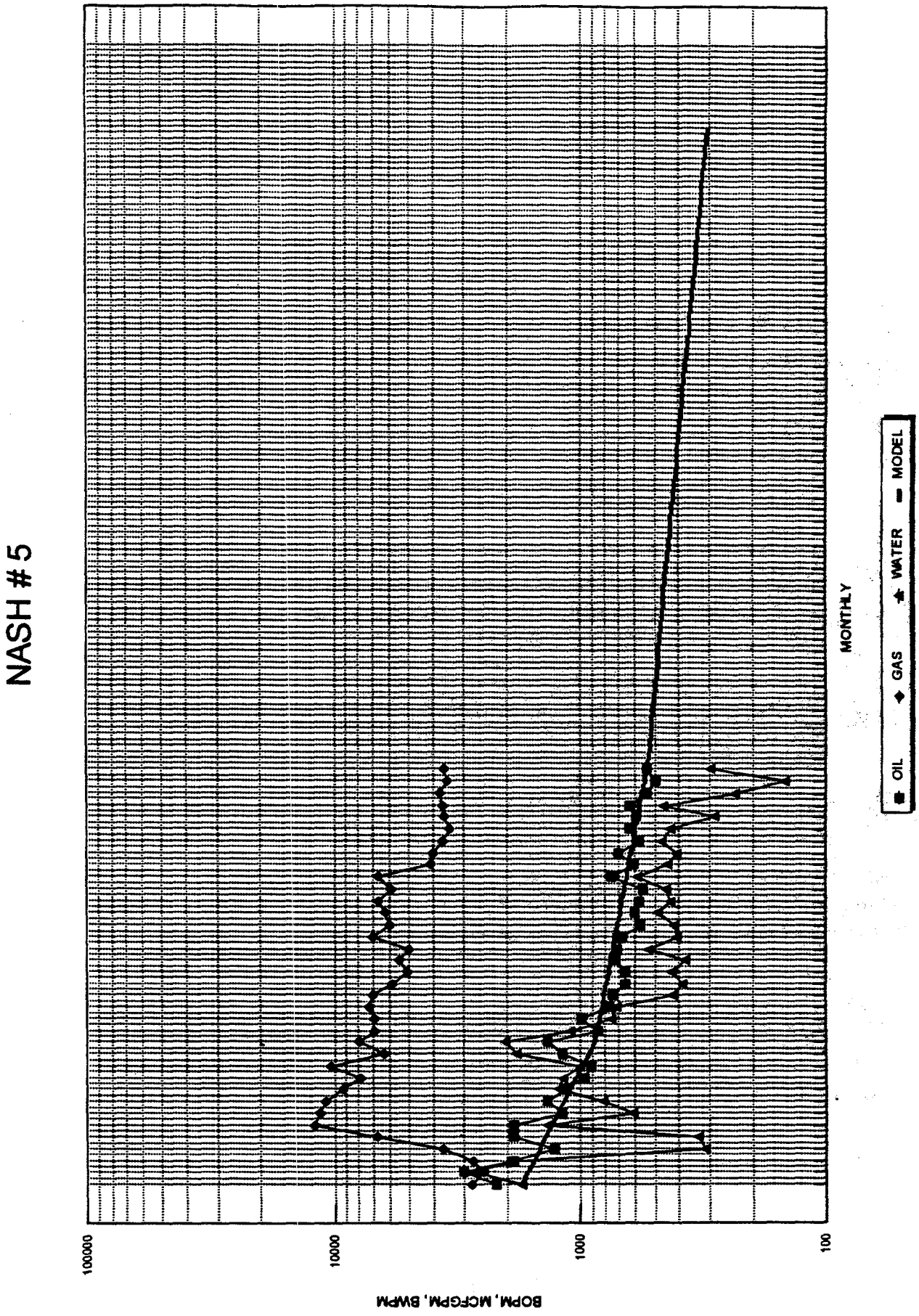

Figure 29. Typical production plot and Delaware Model.

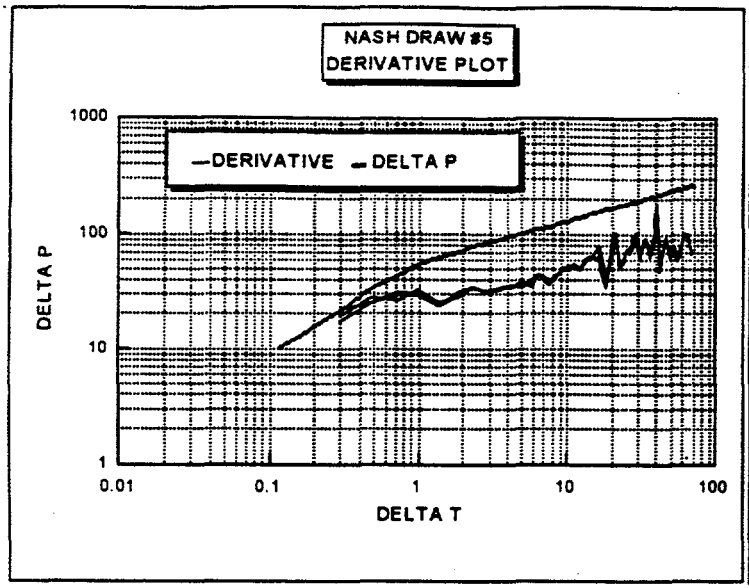

NASH DRAW #5 "L" ZONE AFTER FRAC

[PD/DELTA P]M=	0.0082	
[DELTA T/tDf]M=	7.692308	
[CDf]M=	3E-01	
kh=	41.08595	md-ft
k=	0.838489	md
C=	0.055957	bbl/psi
Lf=	140.8628	
S=	-5.17093	

WELL WITH INFINITE CONDUCTIVITY VERTICAL FRACTURE
INFINITE ACTING RESEVOIR WITH HOMOGENEOUS BEHAVIOR

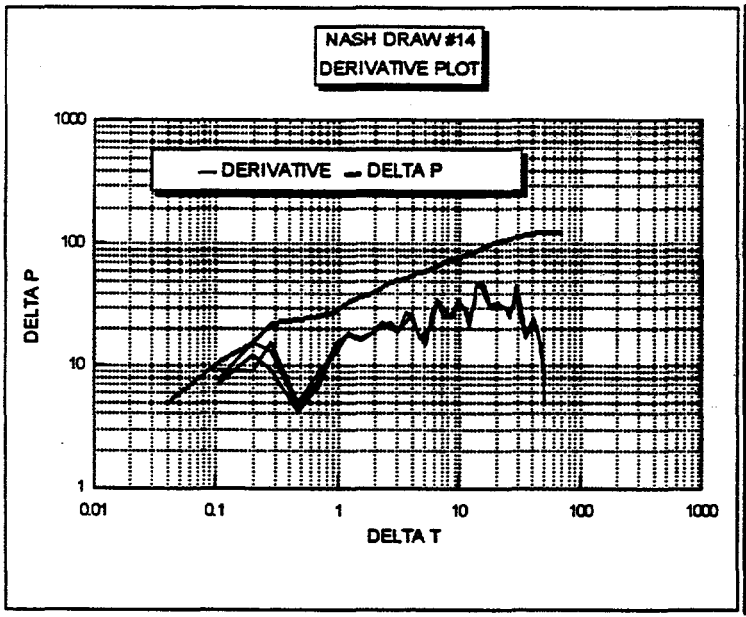

NASH DRAW #14 "L" ZONE AFTER FRAC

[PD/DELTA P]M=	0.015	
[DELTA T/tDf]M=	11.11111	
[CDf]M=	3E-02	
kh=	75.15723	md-ft
k=	1.459364	md
C=	0.015729	bbl/psi
Lf=	246.3285	
S=	-5.72981	

WELL WITH INFINITE CONDUCTIVITY VERTICAL FRACTURE
INFINITE ACTING RESEVOIR WITH HOMOGENEOUS BEHAVIOR

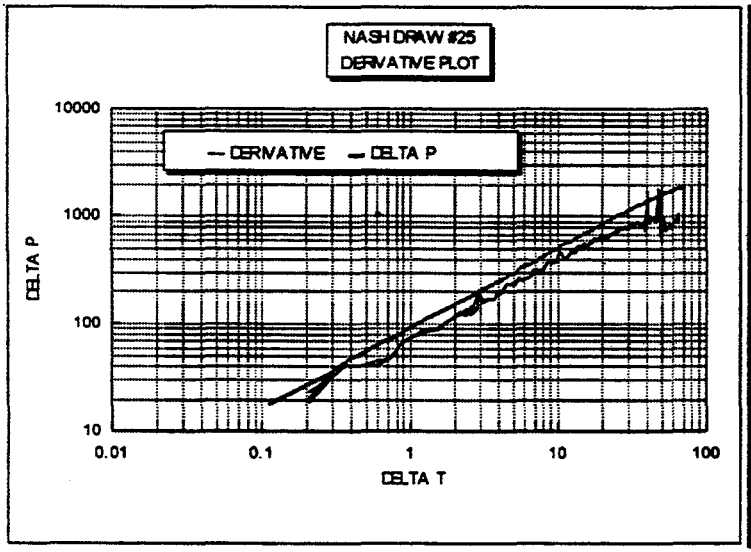

NASH DRAW #25 "K" ZONE AFTER ACID

[PD/DELTA P]M=	0.00193	
[DELTA T/tD/CD]M=	0.13	
[CDe^2S]M=	1E+03	
kh=	14.81397	md-ft
k=	0.58094	md
C=	0.001137	bbl/psi
CD=	160.0262	
S=	0.916209	

WELL WITH WELLBORE STORAGE AND SKIN - INFINITE
ACTING RESEVOIR WITH HOMOGENEOUS BEHAVIOR

Figure 30A. BHP tests and analysis.

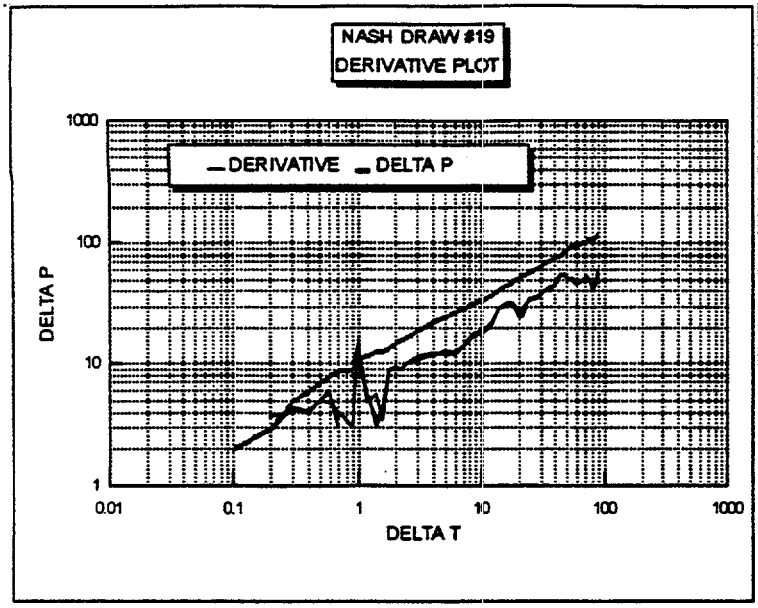

NASH DRAW #19 "K" & "L" ZONE AFTER FRAC

[PD/DELTA P]M=	0.011	
[DELTA T/tDf]M=	40	
[CDf]M=	3E-01	
kh=	117.2666	md-ft
k=	3.553533	md
C=	0.8305	bbl/psi
Lf=	422.4707	
S=	-6.26926	

WELL WITH INFINITE CONDUCTIVITY VERTICAL FRACTURE
INFINITE ACTING RESEVOIR WITH HOMOGENEOUS BEHAVIOR

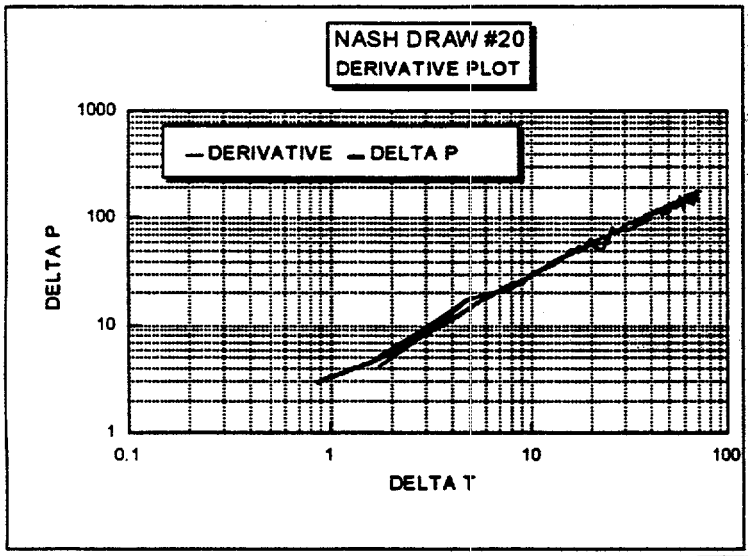

NASH DRAW #20 "L" ZONE AFTER FRAC

[PD/DELTA P]M=	0.015	
[DELTA T/tD/CD]M=	20	
[CDe^2S]M=	1E+11	
kh=	99.14358	md-ft
k=	2.873727	md
C=	1.17025	bbl/psi
CD=	288674.3	
S=	6.377691	

WELL WITH WELLBORE STORAGE AND SKIN - INFINITE
ACTING RESEVOIR WITH HOMOGENEOUS BEHAVIOR

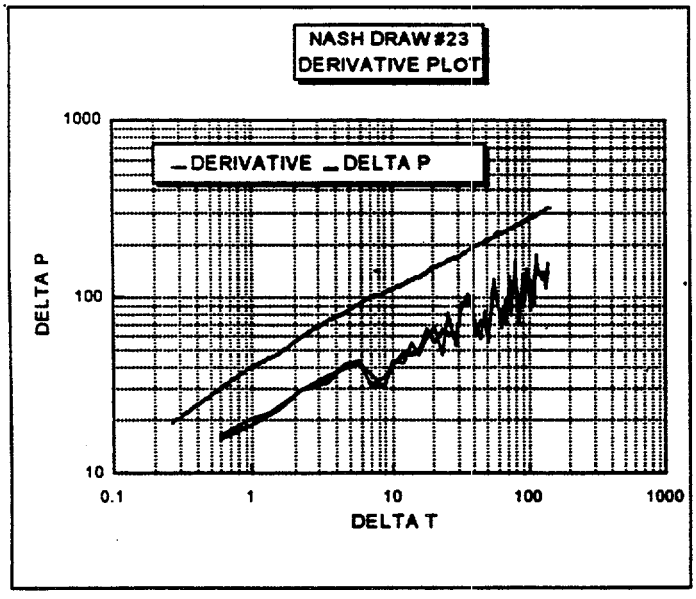

NASH DRAW #23 "K" & "L" ZONE AFTER FRAC

[PD/DELTA P]M=	0.0038	
[DELTA T/tDf]M=	121.9512	
[CDf]M=	3E-03	
kh=	44.2662	md-ft
k=	1.106655	md
C=	0.004084	bbl/psi
Lf=	411.0328	
S=	-6.24182	

WELL WITH INFINITE CONDUCTIVITY VERTICAL FRACTURE
INFINITE ACTING RESEVOIR WITH HOMOGENEOUS BEHAVIOR

Figure 30B. BHP tests and analysis.

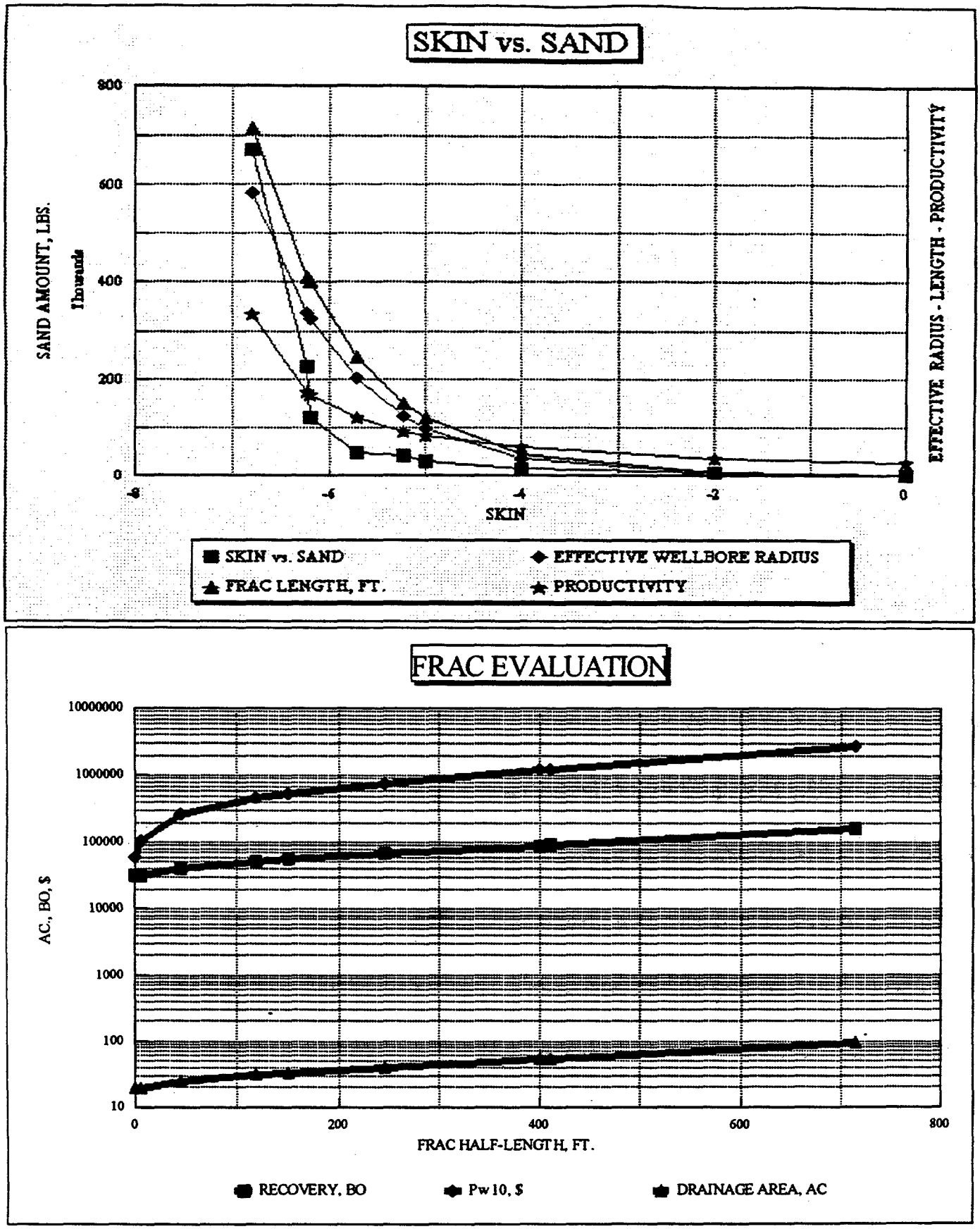

Figure 31. Frac treatment analysis.

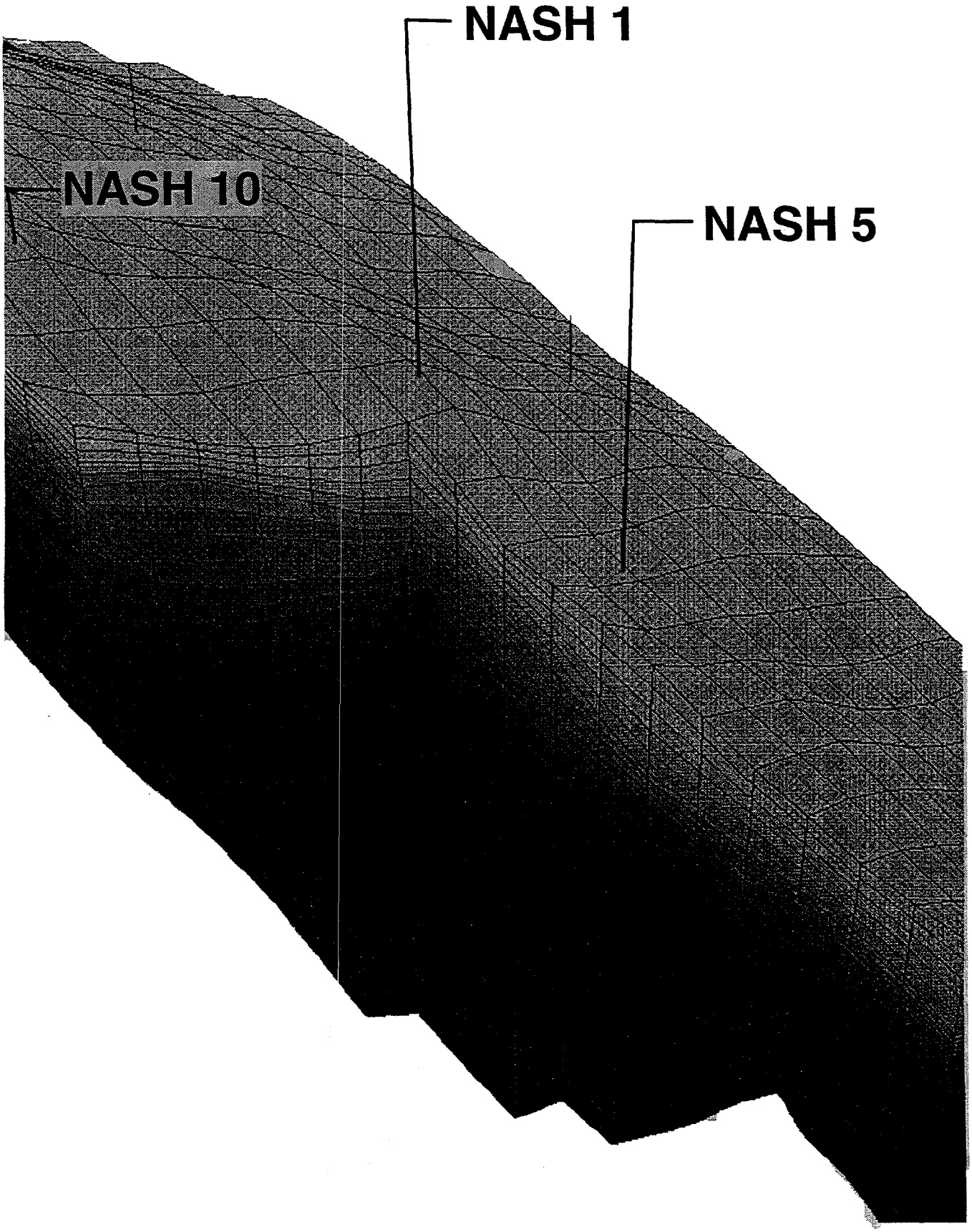

Figure 32. Analog area section 14, T23S - R28E

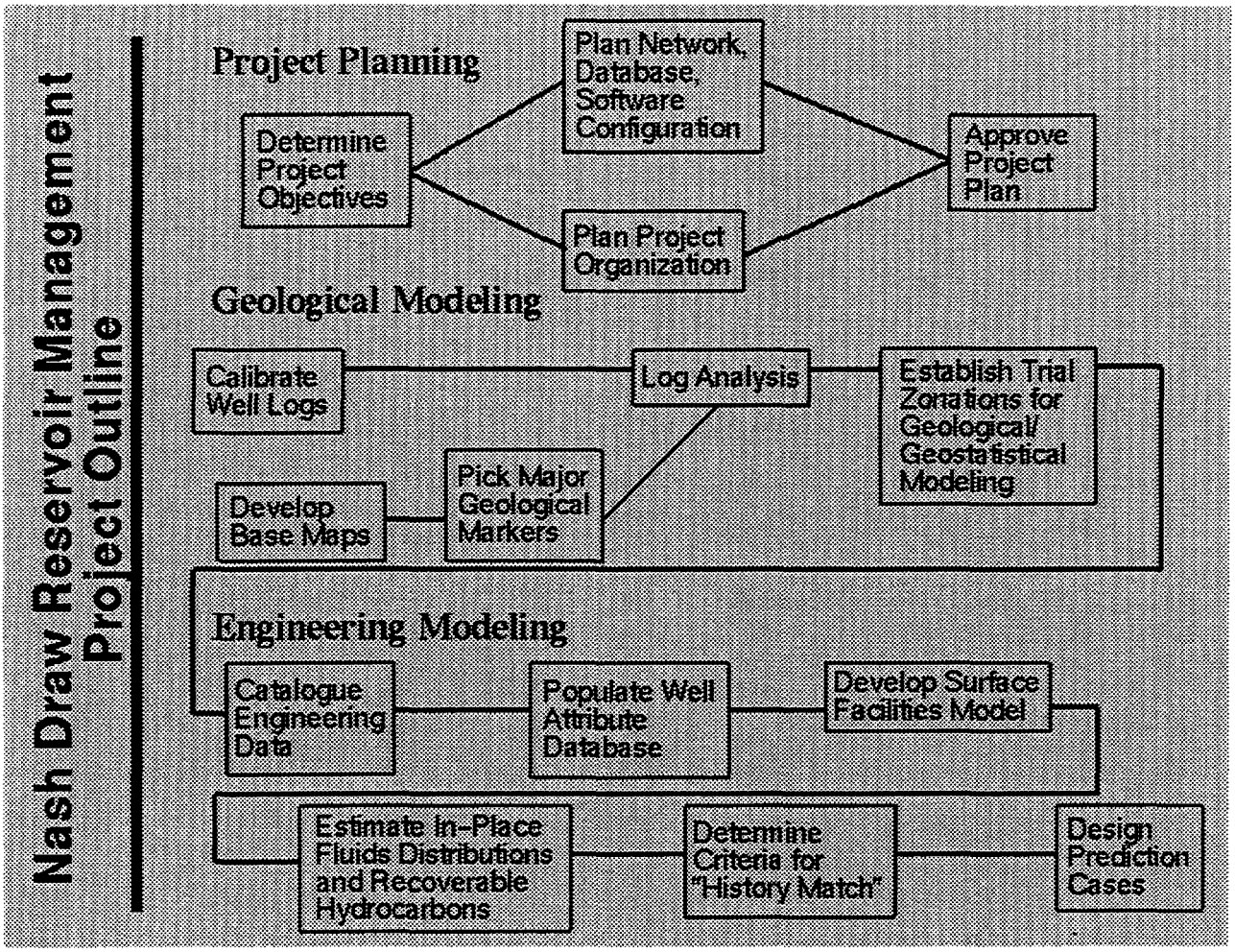

Figure 33. Nash Draw reservoir management project outline.

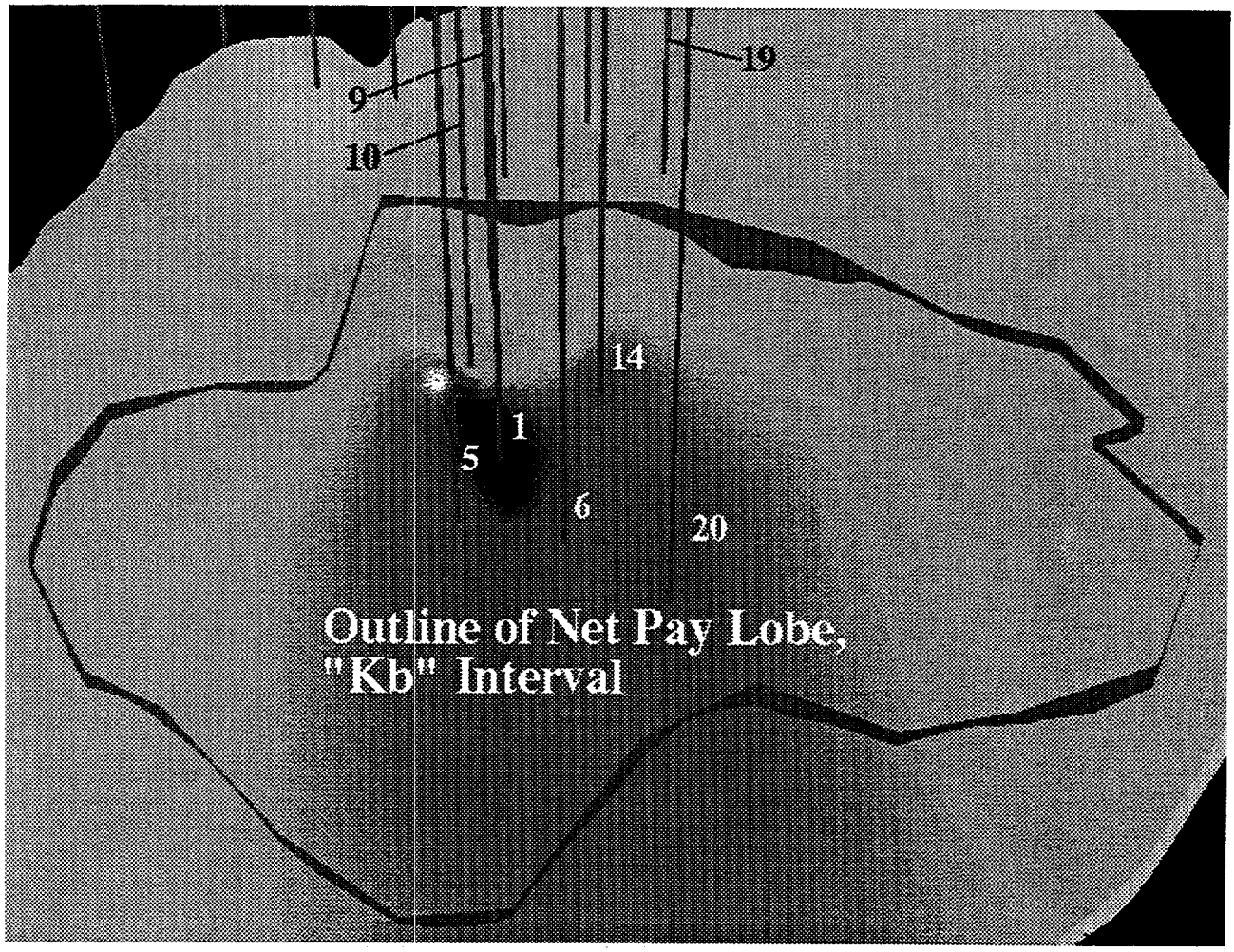

Figure 34. Outline of net pay lobe "Kb" interval.

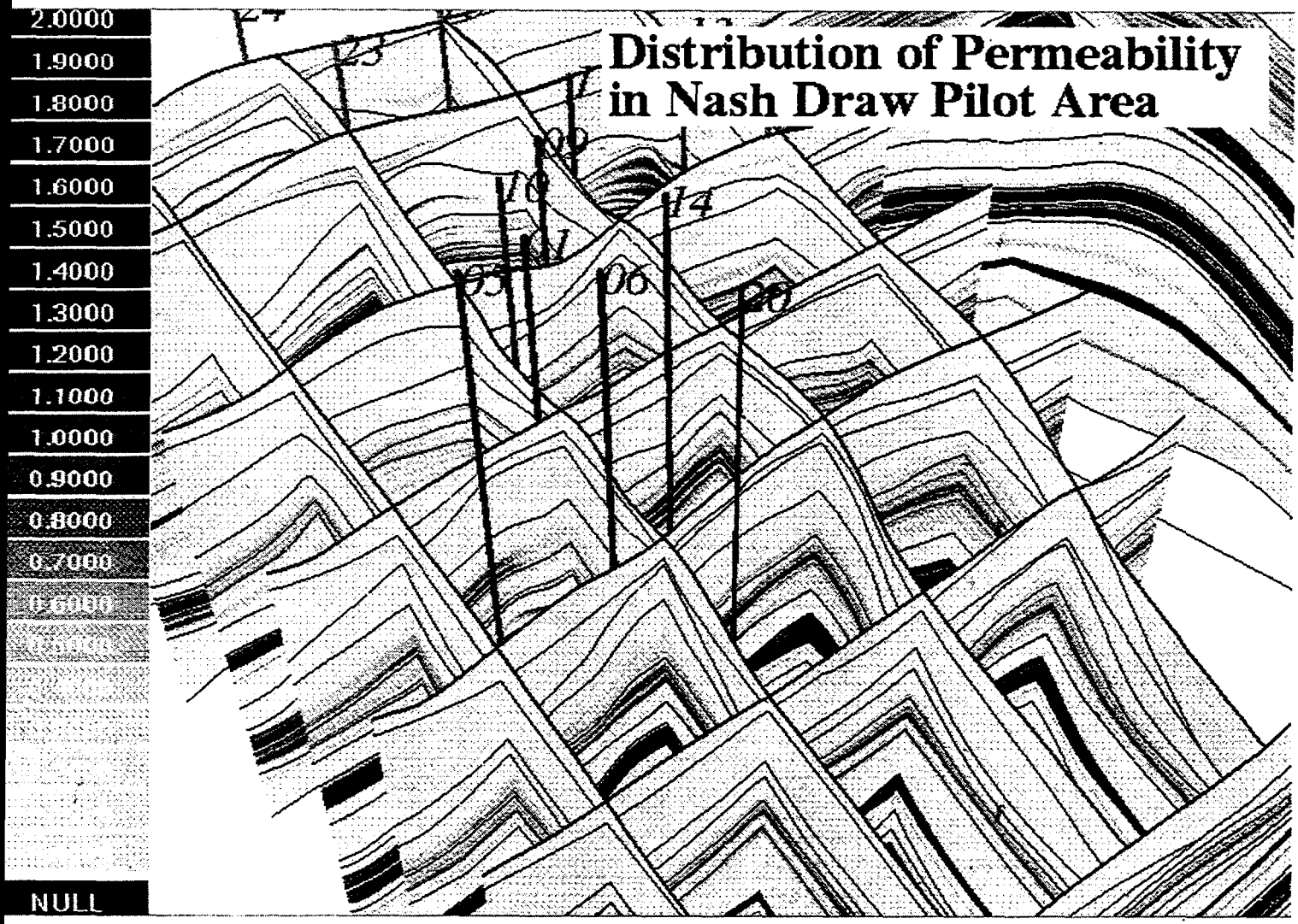

Figure 35. Distribution of permeability in Nash Draw area.

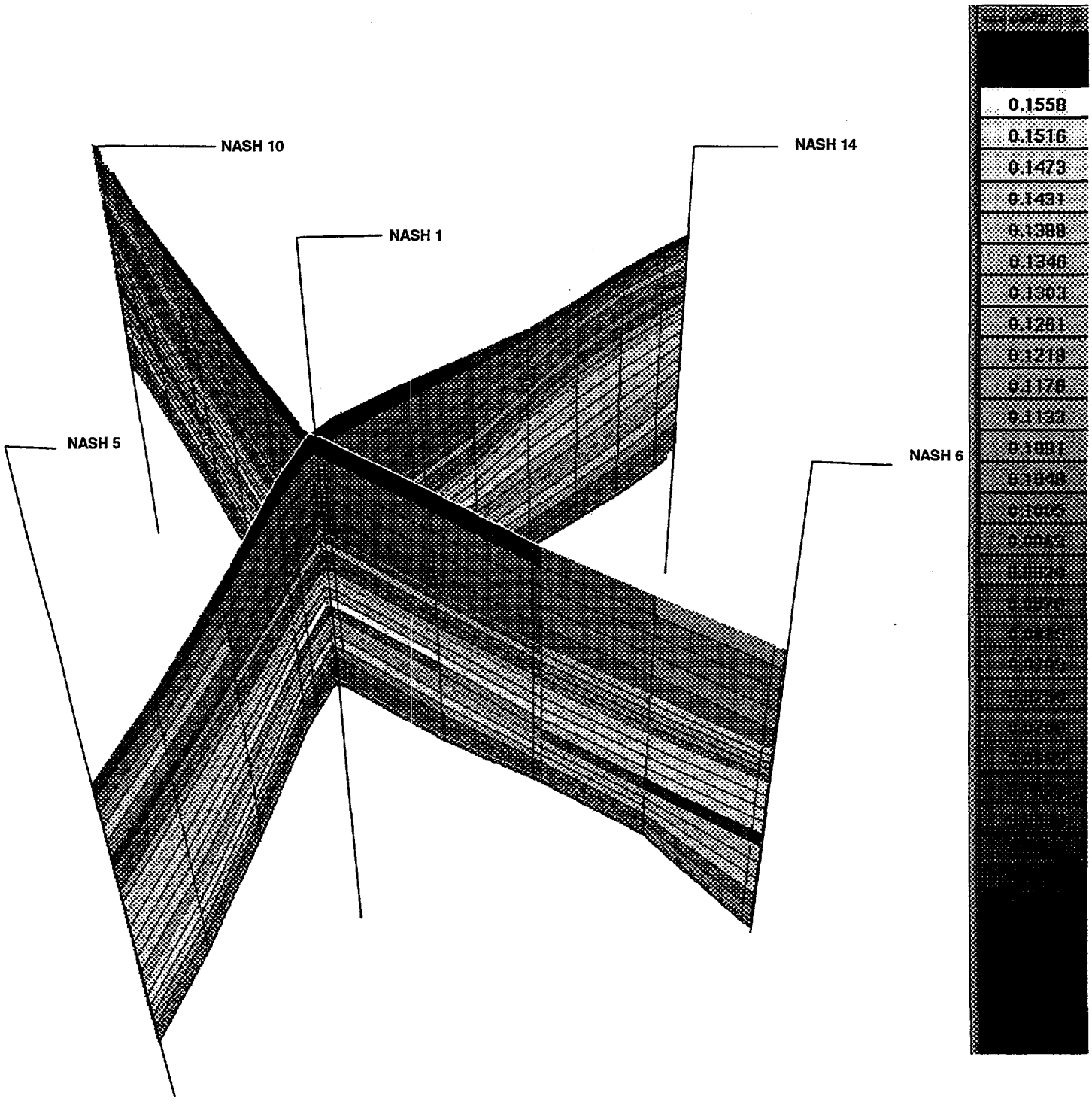

Figure 36. Distribution of porosity in Nash Draw Pilot Area.

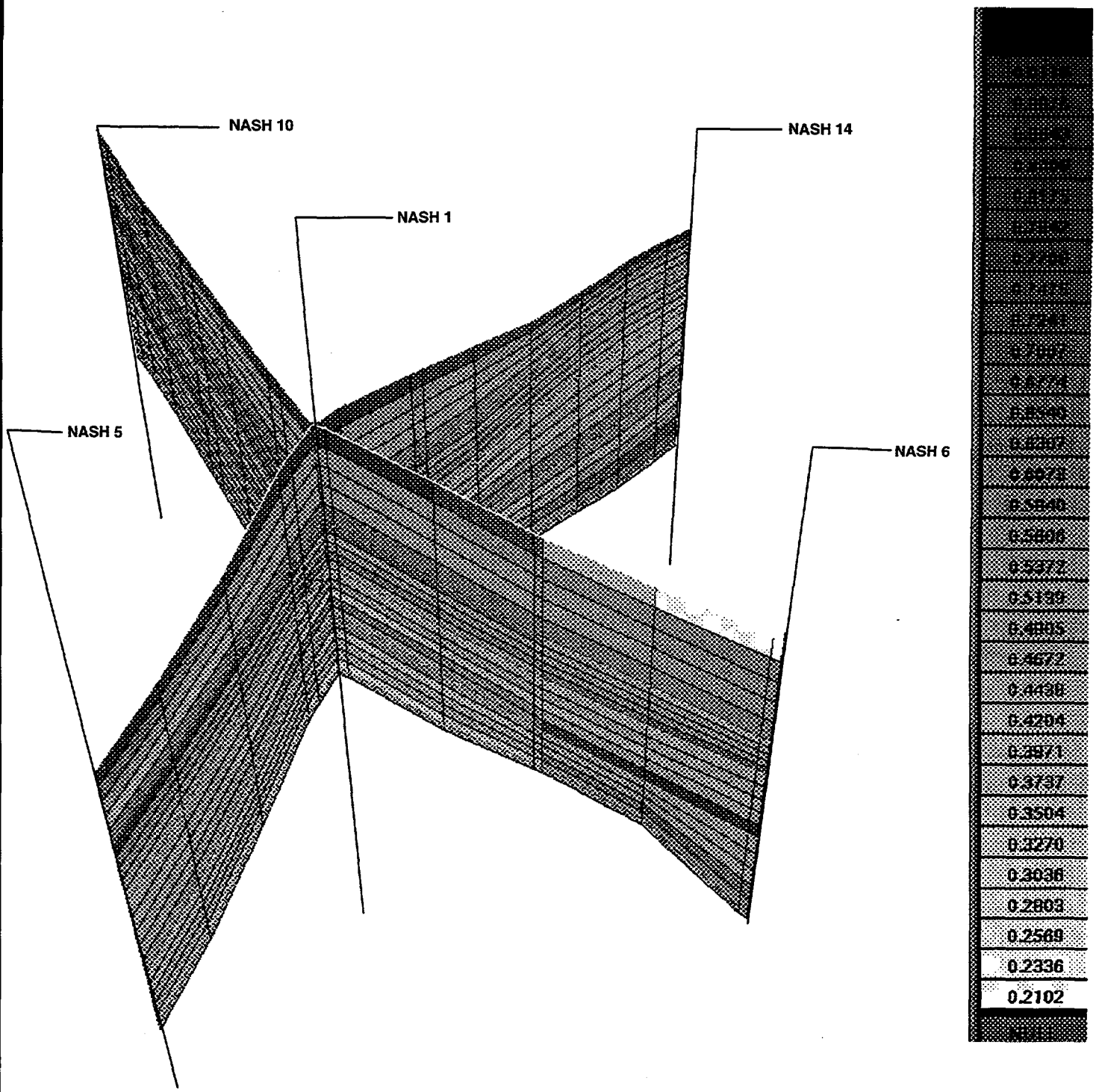

Figure 37. Distribution of water saturation in Nash Draw Pilot area..

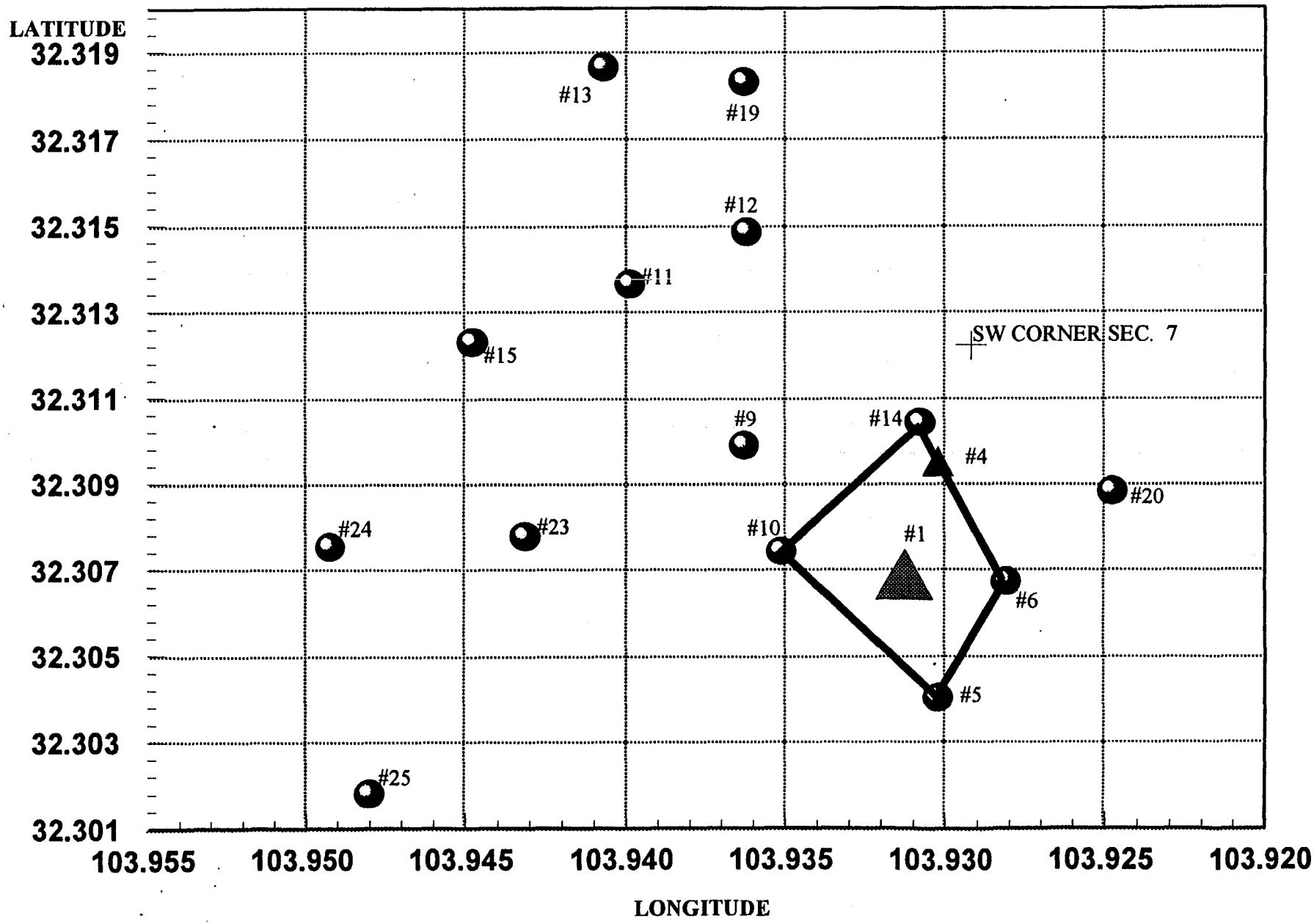

Figure 38. Nash Draw Brushy Canyon Pool field map with pilot area.

INJECTION RATE WATER

NASH DRAW #1

OIL ZONE ONLY

k=	1.1320755	md, ABSOLUTE PERMEABILITY	
krw=	0.22	%, RELATIVE PERMEABILITY TO WATER, FRACTION	("L" @ 70% Sw)
h=	53	FT., HEIGHT	
Piwf=	5000	PSI, INJECTION WELL BOTTOM-HOLE PRESSURE	
Pe=	1000	PSI, PRESSURE AT EXTERNAL BOUNDRY	
Uw=	1.00	CP, WATER VISCOSITY	PRODUCED WATER @ 120 F
rwo=	100	FT., RADIUS OF THE LEADING EDGE OF THE WATER BANK, AT THE WATER-OIL INTERFACE	
r'w=	37.755063	EFFECTIVE WELL RADIUS, FT.	
M=	0.4088889	MOBILITY RATIO	
re=	1144	FT., EXTERNAL BOUNDRY RADIUS	
S=	-4	SKIN	
rw=	0.7	WELL RADIUS, FT.	

iw= 189.44 BWPD

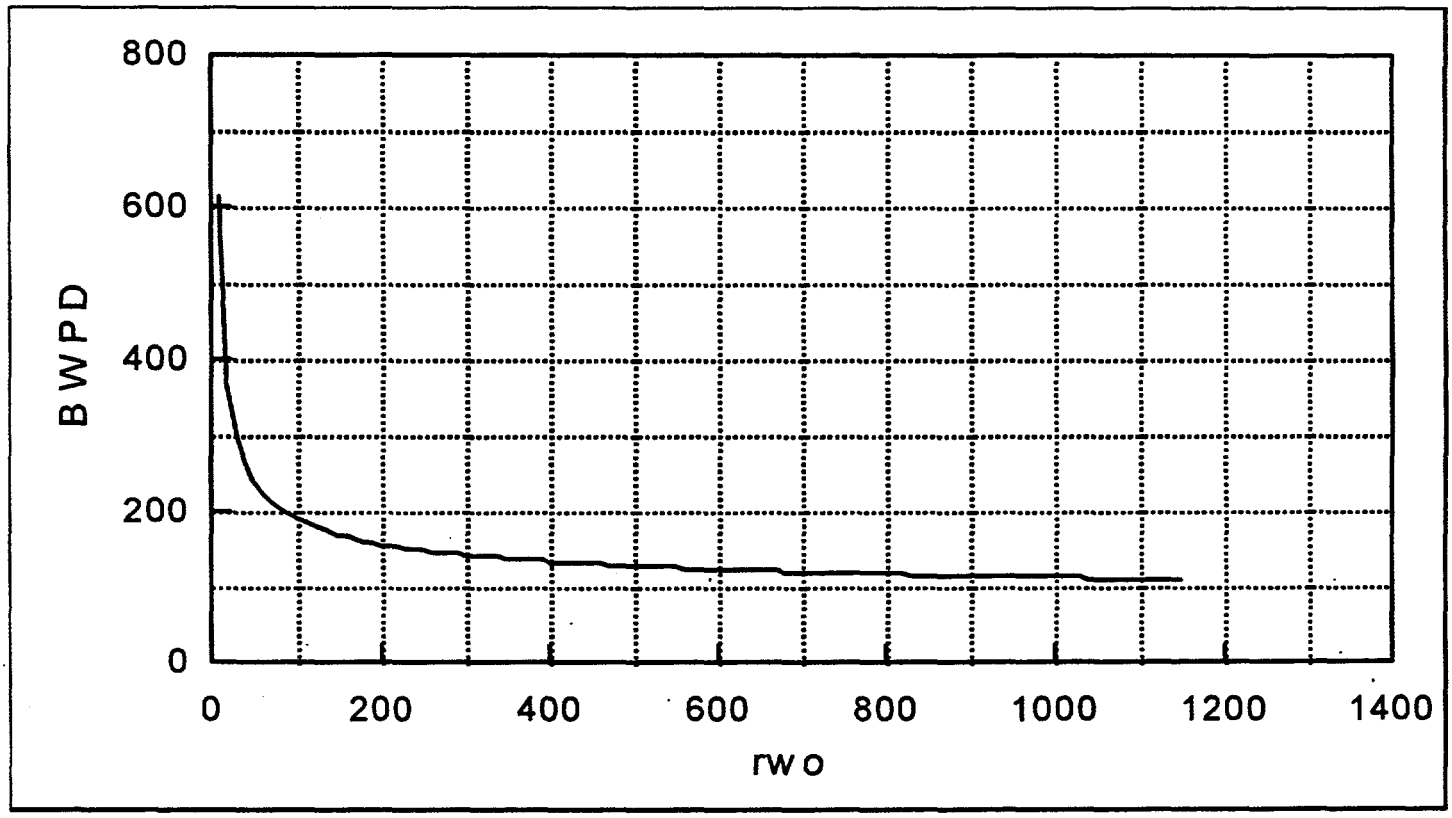

Figure 39. Pilot injection well, water injection rate.